Comparing Cold In-Place Recycling (CIR) and Cold In-Place Recycling with Expanded Asphalt Mixture (CIREAM)

by

Janki Bhavsar

A thesis

presented to the University of Waterloo

in fulfillment of the

thesis requirement for the degree of

Master of Applied Science

in

Civil Engineering

Waterloo, Ontario, Canada, 2015

Author's Declaration

I hereby declare that I am the sole author of this thesis. This is a true copy of the thesis, including any required final revisions, as accepted by my examiners. I understand that my thesis may be made electronically available to the public.

Abstract

Cold Mix Asphalt (CMA) is used in several rehabilitation techniques, which uses 100% Reclaimed Asphalt Pavement (RAP), thus making it a sustainable product in the industry. Using CMA for rehabilitation decreases the energy consumption and greenhouse gas emissions. In Ontario, it has been implemented over the past 17 years. There are two main techniques used for CMA: Cold In-Place Recycling (CIR) and Cold In-Place Recycling with Expanded Asphalt Mixture (CIREAM). It is necessary to determine the performance of these techniques in order to determine the age of the pavement and expand their applications. There is a lack of laboratory and field performance information in Ontario for these two techniques. Thus, in this study, laboratory investigation was carried out to establish and compare the material performance of CIR and CIREAM. In addition, a field study was conducted which involved the evaluation of several road sections which have used CIR and CIREAM techniques.

For this project, the test material was collected from road sections in Ontario, thus, this study was focused on CIR and CIREAM applications in Ontario and tests were based on standards followed by the province. Although the study was conducted for Ontario, the methodology may be applied outside of Ontario with similar climate conditions. However, the results would vary based on the type of material used.

The laboratory study included testing for the overall stiffness, tensile strength, and fatigue behavior of the test samples to simulate their long-term performance. RAP was extracted from southern and northern parts of Ontario to make the test samples. A curing duration test was conducted using the dynamic modulus test apparatus. This test was done to determine a curing time of CIR samples in the laboratory which provided the best stiffness. For the stiffness test, sample mixes were constructed with varying percentages of asphalt cement (AC). From these mixes, the best performing mix was chosen based on its workability, rutting resistance and overall stiffness. The fatigue and

tensile strength tests were conducted using the optimal mix chosen from the stiffness test and the samples were cured according to the results from the curing duration test.

From the curing duration test, it was concluded that curing the CIR samples for 14 days after compaction gave a higher stiffness to the mix. For the CIR mixes using southern Ontario RAP, the mix with 3.2%AC performed well in comparison to the other mixes. The CIREAM mixes with varying percentages of AC had an overall similar performance. The fatigue testing showed that both CIR and CIREAM samples had similar fatigue resistance. The TSRST tests showed that CIR samples exhibited more shrinkage in comparison to CIREAM and they had higher tensile stresses at failure. The dynamic modulus testing of the CIR samples using northern Ontario RAP showed no statistically significant differences between the mixes. The gradation of the RAP used had a large impact on the stiffness and workability of the sample mixes and their performance.

The field study included road sections with varying roadway and pavement attributes. Data was collected from various municipalities which included the City of Waterloo, County of Peterborough, Region of Northumberland, York Region, Haldimand County, County of Perth, County of Wellington, and the united counties of Stormont, Dundas and Glengarry, along with the Ministry of Transportation Ontario (MTO). This data highlighted the limits of all road sections which had implemented CIR or CIREAM within the municipalities. Approximately 200 road sections were identified which had used CIR or CIREAM techniques. These sections were visually inspected in three different municipalities; specifically the City of Waterloo, Perth County, and the united counties of Stormont, Dundas and Glengarry. From the visual inspections large amounts of deteriorations were observed where greater number of trucks, poor drainage and low speeds were prevalent. Field data evaluation showed no significant effect on physical condition, PCI or rut depth of the roadway due to age, AADT or AADTT, respectively.

To date, these techniques are used on low volume roadways but there is also an opportunity to expand to higher volume roadways to promote sustainable use of recycled asphalt. These techniques are sustainable due to their use of 100% recycled aggregates and low energy consumption. Thus, by closing the research gap on their performance information, it would help broaden their application.

Acknowledgements

I would like to acknowledge my supervisor, Dr. Susan L. Tighe, for giving me the opportunity to do my graduate studies with her. Her constant support and guidance has allowed me to achieve my academic goals. I give her my heart-felt gratitude.

I would also like to thank the industry partners at McAsphalt Industries Ltd. and Miller Paving Limited, 4Roads Management Services Inc. and the Department of Civil and Environmental Engineering; specifically Michael Esenwa, Anton Kucharek, the late Keith Davidson, Amma Wakefield, Trevor Moore, Laura Bland, Richard Morrison, Rob Sluban, and Ron Dulay. I greatly appreciate the support of the Natural Sciences and Engineering Research Council of Canada (NSERC) for helping fund this project. I would like to acknowledge the help from Dave Anderson for the field study of this project and the folks from WorkTech for providing a useful tool for the study. I also appreciate the time and efforts put in by the municipalities to provide field information for this project; specifically Warren Lee (MTO), Becca Lane (MTO), Gary Macdonald (Waterloo), Christina Klein (Northumberland), Lloyd Rollinson (Haldimand county), Dave Turkington (Peterborough), and Matt Ash (Perth).

I would like to acknowledge my Centre for Pavement And Transportation Technology (CPATT) colleagues; specifically Dr. Doubra Ambaiowei, Sina Varamini, Magdy Shaheen, Dr. Xiomara Sanchez, Dr. Marcelo Gonzalez, Sonia Rahman, Dan Pickel, Andrew Northmore, Cheng Zhang, Dr. Hassan Baaj, Taher Baghaee, Prabir Das, all the co-op students and research assistants, and the rest of the group members. I appreciate all of their long hours of help, guidance and friendships. They were always supportive and made sure that there was never a dull moment during graduate school. I would like to thank them for making me the captain of our soccer team, CPATT FC, for two consecutive seasons. I would also like to acknowledge and thank Olivier Daigle for helping me proofread my work.

Finally, I would like to express gratitude for my family and friends. They were very supporting and helpful throughout my studies and without them; I could not have achieved any of my goals.

Dedication

I would like to dedicate this thesis to my late grandmother, my niece, Vishwa, and my family.

Table of Contents

List of Figures

List of Tables

Glossary of Terms

AADT	Average Annual Daily Traffic
AADTT	Average Annual Daily Truck Traffic
AASHTO	American Association of State Highway and Transportation Officials
AC	Asphalt Cement
ASTM	American Standard Test Method
AV	Air Voids
AVC	Asphalt Vibratory Compactor
BRD	Bulk Relative Density
CIR	Cold In-Place Recycling
CIREAM	Cold In-Place Recycling with Expanded Asphalt Mixture
CMA	Cold Mix Asphalt
CPATT	Centre for Pavement And Transportation Technology
DT	Duration Test
FPB	Four Point Bending
FWD	Falling Weight Deflectometer
HF	High Float
HMA	Hot Mix Asphalt
IRI	International Roughness Index
ITS	Indirect Tensile Strength
LCC	Life Cycle Cost
LS	Laboratory Standard
LVDT	Linear Variable Differential Transformer
MRD	Maximum Relative Density
MTO	Ministry of Transportation Ontario
NCHRP	National Cooperative Highway Research Program
OMC	Optimum Moisture Content
OPSS	Ontario Provincial Standard Specification

PCI	Pavement Condition Index
PG	Performance Grade
PGAC	Performance Grade Asphalt Cement
RAP	Reclaimed Asphalt Pavement
RCR	Riding Comfort Rating
TSRST	Thermal Stress Restrained Specimen Testing
WMA	Warm Mix Asphalt

CHAPTER 1
INTRODUCTION

1.1 Background

The rehabilitation of an asphalt pavement is carried out in order to increase its service life. Cold Mix Asphalt (CMA) is applied in several rehabilitation techniques, uses 100% Reclaimed Asphalt Pavement (RAP) and it is carried out in-place. It is used when the pavement condition of a roadway is anywhere between good to fair (NCHRP Synthesis 421, 2011)

Since rehabilitation techniques with CMA use 100% RAP and are constructed in-place, they have several benefits such as: reduced fuel consumption and emissions of carbon dioxide and nitrous oxide (Chesner, 2011) and no offsite hauling of aggregates or on-site hauling of virgin aggregates is required (Alkins, Lane, & Kazmierowski, 2008); This helps reduce project costs. For other commonly used rehabilitation techniques such as: Hot Mix Asphalt (HMA) and Warm Mix Asphalt (WMA), the aggregate and bitumen are required to be heated and they do not use 100% RAP; thus, making CMA a more sustainable choice with regards to the environmental and economic benefits (Mallick, Kandhal, & Bradbury, 2008). However, there are a few concerns when using CMA; these are noted as follows: The aggregates are recycled on-site and have unknown properties because it is recycled from what is available and it is used to rehabilitate damaged road ways. Thus, recycling of the damaged road

may result in poor quality of RAP. The existing binder in the aggregate is usually stiff because it is aged (Mallick, Kandhal, & Bradbury, 2008). Using CMA in rehabilitation techniques is not always suitable for pavements with extensive base or subbase problems or pavements of insufficient strength. When a pavement has a structural or subbase layer damages it might require reconstruction to mitigate the damages. CMA is good to use for load associated, environmental associated and material associated distresses (Chan, Tighe, & Chan, 2010) but it is not well suited for road sections with poor drainage (OPSS 335, 2009). These factors lead to an uncertainty about the expected service life and the long term performance of using CMA in rehabilitation. As a result, these uncertainties limit its usage to low volume roadways to minimize its exposure to aggressive traffic conditions (Chesner, 2011).

There are two technologies that are used in Ontario with CMA. These are Cold In-place Recycling (CIR) and Cold In-place Recycling with Expanded Asphalt Mixture (CIREAM).

For CIR construction, the existing pavement is milled, mixed with emulsified asphalt, laid and compacted in a continuous step. The pavement is then left to cure in-place for 14 days. CIREAM construction done similarly to CIR construction but it uses expanded asphalt mixture instead of emulsified asphalt and it only requires a 2 day curing period. Both rehabilitation techniques are usually finished off with a surface layer. This surface layer is a minimum of 25 mm thick layer of Hot Mix Asphalt (HMA) (Wirtgen, 2004). The surface layer is required to protect the open binder layer underneath. Figure 1-1 shows the on-site CIR and CIREAM compaction process.

Recycling pavements using CIR and CIREAM has the potential to decrease energy consumption, reduce adverse environmental impacts and costs associated with asphalt pavement rehabilitation. CIR can conserve around 62% of

aggregate, and reduce 52% of carbon dioxide and 54% of nitric oxide and nitrogen dioxide emissions compared with a traditional rehabilitation technique of 100 mm milling and 130 mm of HMA placement (Alkins, Lane, & Kazmierowski, 2008).

Figure 1-1: Cold In-Place Recycling (CIR) in field (Moore, 2013)

From an economical perspective, CIR and CIREAM have shown many benefits including the reduction in cost by 42% over a 50 year service life period and 5% discount rate are used (Alkins, Lane, & Kazmierowski, 2008). This means that CIR and CIREAM are more cost-effective than the traditional rehabilitation technique (Alkins, Lane, & Kazmierowski, 2008). From the social benefits aspect, CIR and CIREAM improve the transportation safety because it rehabilitates an existing roadway in a distressed state); and it has a high production rate, which is twice the production rate compared to conventional HMA. They have easier recycling processes compared to HMA in uncertain weather conditions (except rainfall), and create less noise because the work is done in place (Alkins, Lane, & Kazmierowski, 2008).

CIR materials can mitigate reflective cracking to extend pavement life (Kazmierowski, Markes, & Lee, 1999). Except for the mitigation of pavement cracking, CIR does require a long curing period. For conventional CIR, it needs at least a 14-day curing period to meet all the compaction requirements. As a result, it usually needs a separate sealing-wearing surface such as a hot-mix overlay or surface treatment because of its susceptibility to moisture intrusion and abrasion (Kazmierowski, Markes, & Lee, 1999).

CIREAM has a shorter curing period compared with the curing period of CIR; CIREAM which only requires a 3-day curing period before a 25 mm HMA surface can be applied (Lane & Kazmierowski, 2006). Also, the dry or warm weather has less influence on the CIREAM process which means there is a longer time window available within which pavement rehabilitation projects could be undertaken. (Lane & Kazmierowski, 2006).

1.2 Problem Statement

Although CIR and CIREAM have been used in Canada and specifically Ontario for several years, there is limited information on their laboratory and long term field performance. Further in-depth study for both techniques, regarding specific construction methods and accurate application is also required to expand its potential to be used more often in the industry. A comparison between the two techniques would be beneficial to assess the technical, economic and environmental cost and benefits of CIR and CIREAM.

1.3 Research Scope and Objectives

The overall objective of this research is to evaluate CIR and CIREAM and to highlight performance differences between them. The specific sub-objectives include:

1) Evaluation of the field performance differences between of CIR and CIREAM;

2) Evaluation of the laboratory performance difference between CIR and CIREAM; and

3) Investigation on long-term field performance differences between CIR and CIREAM.

The scope of the work involved a laboratory study, field study and analysis of the data obtained from these studies. The laboratory study included a strength test using dynamic modulus setup, thermal stress restrained testing and a four point bending test for the samples. This gave an overall comparison between the two techniques with regards to strength, tension and flexural abilities of the mixes. The field study provided information on long-term performance for different in-situ scenarios.

1.4 Organization of Thesis

This thesis is organized in six chapters. Chapter 2 is the literature review of the subject matter and the studies done to date. It presents the materials used and the existing research gaps. Chapter 3 discusses the research methodology for the project and a detailed description of the different tests carried out. Chapter 4 provides the test results, analysis and discussions of all the tests data collected. It also provides a detailed discussion on the material performance in the lab. Chapter 5 provides a detailed description of the field performance collected from the field studies. Chapter 6 summarizes the findings and provides conclusions and recommendations. It also provides recommendations for future research possibilities. Finally, the resources used are listed under the references section. Any additional photographs, graphs, figures, tables and statistical analyses are all provided in Appendix A through H.

CHAPTER 2
LITERATURE REVIEW

2.1 Introduction

This chapter presents the literature review on CIR and CIREAM. The different construction methods, post-construction testing, and type of mixes used in field are discussed for both techniques. The currently available information on lab and field performance of CIR and CIREAM are also discussed. Finally, the research gaps providing the basis of the research conducted for this thesis are discussed.

2.2 Stabilising RAP with Bitumen Emulsion and Foamed Bitumen

CIR is a rehabilitation technique for roadways, which uses emulsion asphalt cement (AC) with water, with 100% Reclaimed Asphalt Pavement (RAP). It has a 14-day curing period to allow the mixture to lose moisture and gain strength. CIREAM is another such rehabilitation technique, which uses expanded/foamed AC and has a curing period of 3 days.

Table 2-1 shows a brief comparison of the advantages and disadvantages of using Bitumen Emulsion and Foamed Emulsion with RAP.

Table 2-1: Advantages and disadvantages of using Emulsified and Expanded/Foamed AC (Wirtgen, 2004)

Stabilising with Emulsified Asphalt Cement	
Advantages	Disadvantages
1) Flexible, viscoelastic 2) Resistance to deformation 3) Ease of application 4) Ease of availability in the industry 5) Standard test methods and specifications are available.	1) Emulsifiers are expensive. Transport costs inflated by hauling the water component, not only bitumen. 2) Where the moisture content of material in the existing pavement is close to OMC, saturation occurs when emulsion is added. 3) Curing can take a long time. Strength development is dictated by moisture loss.
Stabilising with Foamed or Expanded Asphalt Cement	
Advantages	Disadvantages
1) Flexible, viscoelastic 2) Resistance to deformation 3) Ease of application 4) Foamed bitumen uses standard Performance grade AC (PGAC). There are no additional manufacturing costs. 5) Quicker rate of gain of strength.	1) Foamed bitumen demands that the bitumen is hot, usually above 160 ºC. This often requires special heating facilities and additional safety precautions. 2) Saturated material and material deficient in the fraction smaller than 0.075 mm cannot be treated with foamed bitumen without pre-treatment or the addition of new material.

Emulsion asphalt has an advantage in comparison to hot asphalt and cut back binders due to its low application temperature and compatibility with other water-based binders such as performance grade (PG) binders (Salomon, 2006). Foamed asphalt has the advantage that it could be used with a wider range of aggregate types and it requires less binder and water. The foam remains workable and can be constructed in adverse weather conditions, such as cold weather or light rain (K.M. Muthen, 1998).

2.3 Field Construction methods of CIR and CIREAM

The construction process for both CIR and CIREAM requires a milling machine, mobile screening of aggregates and a crushing deck. The milling equipment is essential for removing the old pavement on the existing roadway.

For CIR, the RAP aggregate feeds into a mix paver that adds emulsified asphalt and places the material on the milled roadway. For CIREAM, the RAP aggregate is sent to a twin-shift pug mill where the expanded asphalt is added and mixed. The mixture is conveyed into a paver and placed on the milled roadway. The layers, in both cases, are then compacted using rollers. Compaction for both techniques provides a tighter bond between the RAP aggregates and the emulsified or expanded asphalt. Generally, pneumatic rollers are used for the compaction process. The compacted material is then allowed to cure (Lane & Kazmierowski, 2006). The curing stage is needed to allow the solvent in the CIREAM to evaporate and the emulsified asphalt in CIR to set. The evaporation stiffens the CIREAM binder course and hardens the expanded asphalt. Even though they are both compacted prior to curing, the surface may not be smooth because the material used is reclaimed instead of virgin. Thus, as a final construction stage a layer of overlay is typically placed to smooth the surface. A tack coat is used before the overlay for proper bonding between the binder layer and the surface layer (Chan, Tighe, & Chan, 2010).

Figure 2-1 shows the process diagram for CIR construction. It represents the continuous multi-step process showing the milling, mixing and placement of the RAP.

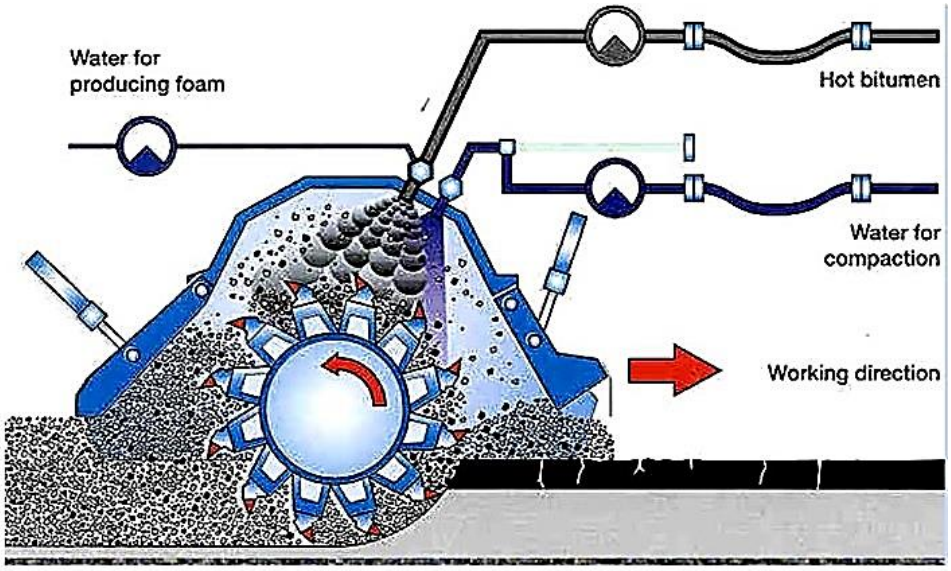

Figure 2-1: CIR field placement process diagram (Wirtgen, 2004)

For CIREAM placement there is a stream of water added (typically 2% by mass of aggregate) to the hot bitumen (heated to 160 – 180 °C) which causes instant evaporation of the water (Wirtgen, 2004). This process causes an expansion of about 1500 times the original liquid volume at normal atmospheric pressure. When the water particles are exposed to the bitumen, the heat energy from the bitumen transfers over to the water and as soon as the water reaches its boiling temperature, it changes state. This creates a thin-filmed bitumen bubble filled with water vapour (Wirtgen, 2004).

In the foamed state, the bitumen can be added and mixed with aggregates at in-situ temperatures and moisture content (Wirtgen, 2004). Figure 2-2 shows a diagram of the foaming process. The bitumen turns into bubbles of thin films and occupies a greater volume. This causes the bitumen to become less viscous and helps it evenly distribute among the aggregates.

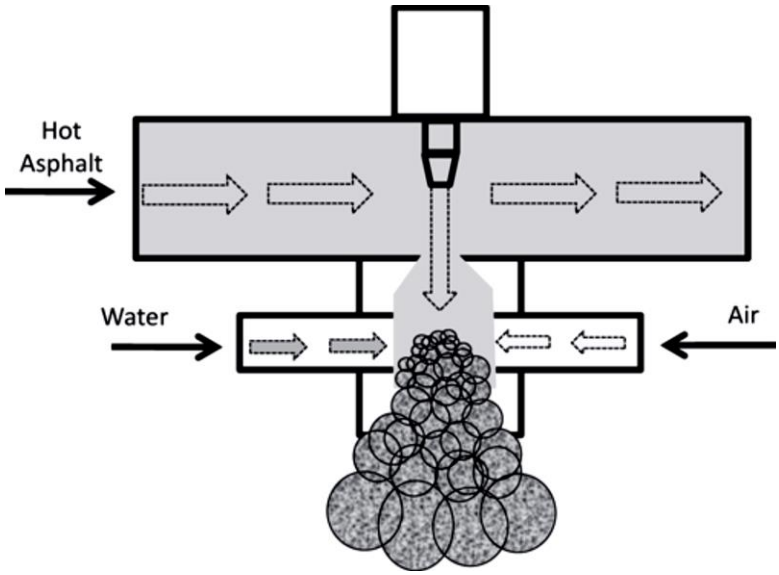

Figure 2-2: Asphalt Cement foaming process (NCHRP Synthesis 421, 2011)

Figure 2-3 shows an example of the post construction cross-section after a CIR or CIREAM mix is used to rehabilitate a section of pavement. It shows the 25 mm untouched asphalt pavement, the CIREAM layer and the asphalt overlay layer.

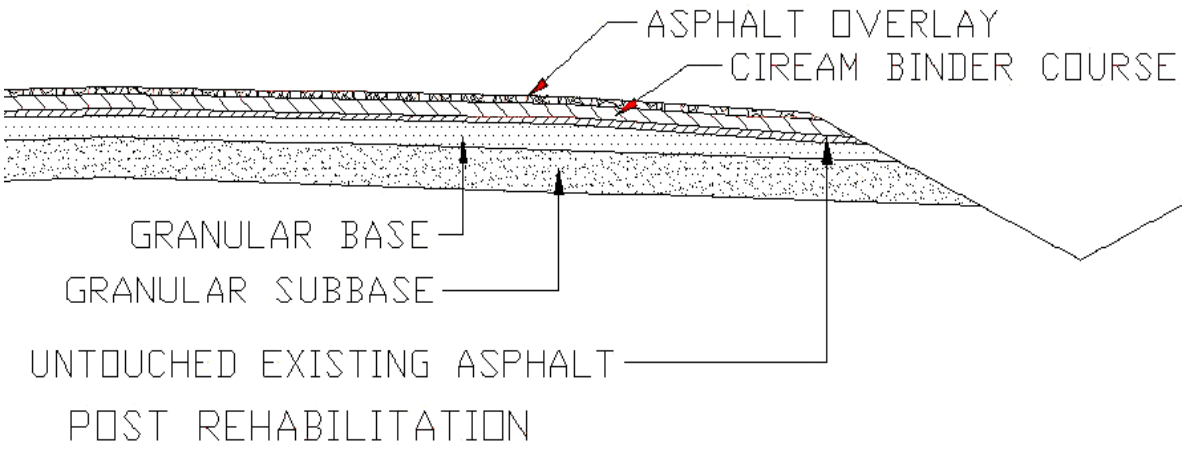

Figure 2-3: Cross section of a pavement rehabilitated with CIR or CIREAM (Chan, Tighe, & Chan, 2010)

2.3.1 Regular Construction mixes

CIR mix design contain RAP, emulsified AC and water. The ratio of AC emulsion and water content is critical to achieve the expected mix density, air void, and stability (Kazmierowski, Markes, & Lee, 1999). In many cases, the mix required 1.5 to 2.2% emulsion content, and 3.5 to 4.5% water content (Kazmierowski, Markes, & Lee, 1999). The maximum amount of emulsion or water (total liquid content) that can be added to the mixes is 4.5% AC following the Ontario Ministry of Transportation (MTO) Laboratory Standard, LS-300 R16 (MTO-LS, 1996). The calculations for the different mixes used for the laboratory testing for this project are shown in Appendix A.

For the CIREAM mix design, the mixes are composed of RAP, expanded or foamed AC and water. Expanded or foamed AC can be characterised by two primary properties:

1) Its Expansion Ratio, which is a measure of the viscosity of the foam and determines how well it will disperse in the mix. It is calculated as the ratio of the maximum volume of foam relative to its original volume; and

2) Its Half-Life, which is a measure of the stability of the foam and provides an indication of the rate of collapse of the foam. It is calculated as the time taken in seconds for the foam to collapse to half of its maximum volume (Wirtgen, 2004).

A general trend of half-life and expansion is shown in Figure 2-4. Thus, the higher percent water added, the higher the expansion grows but the half-life decreases. The optimum percentage of water is at the breakeven point of the two graphs. This ensures the maximum expansion for the maximum half-life that can be achieved with the given AC.

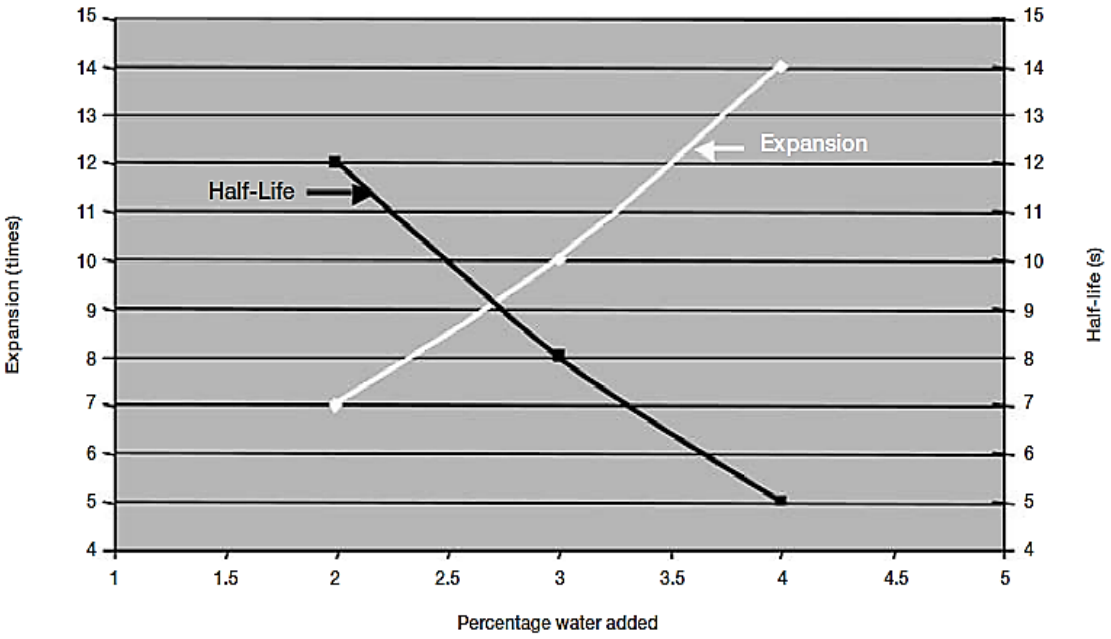

Figure 2-4: Relationship between foaming properties of asphalt cement (Wirtgen, 2004)

It was crucial to determine the peak percent of water, which provides a reasonable half-life and expansion for the performance graded AC (PGAC) used for the laboratory testing. A.2: CIREAM Mix Design shows the calculations for peak water content. 3 percent of water is added to the AC gave an optimized half-life and expansion ratio for the PGAC used.

2.3.2 Post Construction Testing

For both techniques, post construction testing, quality control and quality assurance is crucial in order to ensure their short-term and long-term performance. Since these technologies are relatively new to the industry, most of the information available at this time is for short-term performance.

For CIR or CIREAM, the typical tests that are carried out post construction are indirect tensile strength, resilient modulus, Falling Weight Deflectometer (FWD) tests, and roughness and rutting tests (Lane & Kazmierowski, 2006).

These are performed typically to obtain the wet and dry tensile strength and the tensile strength ratio following the American Standard for Testing Materials method given in ASTM D6931-12 (ASTM, 2012).

2.4 Usage of CIR and CIREAM in Ontario

In Ontario, CIR is an established pavement rehabilitation method. Ontario has been using CIR with emulsified asphalt binder since 1980. In 2003, a new development in CIR technology was introduced using expanded (foamed) asphalt rather than emulsified asphalt to bind the mix (Lane & Lee, 2014). This was the introduction of CIREAM in the pavement industry in Ontario. Over the past 17 years the MTO has successfully recycled—with either CIR or CIREAM—approximately 3,500,000 m^2 of HMA pavement (Alkins, Lane, & Kazmierowski, 2008). With increasing cost of fuel and environmental awareness, CIR/CIREAM have become popular design alternatives when selecting rehabilitation strategies for Ontario's highways and are frequently replacing traditional techniques such as milling, full depth reclamation and new HMA paving (Alkins, Lane, & Kazmierowski, 2008).

Several municipalities in Ontario have successfully used this technology. However, most of the roadways that they are implemented on are rural arterial highways with high speed limits and low traffic volumes (Lane & Kazmierowski, 2006). The use of these techniques is limited to low volume roads because the aggregates used are from existing roadways which are potentially deteriorated and aged.

2.5 Laboratory Evaluation of CIR and CIREAM to date

In 2009, research personnel (Kim, Im, & Lee, 2011) at the University of Iowa carried out a laboratory performance evaluation of CIR and CIREAM. The main

objective of their study was to compare their performance and to see if curing the samples at different times showed any improvement in strength of the samples. Most laboratory and field test results that were obtained indicated that the curing temperature and the curing period length significantly affect the properties of the CIR and CIREAM samples. In Iowa, the industry standard for the curing time is 10–14 days (in Ontario, the standard is 14 days of curing) or a maximum moisture content of 1.5%. However, these criteria were not developed on sound engineering principles or proper experimental results as stated by the engineers who completed the study (Kim, Im, & Lee, 2011). Thus, the study was carried out to contest these specifications and to obtain a more specific in-field curing time (Kim, Im, & Lee, 2011).

The Kim et al, 2011 study involved a set of indirect tensile strength (ITS) tests, dynamic modulus tests, and repeated load tests to evaluate how the moisture, curing temperature, and curing time affected CIR and CIREAM samples. The ITS test was chosen because it is a typical test used to determine the moisture susceptibility of asphalt mixtures. The dynamic modulus and repeated load tests were performed to determine how the moisture content affected the overall stiffness and the permanent deformation of the samples. The dynamic modulus and repeated load tests were conducted using simple performance test (SPT) equipment (Kim, Im, & Lee, 2011).

Figure 2-5 and 2-6 show the test results from the study. In Figure 2-6, the red continuous curve represents the overall trend for the CIREAM samples and the green dashed curve represents the CIR samples for Story County RAP material (Shatec Engineering Consultants, 2013).

The laboratory test results confirmed that the amount of moisture and length of the curing period significantly affected the properties of the CIR mixtures. Given the same curing time, CIREAM specimens exhibited more

tensile strength and less moisture content than CIR emulsion specimens did. When the cured CIR specimens were submerged in water for 24 hours to simulate rain conditions, after the CIR layer was cured, their indirect tensile strength values significantly decreased. Given the same curing time, the CIREAM specimens exhibited higher dynamic modulus than the CIR specimens did. CIREAM exhibited larger flow numbers than CIR specimens. The CIR and CIREAM specimens with a longer curing duration also exhibited larger flow numbers (Kim, Im, & Lee, 2011).

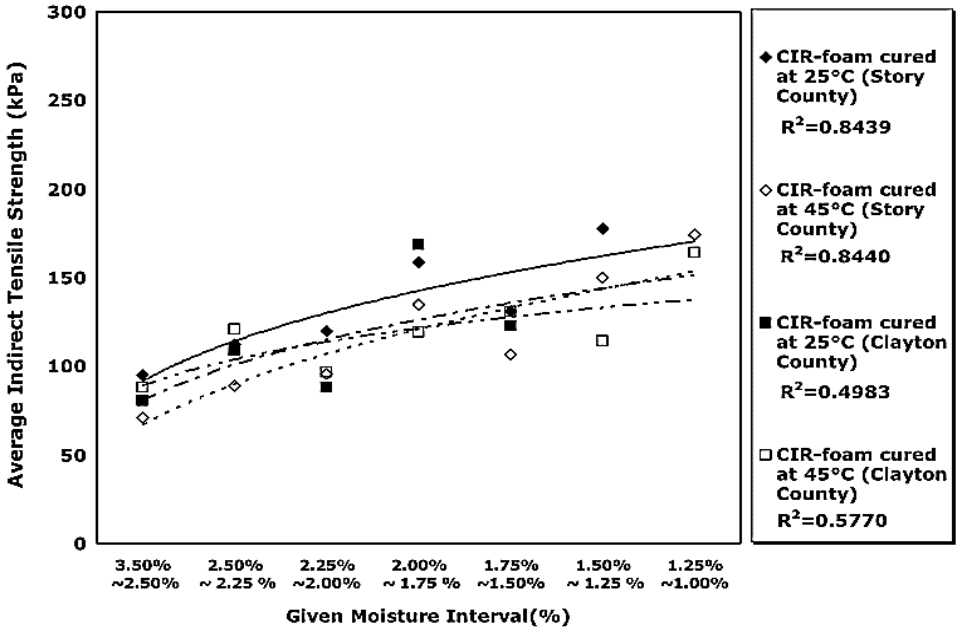

Figure 2-5: Average ITS against ranges of moisture content for CIREAM and CIR specimens cured at 25°C and 45°C (Kim, Im, & Lee, 2011)

Other laboratory performance testing for CIR and CIREAM in Ontario and Canada which are completed by research teams and the MTO mainly include field sample testing for ITS and strength tests.

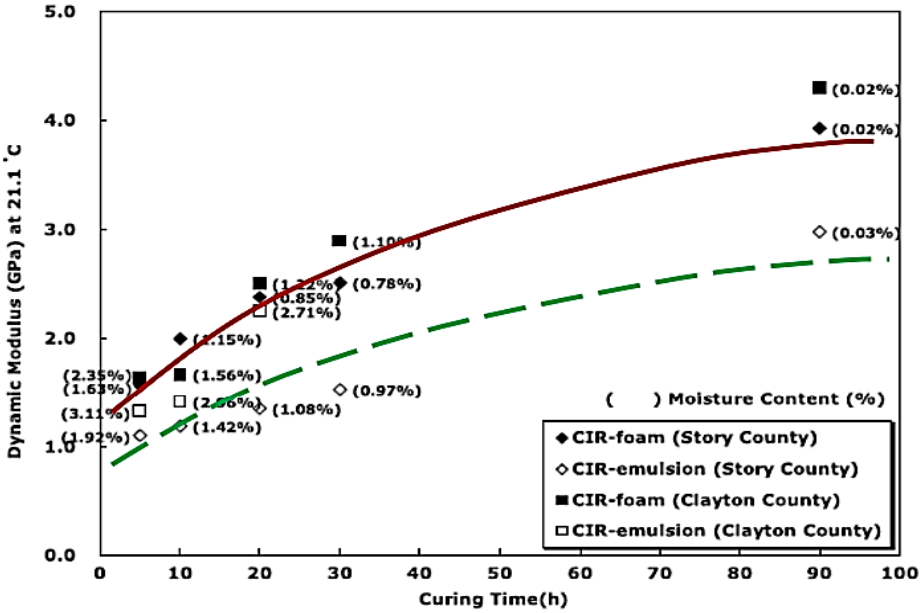

Figure 2-6: Comparison of dynamic modulus of CIREAM and CIR at various curing durations. (Shatec Engineering Consultants, 2013)

Figure 2-7 shows the results of an ITS test done on CIR and CIREAM samples by the MTO for their test section on Highway 7 (discussed in detail in the next section). The test showed that the tensile strengths of both materials were dependent on density (Lane & Kazmierowski, 2006); the denser the material and the more compacted it was, the better the resultant tensile strength.

Resilient modulus tests were conducted on core samples of the CIR mix and CIREAM obtained 8 months after construction. The results were statistically similar for both CIR and CIREAM (Lane & Kazmierowski, 2006).

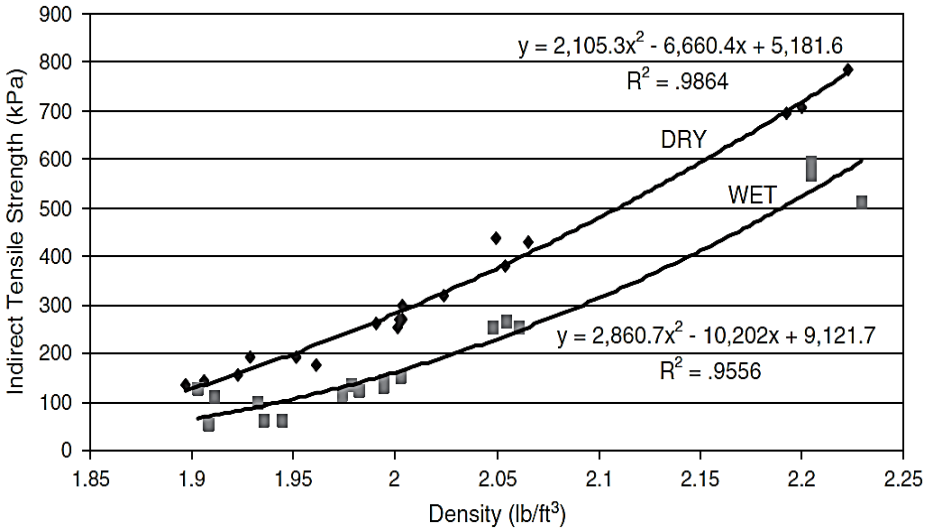

Figure 2-7: Indirect tensile strength versus briquette density for samples of CIR and CIREAM (Lane & Kazmierowski, 2006)

2.6 Field Evaluation of CIR and CIREAM to date

A construction project was developed by the Ontario Ministry of Transportation (MTO) in order to establish the field performance evaluation of CIR and CIREAM. Following the rehabilitation, the performance of the rehabilitated pavement was monitored over a period of ten years. The performance monitoring indicated that the CIREAM section performed as well as conventional CIR at a similar cost. Both treatments performed remarkably well on the tested sections in comparison to the milling, crack repairs and two lift overlays performed on the adjacent road contract (Lane & Lee, 2014). These results are specific to the test site. For a clearer understanding of the field performance comparison of CIR and CIREAM, further field evaluation is required for greater number of sections. Different road sections have varying average daily traffic and loading, thus, evaluating a variety of sections can help provide a more accurate prediction of the service life after applying CIR or CIREAM.

2.6.1 MTO Case Study

In July 2003, the MTO performed a CIR and CIREAM comparison project on a road section located on Highway 7, between the town of Innisville and the town of Perth in Ontario, Canada, as shown in Figure 2-8. The section spanned over 15.4 kilometers in length. It was a rural arterial undivided highway with a posted speed of 80 km/h and an Average Annual Daily Traffic (AADT) of 9000 vehicles as of 2004. Pavement investigation showed an average HMA thickness of 207 mm. The resurfacing consisted of 40 mm of recycled surface course over 40 mm of open-graded binder course (Lane & Kazmierowski, 2006). The two sections of rehabilitation included an 8 km conventional CIR section and a 5 km CIREAM section (Lane & Kazmierowski, 2006). Pre-construction and post-construction tests were carried out on field samples obtained from these trial sections.

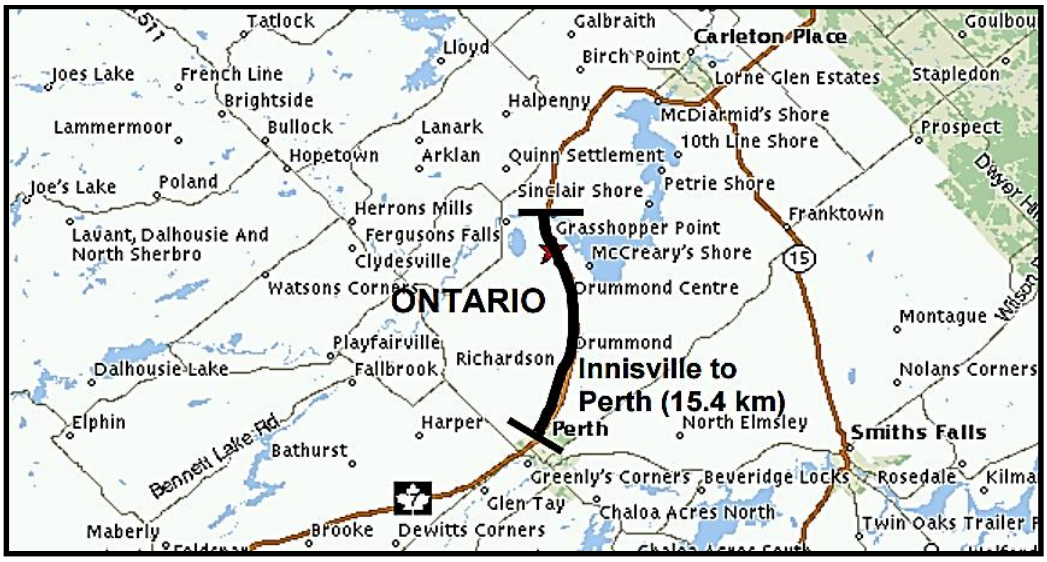

Figure 2-8: Contract 2002-4040 limit on highway 7 from Innisville to town of Perth (Lane & Lee, 2014)

The existing pavement had distresses, which consisted of frequent severe full-depth transverse cracking, localized severe rutting in both wheel paths, longitudinal cracking in wheel paths, intermittent centreline cracking and

moderate alligator cracking. As of 1995, the highway had an average pavement condition index (PCI) of 55 out of 100 and a ride comfort rating (RCR) of 6.2 out of 10. Thus, the highway was a good candidate for rehabilitation. (Lane & Kazmierowski, 2006)

Post construction testing included: ITS testing, falling weight deflectometer (FWD) testing, and MTO's automatic road analyzer (ARAN), which is used to evaluate the roughness and rutting of pavement, for both CIR and CIREAM. In a short time period, the pavement structure of CIR with 50 mm overlay and CIREAM with 50 mm overlay performed similarly at a similar cost (Lane & Kazmierowski, 2006). In addition, both of the materials had a similar performance resilient modulus, FWD, and ARAN test (Lane & Kazmierowski, 2006). After one year, the review of the structure showed that there were no significant distortions, rutting, or cracking for both sections (Lane & Kazmierowski, 2006).

A field review of the pavement sections was carried out a year after construction to measure the short-term performance. Overall, both sections performed well. The overall RCR was 9 out of 10 and PCI was 93 out of 100 (Lane & Kazmierowski, 2006). There was no distinguishable rutting, distortion or cracking observed in either section. However, the CIR section was performing slightly better than the CIREAM pavement in terms of pavement ride quality (Lane & Kazmierowski, 2006).

The results of the field review indicated that the CIREAM section provided equivalent performance to the conventional CIR material and the cost of construction was similar. However, based on the pavement structure analysis, constructability and pavement ride quality, CIR to a depth of 110 mm with a 50 mm HMA overlay was selected as the preferred pavement rehabilitation

technique for this project. It proved to be an effective treatment for extensive reflective cracking in the underlying pavement. (Lane & Kazmierowski, 2006)

MTO had successfully carried out more than 50 contracts with CIR since 1980s (Lane & Kazmierowski, 2006) and CIREAM was a new development at that point; thus, CIR appeared to be a better choice in this scenario.

2.6.2 Life Cycle Cost of Case Study

In order to assess the cost savings of CIR and CIREAM versus mill and overlay using HMA, a life cycle cost analysis was carried out by MTO for these rehabilitated sections on Highway 7. Given the initial construction cost, a 50-year life cycle cost (LCC) was determined.

Table 2-2 shows the calculated life cycle cost values. The 50 year predicted LCC of CIR/CIREAM resulted in cost savings of over $20,000 per km of the section. This was based on the prediction model calculated by the MTO using a 5% discount rate.

Table 2-2: Life Cycle Cost Analysis (Lane & Kazmierowski, 2006)

	CIR and CIREAM	**Mill and Overlay (HMA)**
Depth: milling	-	100mm
Depth: CIR	100 mm	-
Width	7.5 m	7.5 m
Surface course	50 mm	40 mm
Binder course	-	90 mm
Initial const. cost	$100,000/km	$173,000/km
50-year life-cycle cost (LCC)	Yr 15 $100,000→$48,101.71 Yr 30 $100,000→$23,137.74 Yr 45 $100,000→$11,129.65 Yr 50 (salvage) →$5,813.52 Total LCC $76,555/km	Yr 18 $173,000→$71,885.07 Yr 36 $173,000→$29,869.73 Yr 50 (salvage) →-$3,352.50 Total LCC $98,402/km

2.7 Research Gaps

The literature review on CIR and CIREAM presented in this chapter highlighted the research gaps that needed to be filled:

1) There was a lack of performance data and a lack of variety of tests conducted on CIR and CIREAM samples particularly for Ontario. Many of the tests were done on field samples. These tests reported tensile strength (using ITS) and moisture susceptibility of the samples. Although some interesting conclusions were made in terms of the moisture susceptibility and tensile strength,

additional laboratory testing would help shore these conclusions and provide additional information on these rehabilitation techniques. Moreover, a lot of the testing was conducted in the USA. Given the influence of climate on pavement conditions (Mills, Tighe, Audrey, Smith, & Huen, 2009) (and consequently, on the properties of RAP aggregate) testing the performance of CIR and CIREAM using Ontario RAP would be beneficial to local industry

2) MTO made a test section to check the performance of CIR in comparison to CIREAM on Highway 7. However, one section is not sufficient to draw concrete conclusions about their comparison.

In this study, further laboratory investigation was carried out to establish and compare the performance of CIR and CIREAM. In addition, a field study is done on several road sections which have implemented CIR and CIREAM at different times, to examine their overall field behaviour and performance. The field study includes road sections of different speeds, traffic volumes and loading.

CHAPTER 3
RESEARCH METHODOLOGY

3.1 Introduction

This chapter discusses the methodology and goals of the research project. A detailed description of the materials and experiments is provided. Finally, some conclusions and observations are drawn from these experiments. All testing was performed in the laboratories of the Centre for Pavement and Transportation Technology (CPATT) at the University of Waterloo, McAsphalt Industries Limited and Miller Paving Limited.

3.2 Research Methodology

The research methodology included a series of tasks to evaluate the difference between Cold In-place Recycling (CIR) and Cold In-place Recycling with Expanded Asphalt Mixture (CIREAM). The aim of the experimental programme was to determine the laboratory and field performance of CIR and CIREAM. The research methodology summarized in Figure 3-1.

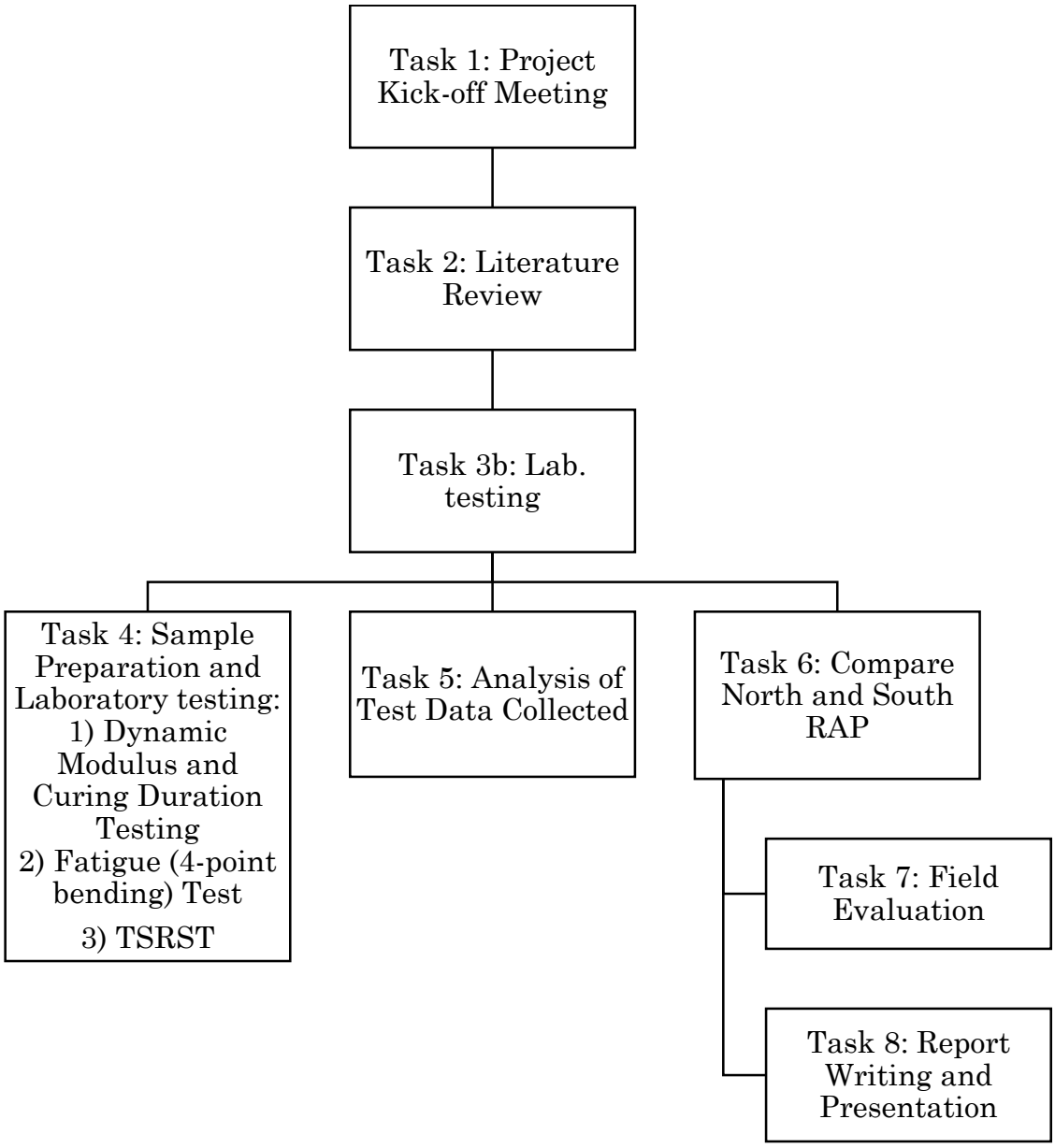

Figure 3-1: Research Methodology

3.3 RAP Material Details

For the purpose of the laboratory component of this study, RAP was obtained from stockpiles from Miller Paving Limited. The Miller Paving Limited stockpiles have road grinding and crushed RAP from Southern and Northern Ontario (Highway 400, 401 projects and other job sites that bring crushed RAP

material for use in HMA paving jobs). The RAP material mainly consisted of crushed rock material, trap rock, limestone and some gravel. Table 3-1 shows the dry gradation of the RAP material obtained from the stockpile. The gradation is presented in Figure 3-2. The gradation is compared with a conventional Hot Laid 3 (HL3) asphalt gradation requirement. HL3 is a dense-graded surface course mix for intermediate volume roads with a maximum aggregate size of 16 mm (OPSS 1150, 2010)

Table 3-1: RAP gradation

	Percent passing			
Sieve	Southern Ont. RAP	Northern Ont. RAP	Max. HL3	Min. HL3
26.5	100	100	100	100
19	100	97.6	100	100
16	98.9	93.6	100	100
13.2	98.4	89.2	98	100
9.5	88	66.6	75	90
4.75	69.1	35.8	50	60
2.36	56.3	20.3	36	50
1.18	46.1	18.3	25	40
0.6	35	10.4	16	30
0.3	24.4	5.1	7	20
0.15	14.4	2.3	3	10
0.075	9.2	0.7	0	5
% AC Extraction	4.77	3.73	-	-
Penetration Value	30	25	-	-

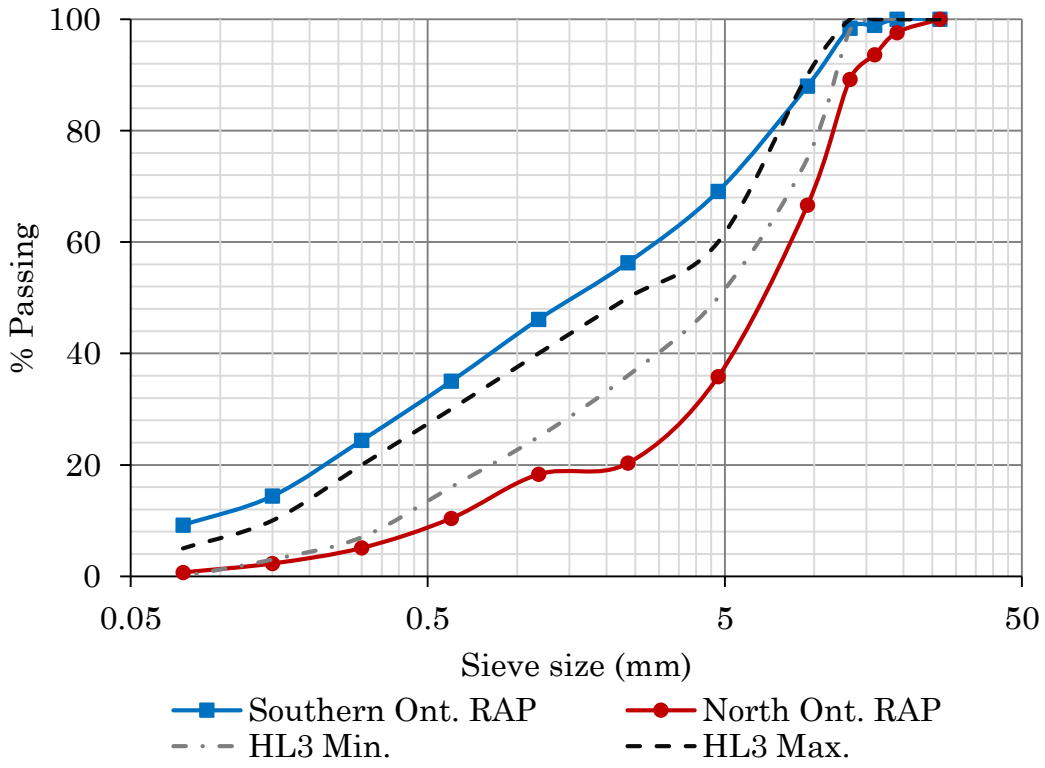

Figure 3-2: RAP gradation in comparison to conventional HL3 gradation

Extraction and penetration tests were performed to determine the percent of asphalt in the RAP and the stiffness of the binder. Southern RAP contained 4.77% existing binder and had a penetration value of 30 mm; Northern RAP contained 3.73% existing binder and had a penetration value of 25 mm. The extraction and penetration tests were performed in accordance with MTO Laboratory standard method LS-282 (MTO-LS, 2009) and ASTM D5/ D5M-13, respectively. Higher values of penetration mean a softer binder consistency (ASTM, 2013). Value of 30 and 25 mm correspond to a very stiff binder consistency (Pavement Interactive, 2007).

Figure 3-3 shows the target grading of the RAP material which is considered ideal for CIR and CIREAM projects (Wirtgen, 2004). In comparison to these limits, the Southern RAP, as shown in Figure 3-2, is closer to the upper limit of the target grading, and the Northern RAP is closer to the lower limit of

the target grading and the typical RAP grading. However, having a large percent of small (between 1 mm to 10 mm sieve sizes) and sandy particles may result in higher absorption of the bitumen within the mix because of a higher surface area of the aggregates.

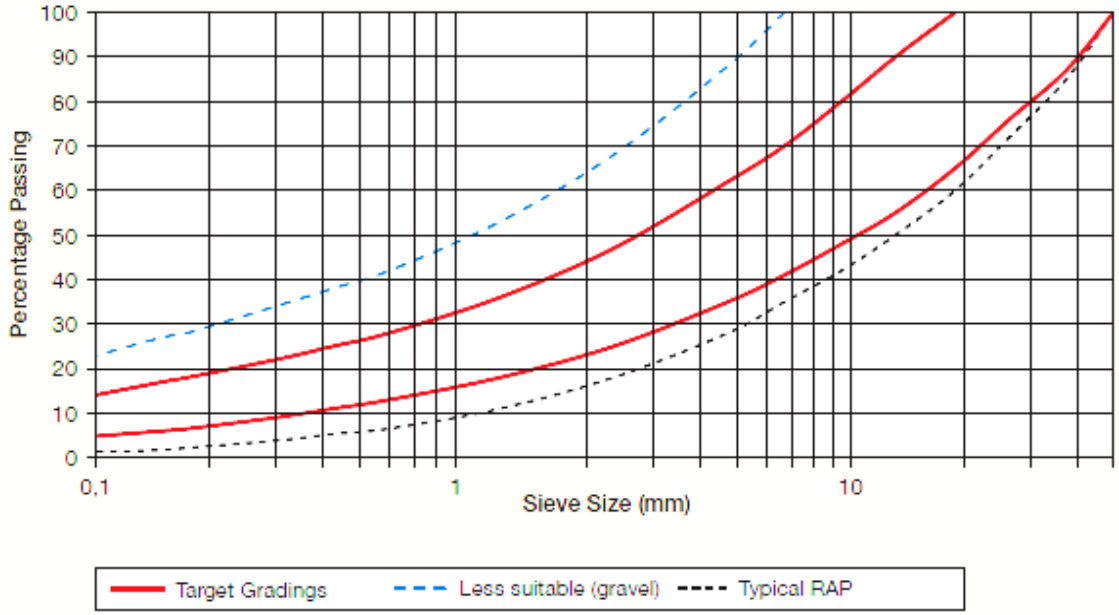

Figure 3-3: Target grading curves for bitumen stabilization (Wirtgen, 2004)

For all the mixes that needed to be constructed in the lab, conventional PGAC was used; specifically PG 58-28. It is a commonly used binder in Ontario and it can withstand a 7-day average high temperature of 58°C and a low temperature of -28°C. A polymer modified emulsion was used for the CIR mixes; specifically a high float (HF) emulsion of HF-150P. The AC was used as is for the CIREAM mixes.

3.4 Test Samples Preparations

The RAP used in these experiments was first air dried for at least 24 hours in order to rid of any moisture. Figure 3-4 shows RAP that was air dried with a fan

before mixing. The fans helped the material dry faster to rid of its moisture. The mixes were all constructed in accordance with MTO LS-300 (MTO-LS, 1996) for CIR and LS-297 (MTO-LS, 2011) for CIREAM samples. Following the drying process, the material was screened over a 26.5 mm sieve. Any material retained on the 26.5 mm sieve was considered too large for the mix according to the standard. The mix design was then calculated as shown in Appendix A. The samples were constructed with specific asphalt cement (AC) and water contents, measured as a percentage by weight of the RAP.

For CIR samples, the mix was constructed using a Hobart industrial mixer (Model No.A200) where the RAP, water and AC were weighted and mixed together. The RAP was first weighed. Each batch of mix was 5000 g based on the capacity of the mixer. Water was then added to the RAP such that the final liquid content of the mixture was no more than 4.5% of the dry weight. Thus, for each varying percent AC in the samples, the percent water was calculated accordingly. For example, for 1.2% AC there was 3.3% water content added to result in a total of 4.5% liquid content. Once the water was added, the AC was added to the mix. The sample batch was then mixed using the mixer for no more than 90 seconds. Once the mixes were made, the samples were weighed in a baking pan and then allowed to cure in the oven for one hour at 60°C ± 3°C before compaction.

Figure 3-4: RAP pile in the lab left for air-drying with fans

For CIREAM, the RAP was weighted and mixed using a Wirtgen Foaming Machine (Bitumen Plant WLB 10 and twin shaft compulsory mixer WLM 30), as shown in Figure 3-5. It is a specially designed machine used to make foamed asphalt samples in the laboratory. It simulates the foaming process carried out in the field and allows for proper foaming of the AC and mixing of the samples according to standard-practice. Before mixing the foamed samples, the AC was heated to a temperature of 160°C to 180°C overnight (at least 10-12 hours) to ensure proper expansion of the AC during the mixing, as the water needs to evaporate instantaneously when it is exposed to the AC. The machine allows the user to input the desired amount of water and AC that is sprayed into the weighed RAP sample. Once mixed, the samples were compacted right away since the CIREAM samples did not required oven drying. In some instances, when a compactor was not available, the samples were immediately transferred into airtight sample bags in order to minimize exposure to air and aging of the binder. The bags were stored in a cool place with temperatures between 20°C to 25°C. Once the samples were compacted, they were allowed to cure for 72 hours in the oven at 40°C.

Figure 3-5: Wirtgen asphalt foam mixer

Figure 3-6 shows the samples compacted using a Pine Superpave gyratory compactor (Model No. AFG2A). Once the samples were cured the air voids in the samples were calculated. For the CIR samples, the Bulk Relative Density (BRD) was determined for all the mixes, either by volumetric measures or by regular water-immersion method performed on compacted briquettes. The Maximum Relative Density (MRD) was calculated for the briquettes as well. These methods of obtaining BRD and MRD were done in accordance with MTO LS-262 (MTO-LS, 1999) and LS-264 (MTO-LS, 2012), respectively. Finally, Using the BRD and MRD values, the air voids for each briquette was calculated using MTO LS-265 (MTO-LS, 1996).

Figure 3-6: Compacted cylindrical samples before coring test samples

All the compactions were carried out using the Pine SuperPave (SPP) gyratory compactor for cylindrical samples. For beam compactions, a Vibco Inc. Asphalt Vibratory Compactor (AVC) was used.

There were three main tests, which required compacted and cured samples. These tests were Dynamic Modulus Testing (a workability and strength test, and a duration test), Fatigue Beam Testing and Thermal Stress Restrained Specimen Testing (TSRST). The Dynamic Modulus test was first completed with different varying percentages of AC in the mixed samples. After analysing the results from the test, the optimum percentage of AC for each RAP was chosen. The Fatigue beam and TSRST were performed using the optimum percentage of AC for each RAP.

3.5 Dynamic Modulus Testing

The dynamic modulus test is a compressive performance test for asphalt specimen used to determine their overall stiffness, including the binder and the aggregates within the mix samples (H. Di Benedetto, 2001). An axial cyclic compressive load is applied to a cylindrical specimen in a stress controlled process. The resulting applied stress and recoverable axial strain responses of the specimen are measured. The dynamic modulus number ($|E^*|$) is the

absolute value of the complex modulus and is calculated by dividing the maximum peak-to-peak stress by the recoverable peak-to-peak axial strain of the specimen subjected to sinusoidal loading. This set of number is a very good indicator of the overall stiffness, rutting resistance and crack development in a mixture (Copeland et al., 2007). It is used to relate stress to strain for linear visco-elastic materials, such as asphalt mixtures. This relationship can be mathematically described by Equation 3-1 (Witczack, 2005).

$$E^* = \frac{\sigma}{\varepsilon} = \frac{\sigma_o e^{i\omega t}}{\varepsilon_o e^{i(\omega t - \phi)}} = \frac{\sigma_o \sin(\omega t)}{\varepsilon_o \sin(\omega t - \phi)} \qquad \text{Equation 3-1}$$

where,

E^* = Complex modulus

σ_o = peak (maximum) stress amplitude, kPa

ε_o = peak (maximum) amplitude of recoverable strain

ϕ = phase angle, degrees

ω = angular load frequency

t = Time of loading, seconds

The testing procedure outlined in AASHTO TP 62-09 (AASHTO, 2009) was used to determine E* modulus. The test used the CPATT MTS-810 test equipment and an MTS-651 environmental chamber. The modulus values are obtained at the specific temperatures and frequencies of loading. Using these values, a master curve is calculated using the AASHTO TP 62-09 procedure (AASHTO, 2009). All test values are reported in Appendix B Dynamic Modulus Results.

Figure 3-7 illustrates a one-dimensional case of a sinusoidal loading applied during the test. The time lag between the stress and strain curves is the phase angle (Witczack, 2005).

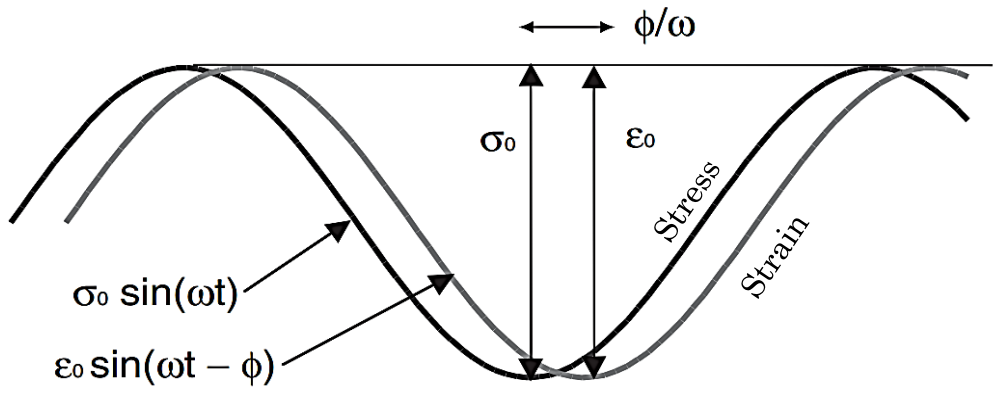

Figure 3-7: Sinusoidal loading during dynamic modulus testing (Witczack, 2005)

The established master curve is, within the pavement industry, an accepted method of evaluating the effect of different temperatures and rate of loading on mixture stiffness (NCHRP, 2011). This master curve is obtained by applying a shift factor to experimental complex modulus (E*) values in order to normalize them to a reference temperature of 21°C (in this case). Shifting of the values is performed using the principal of time-temperature super positioning with respect to time until the curves merge into a simple smooth function (Witczack, 2005).

Asphalt mixtures are sensitive to temperature and loading. Thus, it is possible to capture the impact of such factors with the complex modulus value throughout different seasons. The complex modulus helps model the deterioration of the pavement structure and the dynamic modulus master curve is a critical input for flexible pavement design in the mechanistic-empirical pavement design guide developed in NCHRP Project 1-37A (NCHRP, 2004).

3.5.1 Test Procedure

In this procedure, three replicate specimens for each mixture were tested to get average data. For this test, cylindrical samples are used. The mixed samples are

compacted using a SuperPave gyratory compactor. Figure 3-8 shows the dimensions of these specimens. Each percent AC mixture had three replicate cylindrical specimens measuring 100 mm diameter by 150 mm height. These specimens were cored from the Superpave gyratory compacted specimens (150 mm diameter) as shown in Figure 3-8.

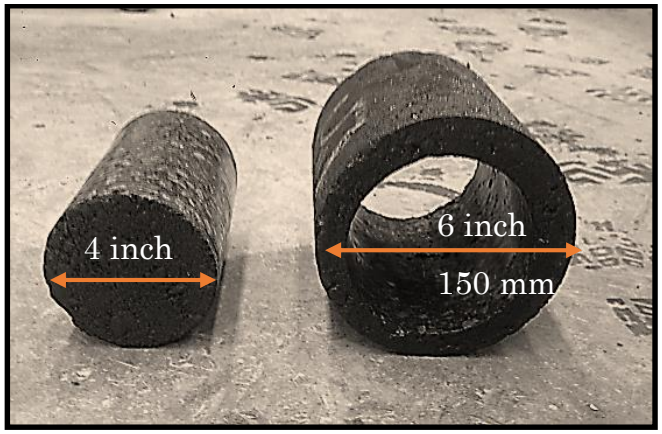

Figure 3-8: A dynamic modulus test specimen cored from a SuperPave specimen

The specimens were tested using the CPATT MTS-810 test frame within an MTS-651 environmental chamber at six different loading frequencies (0.1, 0.5, 1, 5, 10, and 25 Hz) for five different temperatures (-10, 4, 21, 37 and 54°C). For each frequency, specified load cycles (200 cycles for 25 Hz, 200 cycles for 10Hz, 100 cycles for 5 Hz, 20 cycles for 1 Hz, 15 cycles for 0.5 Hz, and 15 cycles for 0.1 Hz) were applied. Refer to Figure 3-9 to see a flow chart of the different cycles, frequencies, temperatures and corresponding loads.

For each temperature, the applied stress and the cross section of the tested samples are kept constant by means of an applied load. An increase in the dynamic modulus value reflects a decrease in the strain corresponding to for a given load, which can also be interpreted as an increase in the stiffness of that mix (El-Hakim, 2013). In contrast, a decrease in the dynamic modulus indicates

an increase in strain and can be interpreted as a decrease in the stiffness of that mix (El-Hakim, 2013).

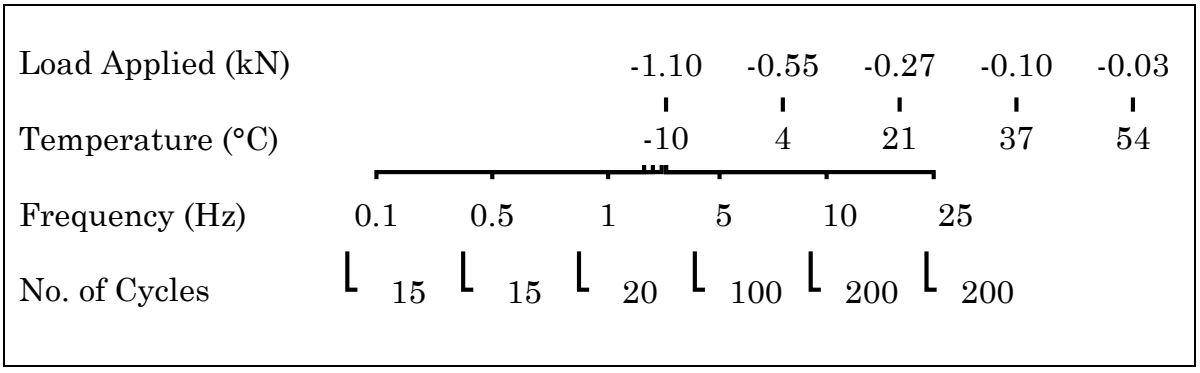

Figure 3-9: Flow chart of the dynamic modulus testing process

The dynamic modulus test was performed by applying a cyclic, sinusoidal axial compressive load to the specimen. The load was applied over the specified range of frequencies and temperatures for their corresponding number of cycles. The resulting recoverable axial strain response was measured using transducers connected to the specimen, and used to calculate the dynamic modulus and the phase angle for each mixture (NCHRP, 2011). Figure 3-10 shows the general setup of the test within the temperature-controlled chamber, with the attached transducers.

Figure 3-10: Dynamic modulus test setup in environmental chamber

3.5.2 Mix Designs

In this study, mixes with five different percentages of AC were tested. The percent AC varied from 1.2% to 3.2% of the mass of the reclaimed aggregate at an increment of 0.5% AC. Three replicate specimen were used for each mix for the dynamic modulus testing to achieve proper averaged results.

Table 3-2 and 3-3 show the different mixes for the CIR and CIREAM samples. In the sample IDs the "S" represents Southern Ontario RAP and the number following it represents the mix number. For example, CIR-S1 is a CIR samples made with Southern RAP and the 1 denotes the first increment of the percentage AC used (i.e., 1.2%). Similarly, an "N" in the sample IDs is later used to denote the use of Northern Ontario RAP in the samples. For the fatigue beam and TSRST tests, a "-F" and a "-T" are added to the sample ID, respectively. For example, the first sample of a fatigue beam test, using 3.2% AC would be CIR-S5-F1 and for TSRST, it would be CIR-S5-T1.

Table 3-2: CIR Sample Mixes

Sample ID	%AC
CIR-S1/N1	1.2%
CIR-S2/N2	1.7%
CIR-S3/N3	2.2%
CIR-S4/N4	2.7%
CIR-S5/N5	3.2%

Table 3-3: CIREAM Sample Mixes

Sample ID	%AC
CIREAM-S1/N1	1.2%
CIREAM-S2/N2	1.7%
CIREAM-S3/N3	2.2%
CIREAM-S4/N4	2.7%
CIREAM-S5/N5	3.2%

3.5.3 Curing Duration Testing

The curing duration test was designed to evaluate the effect of curing time on the sample mix's stiffness. The typical construction standard for CIR prescribes a minimum pavement cure time of 14 days before letting traffic back on that road (Wirtgen, 2004). The surface of the existing pavement is milled and re-paved in one-step. However, during the lab tests, the standard does not require the samples to cure before the mixes are compacted or before beginning the tests. Some inconsistencies in the test results were noticed during the preliminary stage of testing. These discrepancies were caused by inconsistent specimen curing time. The duration test was designed to confirm this hypothesis and determine the optimal curing time for the samples.

For this test, specimens were mixed and compacted on different days in order to vary the curing time. Table 3-4 shows the mixes for the duration testing. The "DT" in the sample IDs represents Duration Test and the "S" represents the use of Southern RAP. The number that follows the "S" is the number of days the mix the allowed to cure before compaction. For example, the sample DT-S2 represents a duration test mix made from southern RAP, which was compacted 2 days after mixing. All mixes were consistent with 1.2%AC. This percentage of AC was chosen as it is the lowest percentage of AC from the strength test and in order to save material. Moreover, the focus of this test was on the duration of curing and, therefore, the percentage of AC needed to be constant. All specimens were mixed on day 0. The first set of samples (DT-S0) was compacted on the same day. The rest of the mix sample was stored in an airtight container to prevent the loss of moisture. The rest of the specimens were compacted on days 2, 7 and 14, respectively; thus allowing for different curing time for the mix, before compaction. The specimens compacted on the initial day, day 0, were cured for 14 days, after compaction, whereas the specimens compacted on day 14 were cured for 7 days. In this manner, the curing time before and after compaction were varied for testing.

Table 3-4: 1.2% AC Sample mixes and corresponding % air voids

Sample ID	Curing time (days)	
	Before Compaction	After Compaction
DT-S0	0	14
DT-S2	2	14
DT-S7	7	7
DT-S14	14	7

The results of the duration test were used to determine the optimal pre- and post-compaction curing times for the specimens for the rest of the testing.

3.6 Fatigue Beam Testing

Fatigue cracking is one of the main damage modes in asphalt pavement. Under repetitive traffic, loading, micro cracks initiate and progress to macro cracks.

A four-point bending (FPB) fatigue beam test is used to estimate the fatigue life of wide asphalt concrete specimens sawed from laboratory or field compacted asphalt concrete and subjected to repeated flexural bending. Figure 3-11 shows the apparatus used in the CPATT laboratory.

In the FPB test setup, four clamps fix the beam specimen in the load frame. This load frame is set up inside a temperature-controlled chamber. The load is applied to the specimen through the inner clamps by means of two actuators. To allow free rotation and horizontal movement (translation) of the specimen at the four supports, a small steel roller is placed in the grooves between the clamp and the frame. The deflection is controlled by a linear variable differential transformer (LVDT) at the center of the beam. The force is measured by a load cell at the bottom. The loading device is capable of applying cyclic loading at a frequency range of 5 to 10 Hz. The desired maximum strain is pre-calculated and used to set the displacement control limits. The deflection at the mid-point (L/2) of the beam specimen is regulated by a closed loop control system (Li, Pronk, Molenaar, Ven, & Wu, 2013).

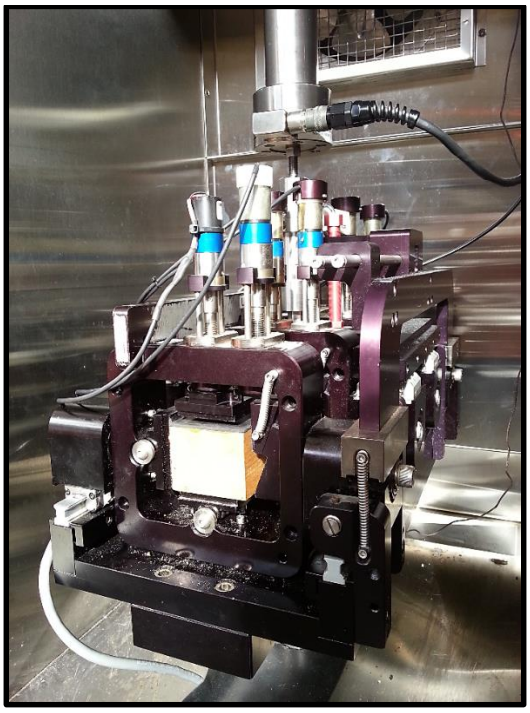

Figure 3-11: Fatigue beam apparatus in an environmental chamber

For this experiment, the asphalt mix samples were compacted using an AVC with an applied vibration force of 115 kPa. Each beam compacted in the AVC could be cut into a maximum of two fatigue beams. Figure 3-12 shows example beams specimens, which were cut and ready for testing. Beams dimensions were 380 mm (14.96 in.) length by 50 mm (1.97 in.) width by 63 mm (2.48 in.) height. The test was performed in accordance to ASTM D7460-10 (ASTM, 2010) and AASHTO T321-07 (AASHTO, 2007).

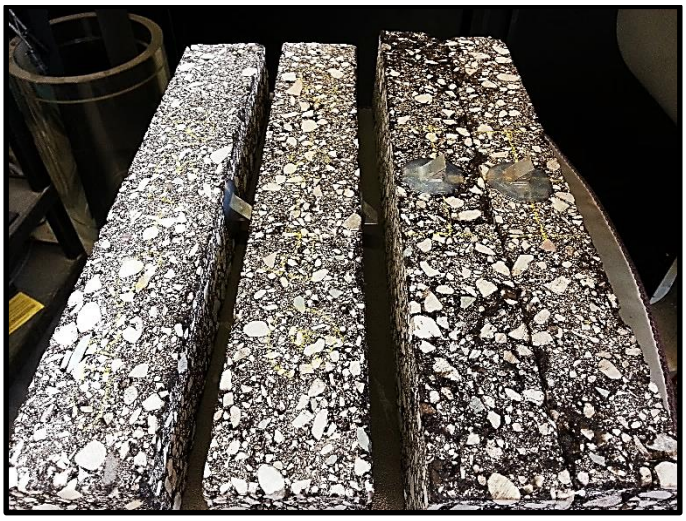

Figure 3-12: Cut out beams for testing purposes

This test is used to estimate the fatigue life of the material under cyclic loading; this simulates traffic loading in the field. The field performance of asphalt concrete is impacted by many factors (traffic variation, speed, climate variation; rest periods between loads; aging; etc.) (Mills, Tighe, Audrey, Smith, & Huen, 2009). One of the most important performance predictor is the strain level at the layer depth induced by the design traffic wheel load. It has been more accurately predicted when laboratory properties are known along with an estimate of the strain level induced at the layer depth by the traffic wheel load traveling over the pavement. Trial tests were carried out, as recommended by standard, to find the desired micro strain for the samples. The strain is back calculated using Equation 3-2 with varying displacements (δ). The displacements were varied between 0.20-0.35.

$$\varepsilon_t = \frac{12h\delta}{3L^2 - 4a^2}$$ Equation 3-2

where,

ε_t = Maximum tensile strain (m/m)

L = Length of beam between outside clamps (0.357m)

h = Height of sample (m)

δ = Maximum deflection at centre of beam (m)

a = Space between inside clamps (0.357/3 = 0.119 m)

The failure cycles were reported for each replicate. Failure is detected when the flexural stiffness of the beam reduces to about 50% of the initial stiffness (defined as the stiffness measured at the 100th load cycle). The number of cycles to failure, sample stiffness and phase angle are reported. A higher number of cycles to failure indicates a more fatigue resistant mix. The data collected during testing is reported in Appendix C.

3.7 Thermal Stress Restrained Specimen Testing

The TSRST is a tension test developed by the Strategic Highway Research Program (SHRP). It is an accelerated performance test to evaluate the low temperature cracking susceptibility of asphalt paving mixtures (Ambaiowei, 2014). This test method determines the tensile strength and fracture temperature of asphalt samples. The test was performed in accordance to AASHTO TP10-93 (AASHTO, 1993) procedure using the CPATT MTS-810 test equipment, which consisted of an MTS-651 environmental chamber, liquid nitrogen tank, temperature cooler and a resistance temperature device.

In Canada, the roadways are subjected to cold temperatures which in turn affect the pavement performance (Mills, Tighe, Audrey, Smith, & Huen, 2009).

TSRST results are crucial because they are used to determine the temperature vs. stress relationship of the asphalt mixtures. Knowing this relationship allows for better pavement design and improved structural analysis. In turn, this reduces thermal cracking on roadways resulting in better pavement performance.

For this test, similar to the fatigue beam testing, the asphalt mix samples are compacted using an AVC with an applied vibration force of 115 kPa and cut into beams of square cross sections. Figure 3-13 shows the cut out beams for the testing. From each of the compacted beams, a maximum of two TSRST test beams could be cut. The specimen dimensions were 50 mm width by 50 mm height by 250 mm length.

Figure 3-13: Mix sample beams cut out for testing

Figure 3-14 shows the testing apparatus with a specimen installed within the environmental chamber

Loctite E20 NS hysol epoxy adhesive was used to bond the top and bottom ends of the specimens to the surface of two cylindrical aluminum platens. The epoxy is allowed to cure for a minimum of 12 – 16 hours prior to conditioning the test specimen in the test chamber at 5°C for six hours.

The environmental chamber is a closed loop system, which is capable of cooling an asphalt sample at a constant rate of 10°C/ hour starting at 5°C. The cooling process is performed by vaporizing compressed liquid nitrogen into the environmental chamber through a solenoid valve. The cool air is circulated with a fan so air is evenly distributed. A temperature sensor monitors the temperature in the environmental chamber and maintains specified temperatures. As the temperature drops, the specimen tends to shrink due to its viscoelastic behaviour. Extensometers are attached to the specimen and monitor shrinkage. A hydraulic actuator counteract the shrinkage and maintains the specimen at its original length by applying a tension force. The temperature of the specimen is gradually decreased which leads to an increase in thermal stresses in the specimen and eventual fracture of the specimen. The maximum stress and temperature at failure are recorded. The collected results are reported in Appendix D.

Figure 3-14: TSRST apparatus in an environmental chamber

3.8 Analysis of Experimental Results

For assessing the test results obtained from the laboratory testing, a statistical analysis was done on the dynamic modulus results. This was carried out to compare the different samples with varying the percentage of AC and eventually determine the optimum percentage of AC to be used for the fatigue beam test and TSRST. The statistical analysis was performed in two steps: The first step involved an Analysis of Variance (ANOVA) of the dynamic modulus master curve dataset of all the mixes and the second step was a pairwise t-test. All calculations and results are shown in Appendix E.

ANOVA is a statistical test used for measuring the relative difference between means of different samples (Statistics Solution, 2013). A single factor e ANOVA was carried out with the data of all samples with varying percentage of AC. The data was sectioned into five different regions based on the range of frequencies to determine if any of the regions had statistically significant difference between the samples.

The t-test was used to determine which specific sample had statistically significant differences from the other samples within the region of significant difference determined by the ANOVA. An independent two-sample, two-tailed t-test was performed with a null hypothesis that the means were equal and an alternate hypothesis that the means were not equal in order to examine whether the alternative mix mean (μ_1) was equal to the control mix mean (μ_o). If $t_{calculated} > t_{critical}$, the null hypothesis was rejected concluding that there was difference in those samples; whereas if $t_{calcualted} < t_{critical}$, there is a failure to reject the null hypothesis. This indicates that there was no statistically significant difference between the two samples (Ambaiowei, 2014) (Statistics Solution, 2013).

Once the regions with statistically significant differences within the master curves were clear, the points on the curve within that region were compared. The

optimum mix was chosen based on its dynamic modulus values in correspondence with the frequency of testing. The optimum mix was then used to carry out the remainder of the tests. A 95% confidence level was used when performing these tests, which was chosen based on the minimum sample size requirement for a two-sided t-test (U.S. Department of Commerce, 2013).

3.9 Field Evaluation

For the long-term field evaluation, several municipalities were contacted within Ontario to collect information regarding sections, which have used CIR and CIREAM as a rehabilitation technique on roadways in their region. The MTO was also contacted in order to get information regarding CIR and CIREAM usage across Ontario.

Figure 3-15 shows a map of Ontario and its different regions as defined by the MTO.

Information regarding Pavement Condition Index (PCI) and any other performance evaluations of CIR or CIREAM sections were collected from the participating municipalities and the MTO. The information collected is shown in Appendix F.

Using the available information, sections of roadways were chosen for a field study. Most of the sections chosen for evaluation were within the Region of Waterloo.

A visual field inspection was carried out in order to determine the current pavement condition. Detailed photographs from the inspection can be found in Appendix G.

Road sections were classified and evaluated based on the available traffic data on each section, the type of rehabilitation and the current condition of the pavement.

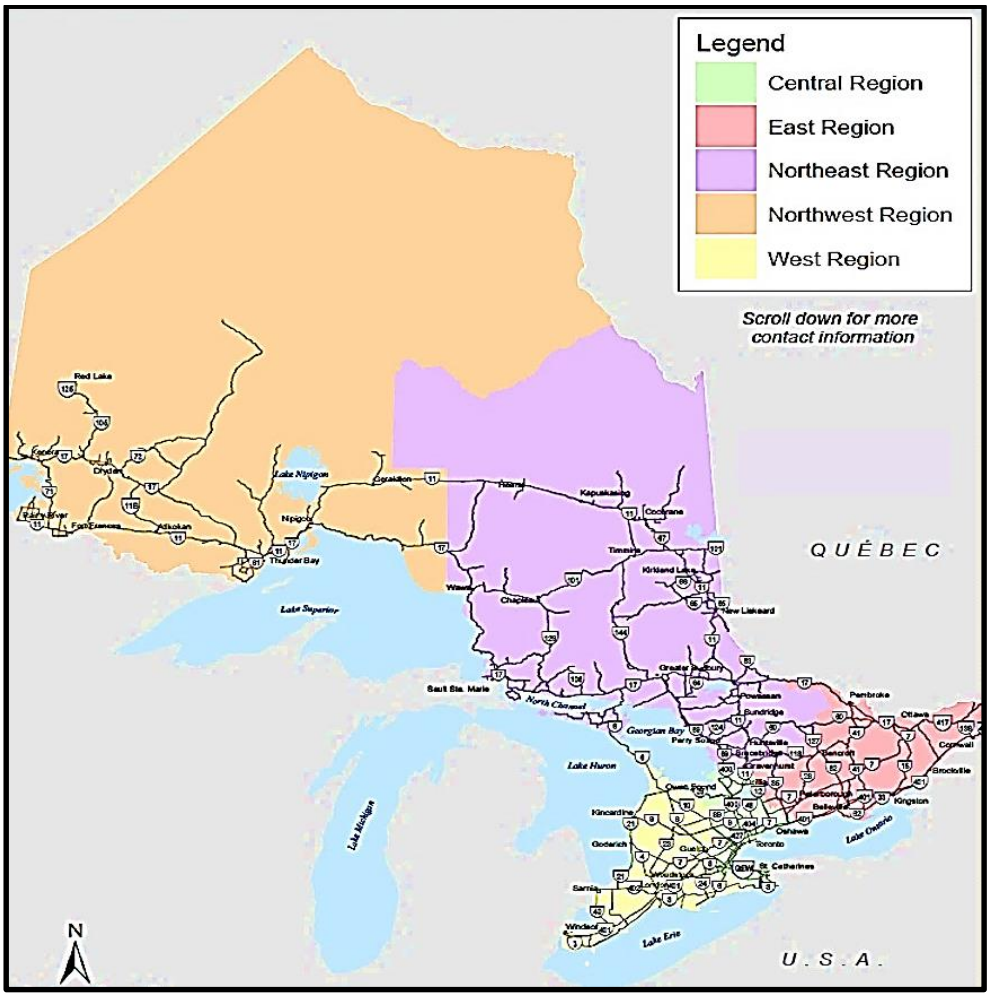

Figure 3-15: Map of Ontario and its different regions classified by MTO

3.10 Summary

The main objective of this study was to gather information and compare the performance of CIR with CIREAM. In order to do this, a set of tasks were defined. These tasks focused on the three different types of lab testing to be carried out on laboratory mixed samples of CIR and CIREAM. The results from the dynamic modulus testing helped determine the optimum percentage of AC

for each type of RAP used and use that optimum percentage of AC for the rest of the testing. The optimum percentage of AC was chosen based on statistical analysis. The next task was focused on the field study. These tasks were used to make conclusions regarding the performance and comparison of CIR with CIREAM.

CHAPTER 4
PERFORMANCE TESTING RESULTS ANALYSIS AND DISCUSSIONS

4.1 Introduction

This chapter presents the experimental test results. It shows the analysis, discusses the results and provides conclusions drawn for the CIR and CIREAM materials used. Finally, it discusses the constraints faced during the testing process.

4.2 Dynamic Modulus Master Curve Development

This section presents the results of the dynamic modulus testing. The first batch of samples was made using the southern RAP material. The duration test samples were first mixed, compacted, cored and cut out, as shown in Figure 4-1. Once these samples were cored, the air voids were calculated by testing the samples to obtain their MRD and BRD values. All the values calculated for MRD and BRD are reported in Appendix A. Table 4-1 shows the average air voids for all the sample mix types. On average the air voids were between 6%-7%. The overall intent of the test was to pick a curing duration for the rest of the experimental programme.

Figure 4-1: Cored samples for dynamic modulus testing

Table 4-1: Average air voids for the sample mixes

Sample Types	%Avg. Air Voids
DT-S	6.21
CIR-S	6.03
CIR-S-F	5.94
CIR-S-T	6.87
CIREAM-S	6.89
CIR-N	6.58

Once the duration test was carried out, all the CIR samples were cured for the optimum time, which was determined using the master curves. The data from the dynamic modulus test were used to develop master curves using Microsoft Excel. All the results and plots for specific temperatures and frequencies are reported in Appendix B. The master curves were evaluated as shown in Appendix E. The regions of the graph that contained statistically significant difference between the curves were further analyzed with a t-test. The t-test helped differentiate the sample mixes which were significantly different from other mixes within that region. Samples with no significant

difference we assumed to be performing similarly within the region. Using that information, the best performing mix and asphalt cement content were chosen for fatigue beam and TSRST testing.

The first CIR test batch was made with five different percentage of AC varying from 1.2 to 3.2 percent AC. The next CIREAM test batch was done using four mixes; the number of mixes was further reduced to three mixes for the CIR samples using Northern RAP. This was necessary due to time and material constraints. The eliminated choices of mixes were determined after examining the results of the first batch where all five were tested. These mixes were eliminated based on their stiffness, workability and rutting resistance. Mixes were very weak and had poor workability were eliminated, as they would realistically not be used in the field.

4.2.1 Evaluation of Rutting and Fatigue Factors From E* Tests

The master curves show the performance with respect to sample stiffness of each mix over a range of frequencies. The tests used to create the master curve were performed in temperatures ranging from -10 to 54°C. The curves are then normalized to 21°C to better compare the results. The overall stiffness of viscoelastic materials does not always have to be high for it to provide good performance (Bahia, Zhai, Bonnetti, & Kose, 1998). At low frequencies and high temperatures, the stiffer the material, the better its rutting resistance. This is because, when there are slow moving vehicles at low frequency (for example: at an intersection), the pavement undergoes the loading at a slower rate and is susceptible to rutting and distortion (Bahia, Zhai, Bonnetti, & Kose, 1998). The stiffer the mix, the better it would be able to withstand loading applied at a slower rate. For higher frequencies, the mix is expected to behave in the opposite manner. At high frequencies (for example: on a highway with greater vehicle speeds), the mix should be more flexible (Bahia, Zhai, Bonnetti, & Kose, 1998).

If the pavement is too stiff at higher frequencies, it is more likely to fail in fatigue in the field as it would not be able to absorb the load as well. Fatigue cracking are prevalent on such pavements (Ambaiowei, 2014). Thus, when analysing the curves, the high and low frequency zones are crucial to determine the overall performance of the mix against rutting and fatigue cracking.

4.2.2 Dynamic Modulus Results

The average dynamic modulus of all replicates was calculated for each temperature and frequency. The data was then normalized to 21°C by using Microsoft Excel's solver function and used to graph the master curves. The master curves are shown in Figures 4-2 to 4-5. All the values obtained for the master curves and the plots for all the temperatures are reported in Appendix B. These master curves were used for the statistical study and determine the overall best performing mixes from each set.

The statistical analysis of the points on the master curves, as shown in Figure 4-2, show that the sample DT-S0 was significantly different from the other mixes for the low frequency (10^{-7} Hz to 10^{-4} Hz) and high frequency (10^{5} Hz to 10^{8} Hz) regions. In the low frequency region, DT-S0 has the highest stiffness in comparison to the other mixes and thus has an overall better predicted performance against rutting. For the high frequency region, DT-S7 and DT-S14 have a slightly better fatigue resistance performance. In the other frequency regions, there were no statistically significant differences between the mixes. DT-S0 was chosen as the better performing mix because the difference in rutting resistance performance of DT-S0 relative to other mixes is more significant than the difference in fatigue resistance performance of DT-S7 and DT-S14 relative to other mixes. As a result, for the remainder of the CIR testing, all samples were allowed to be cured for 14 days after compaction. When the mix was not allowed to cure before the compaction, it provided optimistic low frequency performance.

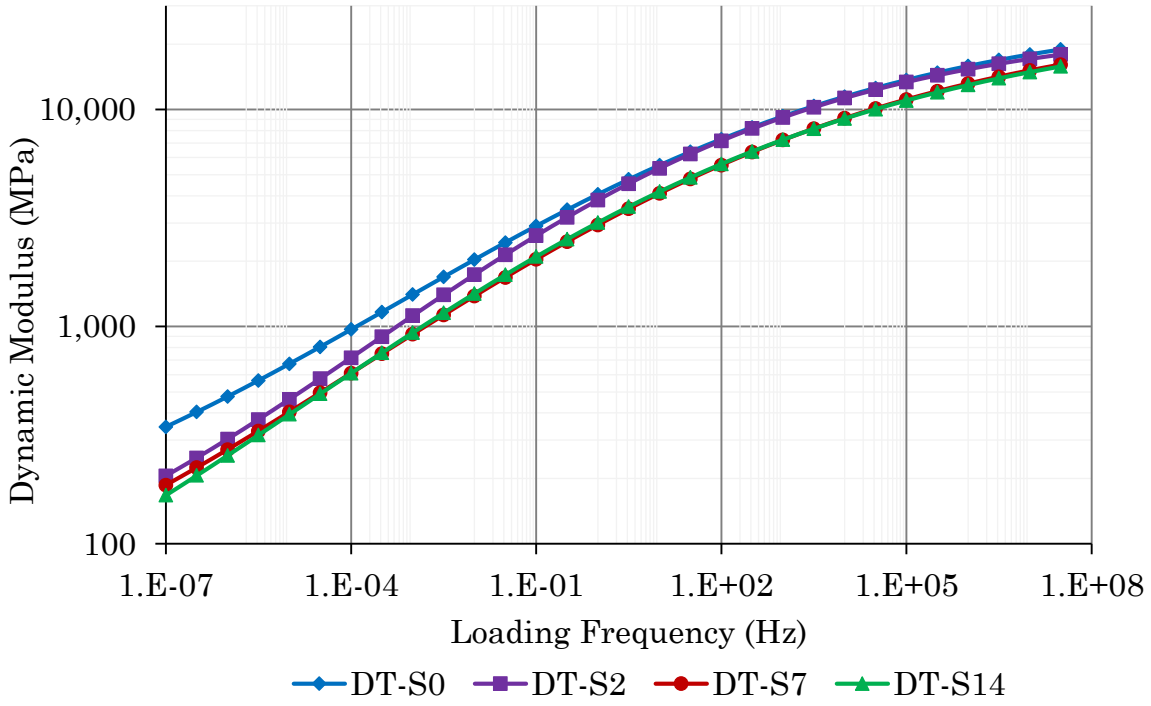

Figure 4-2: Dynamic modulus master curve - duration testing

The master curves developed for southern RAP CIR shown in Figure 4-3, show that there were statistically significant differences between some of the samples in the low frequency region (10^{-7} Hz to 10^{-4} Hz). Appendix D shows the ANOVA for all the regions and it can be seen that the low frequency region has statistically significant differences between the points. In this region, CIR-S5 has a much higher dynamic modulus compared to the other mixes. Thus, a higher percentage of AC helped improve the rutting resistance and overall performance of the mix. Moreover, it was observed that CIR-S1 (with 1.2% AC) showed poor performance against rutting and fatigue performance, and had a low dynamic modulus in the low frequencies. This is due to the fact that CIR-S1 had the lowest amount of emulsion in comparison to the other mixes, which led to a poor bonding of the aggregates within the samples and higher percentage of water used.

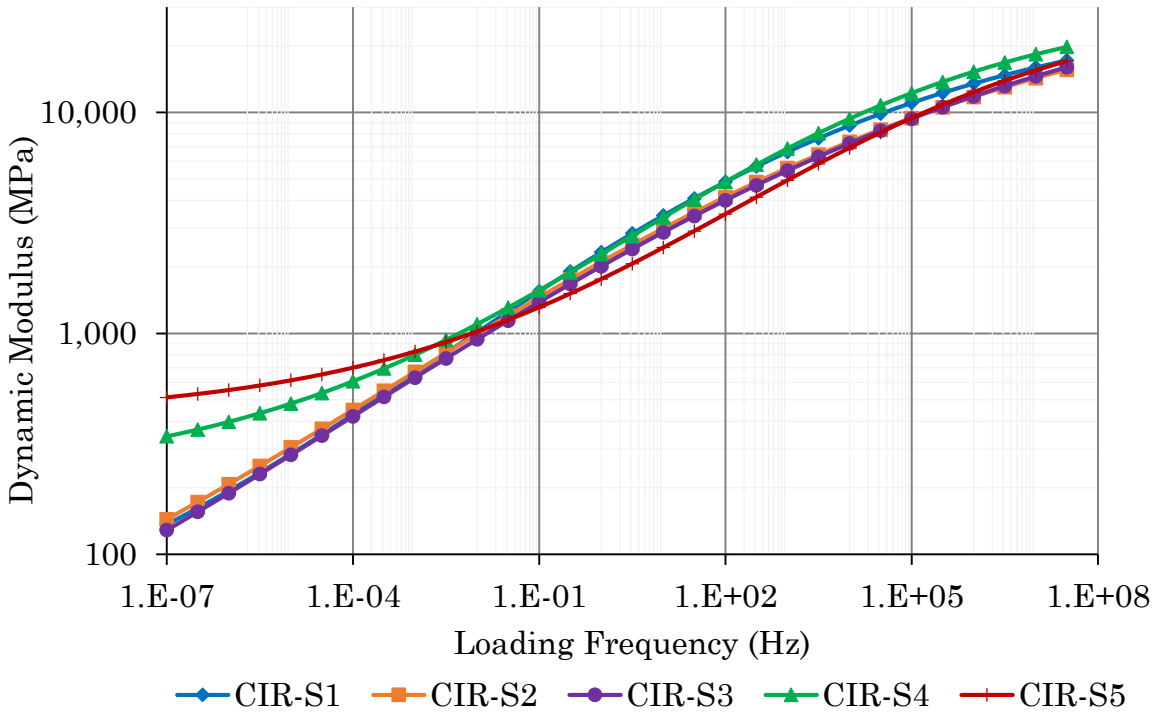

Figure 4-3: Dynamic modulus master curve – CIR-S samples

For the CIREAM samples using southern RAP, the 1.2% AC increment was eliminated because it was considered too low for the mixes and to save material. The test was carried out for 1.7%, 2.2%, 2.7% and 3.2% AC, respectively. The master curves for these mixes, shown in Figure 4-4, and the ANOVA carried out in Appendix D show that there were significant differences between the samples in the low frequency regions (10^{-7} Hz to 10^{-4} Hz) and the high frequency regions (10^{2} Hz to 10^{8} Hz). In the low frequency region, CIREAM-S5 with the highest percentage of AC was performing well with a much higher modulus value. In the high frequency region, CIREAM-S5 had a lower dynamic modulus, which helps against fatigue cracking. Thus, it had an overall better performance when compared to the other mixes.

The overall performance of CIREAM-S compared to CIR-S samples was better due to higher dynamic moduli at low frequencies and lower moduli at high frequencies. However, most of the CIREAM samples were not tested for

temperatures higher than 21°C due to the soft nature of the mixes. A lot of the samples were damaged or broke during the testing procedure at higher temperatures. The samples also sometimes broke easily during the cutting and coring process at higher temperatures.

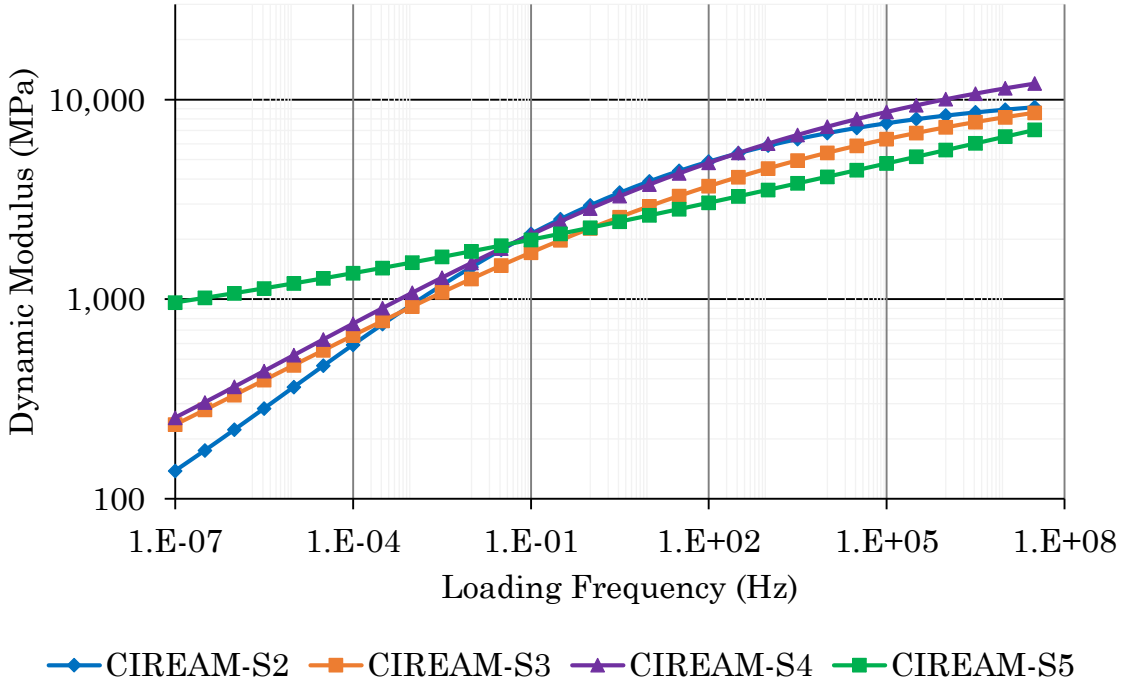

Figure 4-4: Dynamic modulus master curve – CIREAM-S samples

The CIR sample mixes using northern RAP was reduced to just three mixes: 2.2%, 2.7% and 3.2% AC. This was completed because, in the CIR samples using southern RAP, there were no statistical differences between the first two increments of percent AC and they performed poorly in comparison to the other mixes with higher percent AC. For the master curves developed for the CIR-N samples, the statistical study showed that there were no significant differences between any of the mixes as shown in Appendix D. Thus, they could all be considered to be performing similarly. The master curves are illustrated in Figure 4-5.

Overall, in comparison to the CIR-S and CIREAM-S samples, CIR-N samples had lower dynamic moduli at low frequencies and similar moduli at high frequencies. Thus, they had lower rutting resistance in comparison to mix samples using the southern RAP. A four point beam bending test was carried out later on in the project in order to better determine the performance of the mixes against fatigue cracking.

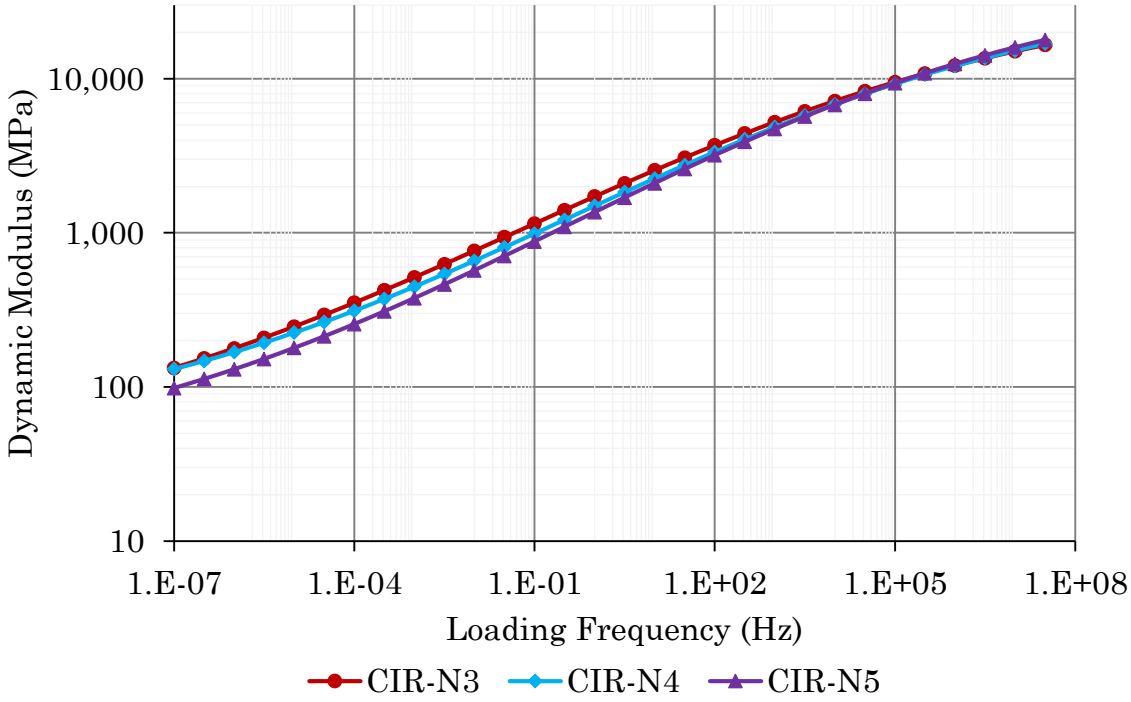

Figure 4-5: Dynamic modulus master curve – CIR-N samples

4.3 Fatigue Performance

For the fatigue beam testing, the CIR-S5 and CIREAM-S5 samples were chosen for comparison because of their overall better performance during the dynamic modulus testing. Four replicates of each of these samples were used to get average values. The beams were also cured for 14 days before testing following the conclusion from the duration test.

The air voids of all the beams were calculated and reported in Appendix A. Trial tests were carried out to find the desired micro strain for the samples. The results of the tests showed that a micro strain of 450 (0.25 to 0.27m deflection) was an ideal strain level for the CIR samples. Similarly, a micro strain level of 370 (0.20 deflection) was chosen for the CIREAM samples. At these strain levels the trial specimens underwent a minimum of 10,000 load cycles prior to failure. A minimum of 10,000 failure cycles as stated in ASTM D7460-10 ensured that the specimens did not decrease in stiffness too rapidly. The strain levels were varied from 370 to 680 for all the trial specimens (ASTM, 2010).

The beams were then tested until failure and the load cycles until failure were reported in Appendix C. Failure in this case occurs at the maximum or peak value of normalized modulus×cycles when plotted versus number of cycles. This peak determines the peak cycles to failure (ASTM, 2010). The summary of the load cycles are illustrated in Figure 4-6. The summary shows that the load cycles for both CIR and CIREAM samples failed at around the same number of load cycles with mean no. of cycles of 19013 and 19513, respectively. They had similar fatigue behaviour. Statistical variances were calculated as stated in ASTM D7460-10 (ASTM, 2010). The calculated covariance values were less than 0.5 for both sets of samples. All the results were within the allowable variances as stated in the standard and, thus, valid.

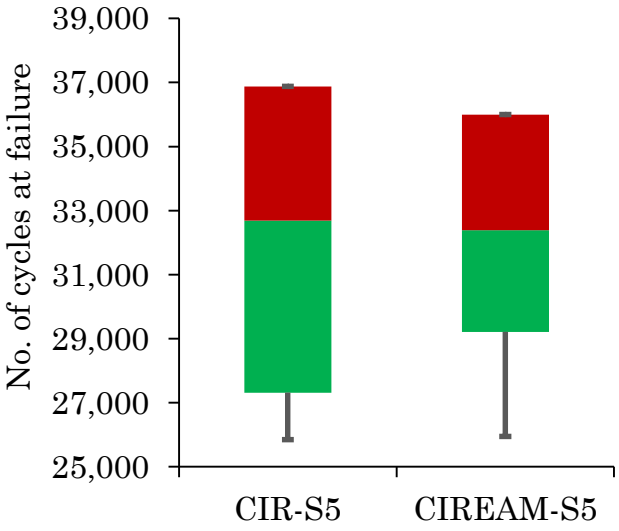

Figure 4-6: Cycles to failure for fatigue testing

4.4 Thermal crack characterization of evaluated samples

The TSRST tests used four beam replicates for CIR-S5 and CIREAM-S5 samples. Similar to the fatigue beam testing, these mixes were chosen based on their performance during the dynamic modulus testing. The beams were cured for 14 days before testing and air voids are reported in Appendix A. The peak load at failure and failure temperature are reported in Appendix D. Using the peak load the tensile stress on each specimen at failure was calculated by dividing the failure load by the cross sectional area of each sample.

The summary of the tensile stress at failure and temperatures at failure are plotted in Figure 4-7and 4-8.

The temperature at failure for both samples was on average -28°C and - 27°C for CIR and CIREAM, respectively. The PGAC used for both emulsion and foamed asphalt was PG 58-28. Thus, the failure temperatures were expected to be around -28°C. For peak loading, the CIR samples had much higher tensile stress at failure (mean value of 2.24 MPa) in comparison to the CIREAM samples

(mean value of 0.54 MPa). Since the cross section area on each specimen was kept constant, it means that the test apparatus had to apply a higher load on the CIR samples to maintain a state of zero strain. Thus, the CIR samples shrank at a higher rate in comparison to the CIREAM samples as the temperature decreased within the chamber.

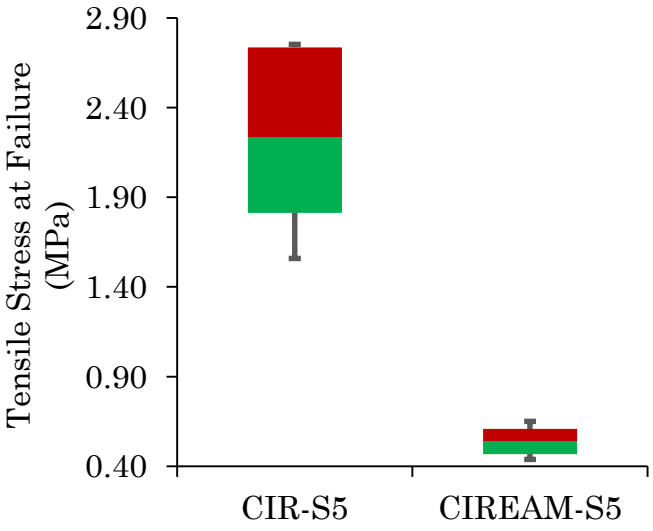

Figure 4-7: Tensile stress at failure for CIR and CIREAM samples

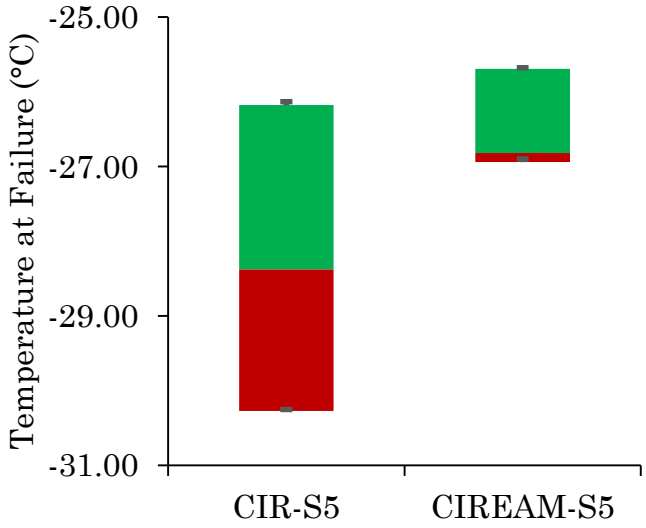

Figure 4-8: Temperature recorded at failure of CIR and CIREAM samples

4.5 Comparison of Materials

The different materials used had a large impact on all of the test results. The constituents of the RAP played a big factor in how the samples performed. Moreover, the use of emulsified AC and expanded AC also affected their behaviour.

Southern RAP had a coarser gradation in comparison to the northern RAP. The northern RAP had a larger percentage of sand and smaller material in comparison to the southern RAP. This resulted in a larger absorption of the AC when the mixes were made. The CIR-N samples were looser due to the higher percentage of fines in the gradation. As a result, the dynamic modulus values were much lower in comparison to CIR-S and CIREAM-S.

For CIREAM-S samples, the expanded asphalt had a lower viscosity in comparison to the emulsified asphalt used in CIR-S/N and thus was able to mix easier with the aggregates. However, the lack of viscosity affected the bond between the aggregates and thus the samples were looser. A large number of CIREAM-S samples were moisture susceptible and failed during the coring and cutting process when making test samples. As a result, the samples had either cracks or were broken completely and could not be tested further. There were differences in shrinkage behaviour between emulsified asphalt and foamed asphalt during TSRST.

4.6 Summary

Dynamic modulus tests were carried out using the southern and northern RAP material for CIR and CIREAM. The duration test helped conclude that curing the samples for 14 days after compaction improved sample stiffness for the low frequencies of the testing. CIR testing using southern RAP shows that used 3.2% AC within the mix gave an overall better performance in comparison to the other

mixes. Similarly, using 3.2% AC for the CIREAM samples also showed improved performance. CIR-N samples all performed similarly.

CIR and CIREAM samples using 3.2% AC had similar performances against fatigue cracking under fatigue beam testing and the failure temperatures for both samples were similar for the TSRST testing. However, the tensile stresses on the CIR samples were much higher in comparison to CIREAM samples.

The properties of the RAP and the usage of emulsion and foamed asphalt were the primary reasons for the differences in performance.

CHAPTER 5
FIELD PERFORMANCE EVALUATION AND DISCUSSIONS

5.1 Introduction

This chapter presents the results from the field evaluations. It also discusses the data received from different municipalities and draws conclusions on the field performance of CIR and CIREAM. The field evaluations are empirical and based solely on observation.

5.2 Road Sections Data

For the field evaluation, nine municipalities in the province of Ontario were contacted in order to gather current information on their CIR and CIREAM road sections. These municipalities were asked to highlight road sections and road limits where CIR and CIREAM were implemented in the past 10 to15 years. Information on the pavement types, the traffic count and the current pavement condition were requested. MTO was also contacted in order to provide similar information on any road sections that implemented CIR and CIREAM within Ontario.

The information was received mainly from municipalities from the Southern parts of Ontario. MTO also provided information on road sections in Ontario. Some of the information provided by the municipalities that responded

to the survey was incomplete with respect to the pavement condition of the sections. Since there was limited information, the road sections needed to be inspected to get a better idea of the pavement performance. Municipalities provided information on about 300 sections. Due to time constraints, road sections in local municipalities were inspected; specifically the Region of Waterloo, Perth County, and United Counties of Stormont, Dundas and Glengarry (SDG). Around 200 road sections were inspected in these municipalities. The MTO data was used as is since they provided a PCI value for the road sections that were provided. All the relevant data collected is reported in Appendix F.

5.3 Field Performance Results

The physical condition of each road section was evaluated. This physical condition evaluated the amount of deterioration present on the pavement, the severity of the deterioration and other road features such as: proper drainage, car traffic, truck traffic, geometry and speed limits, surface type, surface width, and structural adequacy. Table 5-1 shows the classification of the physical condition and how the road sections could be rated anywhere between poor to excellent condition.

Table 5-1: Physical condition value classification (Anderson, 2013)

Physical Condition	0-30	30-55	55-70	70-100
	Poor	Fair	Good	Good to Excellent

WorkTech—an asset management software—was used to maintain consistency in the rating. WorkTech has an asset manager tool that helps track user-defined road attributes and helps complete asset condition inspections

using condition rating formats and calculation methodologies that are used in the industry, such as PCI (MTO, 1991). Using one tool to calculate all the physical condition values helped with the precision and consistency of the results.

For a given road section, the field location of the section was first input into the WorkTech database. Then, the road conditions and the attributes were input. Each attribute had a scale of rating within the software. Finally, WorkTech calculated the overall physical condition which was rated on a scale of 0 to 100, 0 being a completely broken pavement and 100 being a really well performing pavement The overall road condition (the type and severity of deteriorations) and road attributes were input into the database for that given road section into WorkTech. The overall physical condition was then calculated based on the MTO inventory manual rating methodology (MTO, 2009). This type of review identifies the condition of each road asset by its time of need for rehabilitation or maintenance and helps recommend a rehabilitation strategy. However, further detailed review, investigation and design for each section is necessary to address the specific requirements for that road section.

Figure 5-1 illustrates the physical condition of all CIR road sections, which were inspected within the three municipalities, mentioned earlier. Each data point represents a unique road section in the three municipalities. Most of the road sections had an AADT below 10,000 vehicles. Similarly, Figure 5-2 illustrates all the CIREAM road sections inspected. For both CIR and CIREAM, there was a broad range of physical condition for each section, which made it difficult to evaluate the sections based on the traffic counts. CIR and CIREAM both seemed to perform similarly regardless of their AADT.

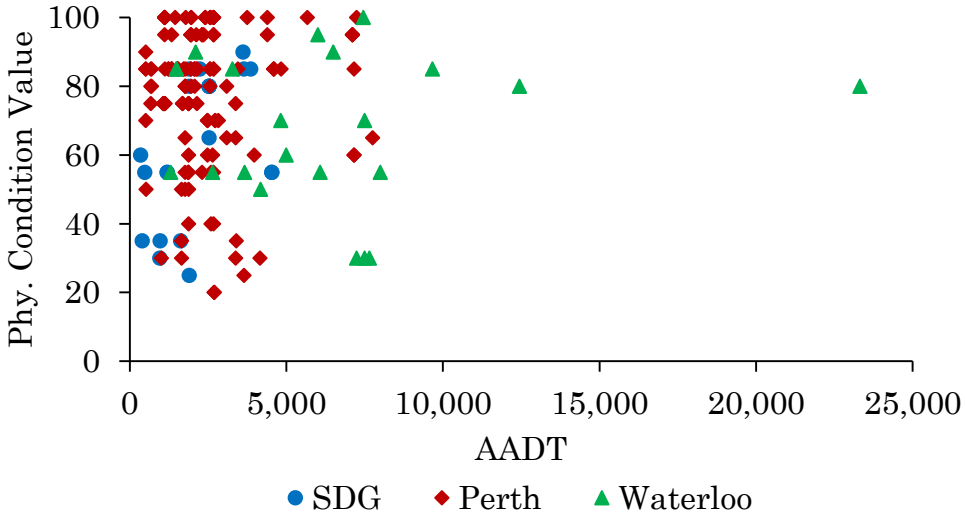

Figure 5-1: Condition of CIR road sections

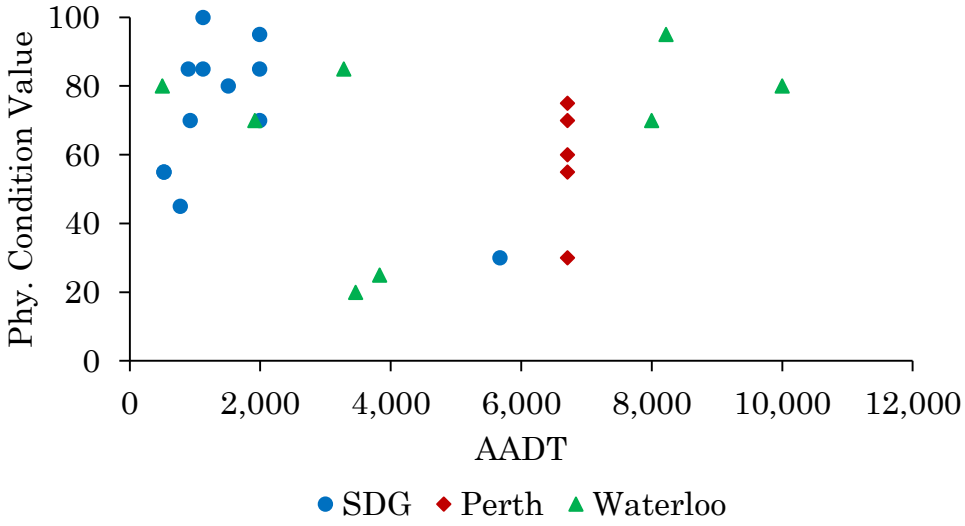

Figure 5-2: Condition of CIREAM road sections

The generalized relationship between the serviceability and the age or the loading on a pavement is a non-linear negative correlation, which means that with increase in age or loading, the serviceability lowers (assuming no maintenance or rehabilitation is carried out) (Witzcak & Yoder, 1975). The serviceability of a pavement is directly proportional to the physical condition value of a pavement as it reflects on the overall condition of the pavement over

a given period of time (Witzcak & Yoder, 1975). Although, the relationship between the PCI or physical condition and the age of a road section is expected to be non-linear, a linear regression analysis was carried out for the collected data, to see the overall effect of the age and the loading on the pavement condition. This was also done because of the comparison between more than one road sections. The regression analysis for all the plots in this chapter is shown in Appendix H.

The age of the road sections which were inspected ranged from one year to 23 years. In order to further evaluate the field performance of these sections, the physical condition values were plotted against the age of the pavement in Figure 5-3 and 5-4.

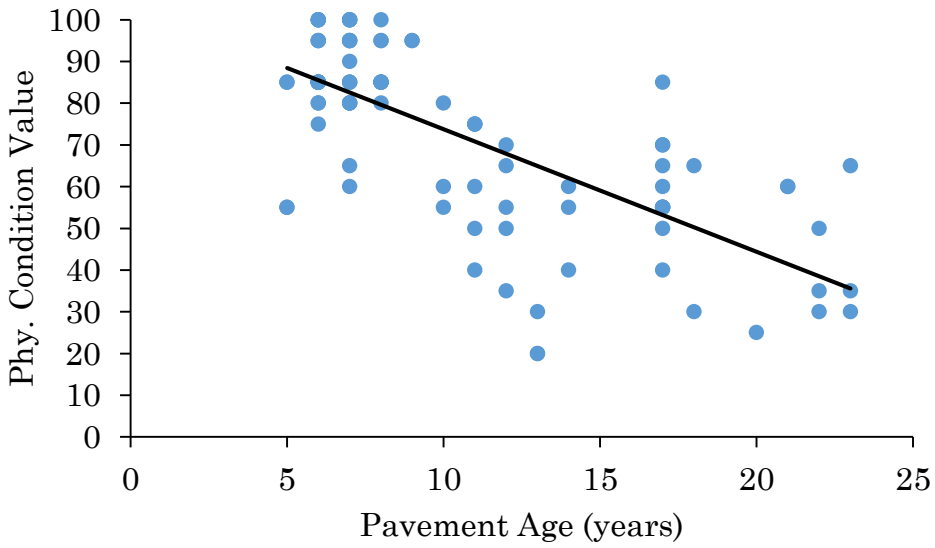

Figure 5-3: Age of pavement vs. physical condition of CIR sections

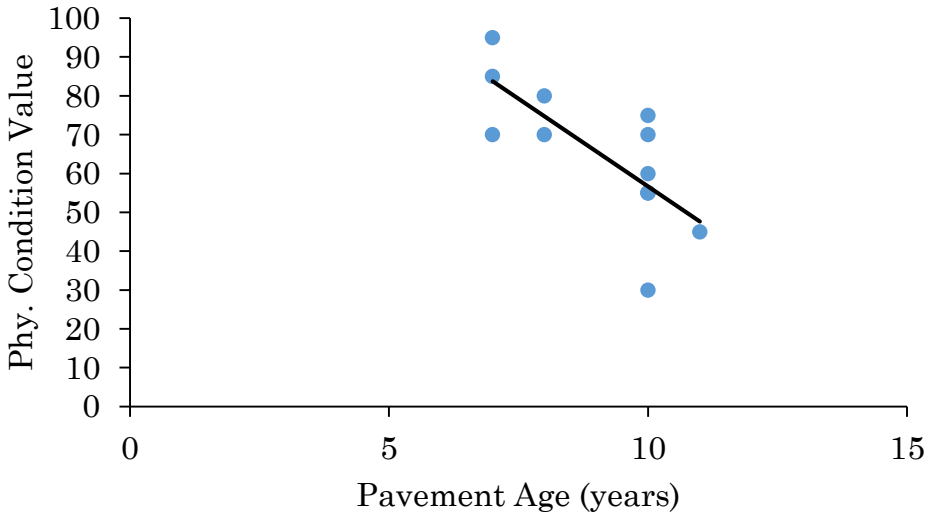

Figure 5-4: Age of pavement vs. physical condition of CIREAM sections

Figure 5-3 and 5-4 showed an overall negative trend for all the sections. The R^2 values for the CIR and CIREAM sections were 0.505 and 0.047, and the p-values were 0.0001 and 0.40, respectively. The p-values for the CIREAM regression suggested an insignificant correlation between the age and the physical condition of the road sections. The age for CIR showed a significant effect on the physical condition of the road sections because of the low p-value. (Frost, 2014)

The physical condition of the inspected road sections was also plotted against the available Average Annual Daily Truck Traffic (AADTT) data for the city of Waterloo in Figure 5-5 and 5-6. These plots were also assessed using linear regression to evaluate an overall effect The R^2 values for the CIR and CIREAM sections were 0.0001 and 0.216, and the p-values were 0.97 and 0.54 respectively. The AADTT showed an insignificant effect on the physical condition of the inspected sections. This maybe the case because the pavement and the road section attributes were not designed to withstand the expected traffic loading. Thus, neither of these attributes affected the pavement, individually.

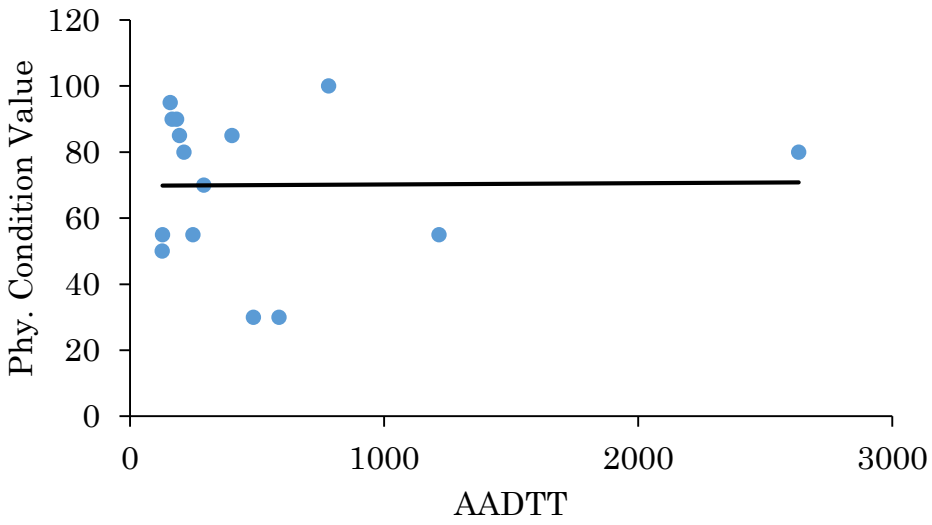

Figure 5-5: Truck traffic vs. physical condition of CIR sections in Waterloo

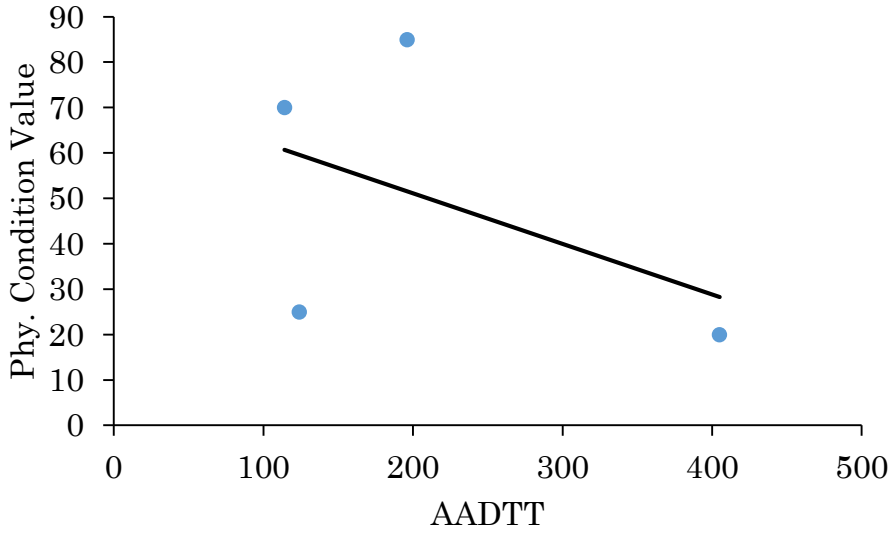

Figure 5-6: Truck traffic vs. physical condition of CIREAM sections in Waterloo

When inspecting the road sections, it was observed that several variables such as: road geometry, structural adequacy and proper drainage could affect the overall pavement performance. Several road sections had severe alligator cracking and potholing occurring when there was poor drainage or no drainage available. Because of poor drainage, there is a buildup of water due to rainfall

and, freezing and thawing due to cold climates within the pavement (Mills, Tighe, Audrey, Smith, & Huen, 2009). This build up can cause stripping and loss of aggregates (Kandhal, 1992). Detailed photographs of the different kinds of deteriorations observed are shown in Appendix G. In addition, they also show cases with a lot of ravelling and aggregate loss. These were mainly observed where there was slow moving traffic or poor to no drainage available.

5.3.1 Performance of MTO Sections

As part of the data collection process, MTO provided information on current road sections in Ontario, which have used CIR and CIREAM as a rehabilitation technique. These road sections already had physical condition inspection data. However, MTO does not use WorkTech to rate their pavement. Thus, their rating was based on a different rating scale using PCI values from zero to 100. They also provided rut depth values for the road sections.

The trend in PCI values compared to the AADT on road sections was examined.

Table 5-2: PCI value classification (ASTM, 2011)

PCI Value	0-10	11-25	26-40	41-55	56-70	71-85	86-100
	Failed	Serious	Very Poor	Poor	Fair	Satisfactory	Good

Figure 5-7 and 5-8 show plots of PCI values with respect to the changing AADT of the road sections. These road sections were rehabilitated between 2003 and 2011 and the PCI values were collected in 2013 by MTO. The placed sections went to a maximum AADT of 35,800. The techniques were usually placed in low volume roadways, rural arterial or rural collectors.

According to the classification of PCI given in Table 5-2, it can be seen that all the sections were performing at least satisfactorily since most of the PCI values are higher than 71, regardless of their age (ASTM, 2011). Linear regression shown in Appendix H, showed the R^2 values for the CIR and CIREAM sections were 0.041 and 0.0001, and p-values were 0.42 and 0.91, respectively. Thus, regardless of an overall adequate PCI values, the correlation between the AADT and the PCI values was insignificant.

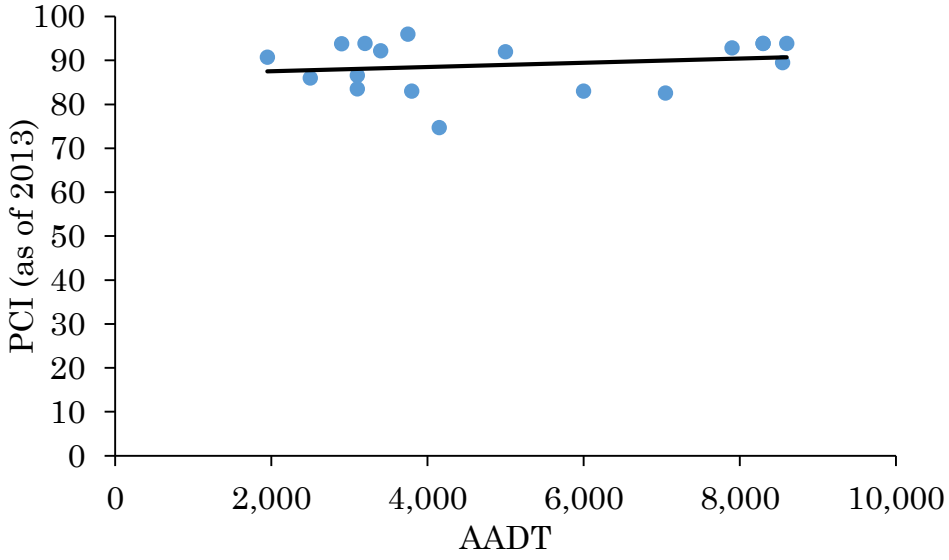

Figure 5-7: PCI values of road sections that implemented CIR

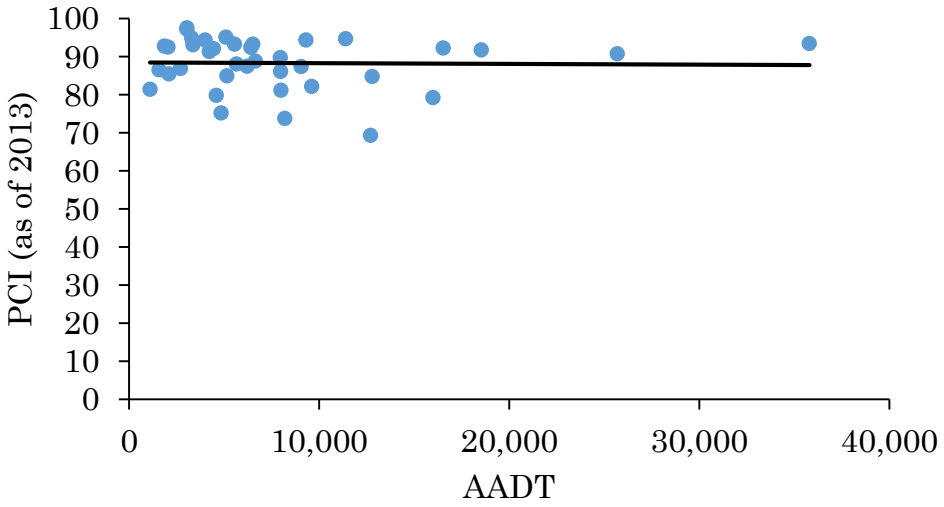

Figure 5-8: PCI values of road sections that implemented CIREAM

To further evaluate the field performance of these sections, the reported rut depth values were also plotted against the AADTT in Figure 5-9 and 5-10. The R^2 values for CIR and CIREAM sections were 0.030 and 0.060 and the p-values were 0.49 and 0.14, respectively. The prediction interval for CIREAM was lower than CIR and thus, showed a better correlation between the rut depth values and the AADTT. However, since both have a low R^2 value and a low p-value, it showed an insignificant correlation. As a result, the AADTT showed no significant impact on the average rut depth values of these road sections.

In contradiction to what the plots (Figure 5-9 and 5-10) illustrate, field inspections in the municipalities showed greater deterioration where high truck traffic was prevalent. These deteriorations included: wheel path cracking, distortion and rutting. Regional Road 3 in the Haldimand County, for example, had severe wheel path cracking and rutting on one side of the road due to heavily loaded truck traffic, as it was located within an industrial area. Other road sections had similar deteriorations due to heavy truck traffic. These inconsistencies in the results may be because of different software used to

evaluate the pavement condition and because they are solely based on visual inspection by different personnel within the respective region.

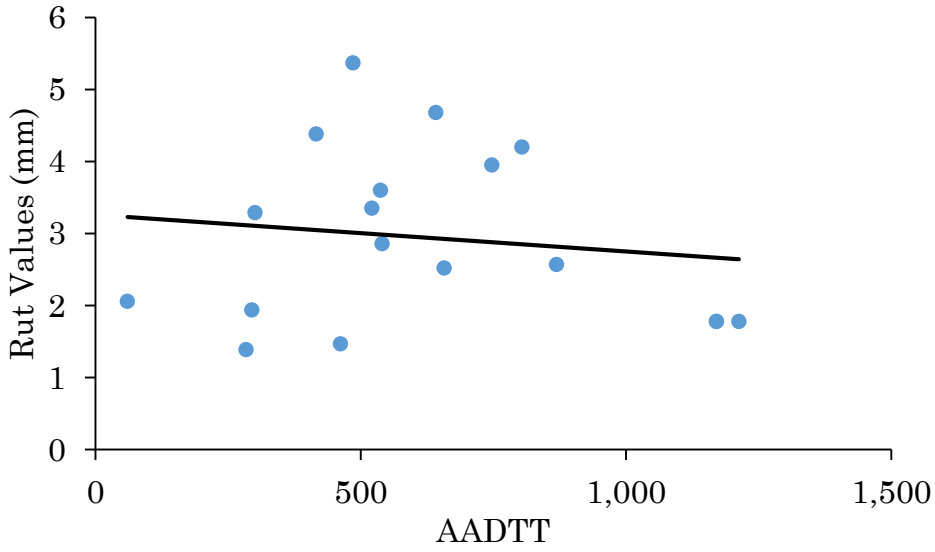

Figure 5-9: Average rut values vs. truck traffic on CIR sections

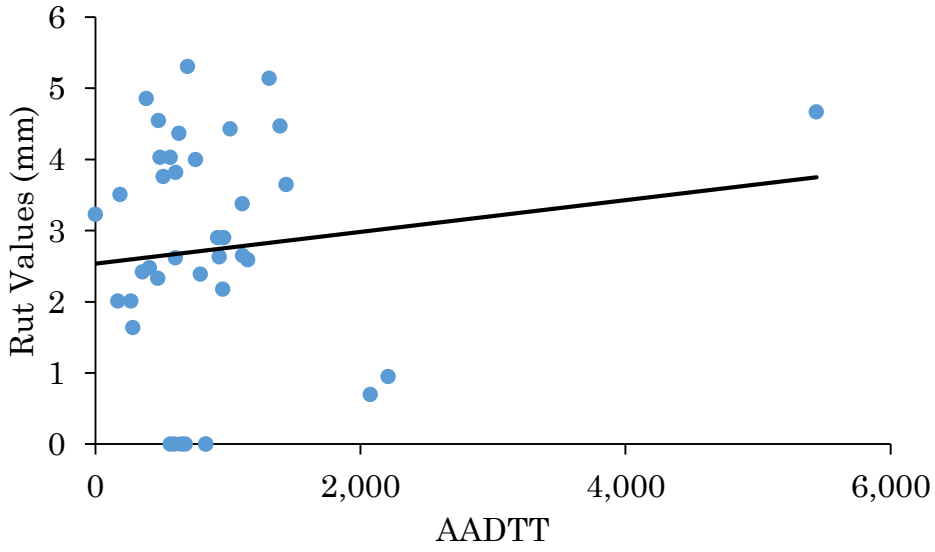

Figure 5-10: Average rut values vs. truck traffic on CIREAM sections

5.4 Summary

Field evaluation was carried out by gathering information from different municipalities from all over Ontario and the MTO. Current information on road sections that had implemented CIR or CIREAM as a rehabilitation technique were gathered. Field visual inspections were carried out in order to examine some of the selected road sections for the type, severity and causes of deteriorations. Relationships between the pavement physical condition, and the traffic, truck loading and pavement age were examined.

For the MTO road sections, none of the examined road features had a significant impact on the physical condition of either of the pavements based on a simple linear regression analysis. The PCI values based on the information provided by MTO showed that most of the inspected sections performed adequately. The reported rut depth values were low and the truck traffic showed no significant effect on the rut depth of those road sections. However, from visual inspections done in the municipalities, a large amount of deteriorations were observed where the road sections had heavy truck traffic in both CIR and CIREAM. In several sections, ravelling was a very common deterioration observed. When a road section had poor drainage and improper road geometry or low speed limits, wheel path rutting and alligator cracking was observed. Both CIR and CIREAM performed similarly in field in comparison.

CHAPTER 6
CONCLUSIONS, RECOMMENDATIONS AND FUTURE RESEARCH

6.1 Conclusions

The literature review on CIR and CIREAM highlighted the research gaps in the current state-of-practice. There was limited information available on the performance data and a lack of performance tests (specifically stiffness, fatigue performance and tensile strength tests) conducted on CIR and CIREAM. Further laboratory investigation was carried out to establish and compare the performance of CIR and CIREAM.

Three different types of laboratory tests were carried out on mixed samples of CIR and CIREAM, to test for their overall strength, their tension cracking and fatigue cracking performance. These tests were conducted on two different types of RAP material.

A duration test was carried out using the dynamic modulus test. It helped conclude that curing the CIR-S samples for 14 days after compaction improved test results in the laboratory for at least the low frequencies of loading. The results from the strength test helped determine the optimum percentage of AC for each type of RAP used. The optimum percentage of AC was used for the rest of the tests. The CIR dynamic modulus testing using southern RAP showed that the use of 3.2% AC within the mix gave an overall better performance in

comparison to the other mixes. Similarly, using 3.2% AC for the CIREAM samples also showed improved performance. CIR-N samples with varying percentage of the AC performed similarly as there were no significant differences between samples. CIR and CIREAM samples using 3.2% AC and the southern RAP had similar performance in terms of resistance to fatigue cracking and the failure temperatures for both samples. Both samples failed at -28°C for the TSRST. However, the tensile stresses on the CIR samples were much higher, on average 4.4 times higher in comparison to the stresses on the CIREAM samples, at failure. The properties of the RAP and the use of emulsion and foamed asphalt were the primary reasons for the differences in performance of the tested samples.

Field visual inspections were carried out in order to examine selected road sections for the type, severity and causes of deteriorations. For the road sections, which were highlighted by MTO, none of the examined road features had a significant impact on the physical condition of the pavements. The PCI values based on the information provided by MTO showed that most of the inspected sections with CIR and CIREAM performed well and all of them were satisfactory. The reported rut depth values for these sections were low and the truck traffic showed no significant effect on the rut depth of those road sections. However, from the visual inspections done in the municipalities, high quantity and severity of deteriorations were observed in both CIR and CIREAM road sections. In several sections, ravelling was a very common deterioration observed along with wheel path rutting and alligator cracking on sections with poor drainage and/or improper road geometry. Overall, both CIR and CIREAM performed similarly in field in comparison.

6.2 Recommendations

The following recommendations related to the materials and the use of CIR and CIREAM are suggested:

1) The Southern RAP used in this research had a higher gradation and was much easier to work with in the laboratory as opposed to northern RAP, which had a greater amount of fine particles in the gradation. The presence of the smaller particles allowed for higher absorption of the AC and thus, made it less workable. The samples prepared with the northern RAP were more fragile in comparison to southern RAP samples. It is recommended that the RAP should be well graded and contain larger particles and to avoid the use of excessive fine aggregates.

2) In the laboratory study, CIR and CIREAM had very similar performance and thus, both techniques are good candidates for rehabilitation on rural arterials. They recycle all the aggregates, thus, it would be recommended to use these techniques in remote areas where there is limited access to virgin material given that the pavement structure is sound. From the TSRST results, CIR underwent a higher amount of tensile stress, which indicated greater shrinkage. Thus, using CIREAM instead for areas with very cold climates would be recommended.

3) In the field, CIR and CIREAM performed adequately (based on the physical condition rating shown in Table 5-1) as long as they were used on roadways with proper geometry, drainage and truck traffic. If the pavement is not designed well for these attributes, the chances of failure could increase. They would make excellent candidates for rehabilitation in areas with low truck traffic and higher speed limits.

6.2.1 Recommended Construction Process

For the construction process of the CIR, it would be recommended to consider different curing times for different types of RAP, given ideal weather conditions.

The existing moisture in the RAP before placement should be determined to account for the added water in the mix. The higher the initial moisture content within the RAP, the longer it is required to cure and rid of all the moisture under ideal weather conditions. Proper curing of the CIR compacted layer is very crucial for strength gain.

When carrying out these techniques in the field, a thorough quality check would be recommended before designing the mix and determining the optimum percentage of AC for that particular RAP. Each RAP behaves and performs differently given the existing amount of AC and the age of the pavement. Thus, carrying out these tests and using the optimum percentage of AC would work for the benefit of the pavement.

6.3 Future Research

In order to further expand on the performance of CIR and CIREAM, the following future studies are recommended:

1) Carrying out the remainder of the testing with the northern RAP would help provide more details on cold temperature behaviour and the fatigue life of the pavement. Further studies would be recommended using RAP of different gradations, different percentages of AC, and different penetration values (AC stiffness).

2) Collecting field samples from the inspected sections and testing for ITS and rutting would help compare the results with their in situ performance, and help predict their long-term performance. Comparing air voids between the field compacted and laboratory compacted samples would also help determine a potential cause for the pavement's strength gain or loss.

3) Collecting a larger set of data from municipalities in different regions of Ontario could also help compare the field performance with the use of different RAP from different roadways.

References

AASHTO. (1993). *Standard Test Method for Thermal Stress Restrained Specimen Tensile Strength; AASHTO TP 10-93*. Washington DC.

AASHTO. (2007). *Standard Method of Test for Determining the Fatigue Life of Compacted Hot-Mix Asphalt (HMA) Subjected to Repeated Flexural Bending; AASHTO T321-07*. Washington DC.

AASHTO. (2009). *Standard Practice for Developing Dynamic Modulus Master Curves for Hot Mix Asphalt (HMA), AASHTO TP 62-09*. Washington DC.

Alkins, A. E., Lane, B., & Kazmierowski, T. (2008). Sustainable Pavements: Environmental, Economic, and Social Benefits of In Situ Pavement Recycling. *Transportation Research Record: Journal of the Transportation Research Board*, 100-103.

Ambaiowei, D. (2014). *Innovative Evaluation of Crumb Rubber Asphalt and Recycled Asphalt Pavement*. Waterloo: University of Waterloo.

Anderson, D. (2013). *WorkTech Asset Classes and Deterioration Curves*. Waterloo, Ontario: 4Roads Management Services Inc.

ASTM. (2010). *Standard Test Method for Determining Fatigue Failure of Compacted Asphalt Concrete Subjected to Repeated Flexural Bending; ASTM D7460-10*. West Conshohocken, PA.

ASTM. (2011). *Standard Practice for Roads and Parking Lots Pavement Condition Index Surveys; ASTM D6433-11*. West Conshohocken, PA.

ASTM. (2012). *Standard Test Method for Indirect Tensile (IDT) Strength of Bituminous Mixtures (2012); ASTM D6931-12*. West Conshohocken, PA.

ASTM. (2013). *Standard Test Method for Penetration of Bituminous Materials; ASTM D5/D5M-13*. West Conshohocken, PA.

Bahia, H., Zhai, H., Bonnetti, K., & Kose, S. (1998). Non-linear Viscoelastic and Fatigue Properties of Asphalt Binders. *Association of Asphalt Paving Technologies*.

Chan, P., Tighe, S., & Chan, S. (2010). *Exploring Sustainable Pavement Rehabilitation: Cold In-Place Recycling with Expanded Asphalt Mix.* Waterloo: Transportation Research Board.

Chesner, W. H. (2011). Evaluation of Factors Affecting the Long Term Performance of Cold In-Place Recycled Pavements in New York State. *Transportation Research Board: Journal of the Transportation Research Board*, 13-22.

Copeland et al., A. (2007). Field Evaluation of High Reclaimed Asphalt Pavement–Warm-Mix Asphalt Project in Florida Case Study. *Transportation Research Record: Journal of the Transportation Research Board*, 93-101.

El-Hakim, M. (2013). *A Structural and Economic Evaluation of Perpetual Pavements: A Canadian Perspective.* Waterloo: University of Waterloo.

Frost, J. (2014, June 12). *How to Interpret a Regression Model with Low R-squared and Low P values.* Retrieved from The Minitab Blog: http://blog.minitab.com/blog/adventures-in-statistics/how-to-interpret-a-regression-model-with-low-r-squared-and-low-p-values

H. Di Benedetto, M. P. (2001). Rilem TC 182-PED Performance Testing and Evaluation of Bituminous Materials. *Materials and Structures*, 66-70.

K.M. Muthen. (1998). *Foamed Asphalt Mixes: Mix Design Procedure.* Pretoria, South Africa: SABITA Ltd. & CSIR Transportek.

Kandhal, P. S. (1992). *Moisture Susceotibility of HMA Mixes: Identification of Problem and Recommended Solutions.* Auburn, Alabama: National Centre for Asphalt Technology.

Kazmierowski, T., Markes, P., & Lee, S. (1999). *Ten-Year Performance Review of In Situ Hot-Mix Recycling in Ontario.* Transportation Research Record,Vol.1684(1), pp.194-202.

Kim, Y., Im, S., & Lee, H. ". (2011). Impacts of Curing Time and Moisture Content on Engineering Properties of Cold In-Place Recycling Mixtures

Using Foamed or Emulsified Asphalt. *American Society of Civil Engineers (ASCE): Journal of Materials in Civil Engineering, 23(5)*, 542–553.

Lane, B., & Kazmierowski, T. (2006). Implementation of Cold In-Place Recycling with Expanded Asphalt Technology in Canada. *Transportation Research Record: Journal of the Transportation Research Board, 1905-02*, pp 17-24.

Lane, B., & Lee, W. (2014). Comparing 10 Year Performance of Cold In-Place Recycling (CIR) with Emulsion versus CIR with Expanded Asphalt on Highway 7, Perth, Ontario. *Transportation Association of Canada*.

Li, N., Pronk, A. C., Molenaar, A. A., Ven, M. F., & Wu, S. (2013). Comparison of Uniaxial and Four-Point Bending Fatigue Tests for Asphalt Mixtures. *Transportation Research Record: Journal of the Transportation Research Board*, 44-53.

Mallick, R. B., Kandhal, P. S., & Bradbury, R. L. (2008). Using Warm-Mix Asphalt Technology to Incorporate High Percentage of Reclaimed Asphalt Pavement Material in Asphalt Mixtures. *Transportation Research Record: Journal of the Transportation Research Board*, 71-78.

Mills, B. N., Tighe, S., Audrey, J., Smith, J., & Huen, K. (2009). Climate Change Implications for Flexible Pavement Design and Performance in Southern Canada. *Journal of Transportation Engineering*, 773-782.

Moore, T. (2013). In-Place Recycling - What to Use and Where. *ARRA Semi-Annual Meeting*. Miller Paving Limited.

MTO. (1991). *Inventory Manual for Municipal Roads*. Downsview, Ontario: Ministry of Transportation.

MTO. (2009). *The formulations to calculate pavement condition indices*. Downsview, Ontario: Ministry of Transportation.

MTO-LS. (1996). *Percent Air Voids in Compacted Dense Bituminous Pavement Mixtures; MTO LS-265*. Ontario.

MTO-LS. (1996). *Preparation of Marshall Specimens for Cold In-Place Recycled Mixtures; MTO LS-300*. Ontario.

MTO-LS. (1999). *Bulk Relative Density of Compacted Bituminous Mixes; MTO LS-262*. Ontario.

MTO-LS. (2009). *Quantitative Extraction of Asphalt Cement and Analysis of Extracted Aggregate from Bituminous Paving Mixtures; MTO LS-282*. Ontario.

MTO-LS. (2011). *Indirect Tensile Strength of Expanded Asphalt Mixes; MTO LS-297*. Ontario.

MTO-LS. (2012). *Theoretical Maximum Relative Density of Bituminous Paving Mixtures; MTO LS-264*. Ontario.

NCHRP. (2004). *Guide for Mechanistic-Empirical Design of New and Rehabilitated Pavement Structures*. Champaign, Illinois: National Cooperative Highway Research Program; Transportation Research Board.

NCHRP. (2011). *A Manual for Design of Hot-Mix Asphalt with Commentary*. Washington: Transportation Research Board: National Cooperative Highway Research Porgram.

NCHRP Synthesis 421. (2011). *Recycling and Reclamation of Asphalt Pavements Using In-Place Methods*. Washington: Transportation Research Board: National Cooperative Highway Research Porgram.

OPSS 1150. (2010). *Material Specification For Hot Mix Asphalt*. Ontario Provincial Standard Specification.

OPSS 335. (2009). *Construction Specification For Cold In-Place Recycling With Expanded Asphalt*. Ontario Provincial Standard Specification.

Pavement Interactive. (2007, August 16). *Materials: Penetration Grading*. Retrieved from Pavement Interactive: http://www.pavementinteractive.org/article/penetration-grading/

Salomon, D. R. (2006). *Transportation Research Circular E-C102: Asphalt Emulsion Technology*. Washington D.C.: Transportation Research Board.

Shatec Engineering Consultants. (2013). *Cold In-Place Recycling With Expanded Asphalt Mix (CIR EAM/Foam) Technology*. Sacramento, California: Shatec Engineering Consultants.

Statistics Solution. (2013). *ANOVA (Analysis of Variance)*. Retrieved from Statistics Solution: Advancement Through Clarity: http://www.statisticssolutions.com/academic-solutions/resources/directory-of-statistical-analyses/anova/

U.S. Department of Commerce. (2013, October 30). *Engineering Statistics Handbook*. Retrieved from National Institute of Standards and Technology: http://www.itl.nist.gov/div898/handbook/prc/section2/prc222.htm

Wirtgen. (2004). *Wirtgen Cold Recycling Manual* (2nd ed.). Windhagen, Germany: Wirtgen Group.

Witczack, M. (2005). *Simple Performance Tests: Summary of Recommended Methods and Database (NCHRP Report No. 547)*. Washington D.C.: Transportation Research Board.

Witczak, M., & Fonseca, O. (1996). Revised Predictive Model for Dynamic (Complex) Modulus of Asphalt Mixtures. *Transportation Research Record: Journal of the Transportation Research Board*, 15-23.

Witzcak, M. W., & Yoder, E. J. (1975). *Principles of Pavement Design*. Hoboken, New Jersey: John Wiley & Sons Inc.

Appendix A Mix Design and Air voids

A.1: CIR Mix Design

Sample weight (g): 5000
Additive %: 0

Emulsion Percentage:	1.2	1.7	2.2	2.7	3.2
Sample Weight (g)	5000	5000	5000	5000	5000
Additive Weight (g)	0.0	0.0	0.0	0.0	0.0
Weight Emulsion (g)	60.7	86.5	112.5	138.7	165.3
Weight Water Added (g)	165.0	140.0	115.0	90.0	65.0

$$\text{Weight Emulsion} = \left(\frac{W_{RAP}}{\left(1-\frac{\%AC}{100}\right)}\right) - W_{RAP}$$

$$\text{Weight Water} = \frac{W_{RAP}(4.5\% - \%AC)}{100}$$

A.2: CIREAM Mix Design

PGAC Grade	PG 58-28
Supplier	McAsphalt Industries Ltd.
Test Temperature	170 °C

WLB-10 Machine Settings							
PGAC Pump		Water					
Quantity Required (g)	500	Quantity Required (%)	2	3	4	5	6
Pump Output (g/sec)	120	Flow Meter Settings (Lit/hr)	8.64	12.96	17.28	21.60	25.92
Timer Settings (sec)	4.17						

Water (%)	Expansion	Half-Life Time (sec)
2.0	9.0	21
3.0	13.5	13
4.0	24.0	7
5.0	30.0	5
6.0	45.0	3

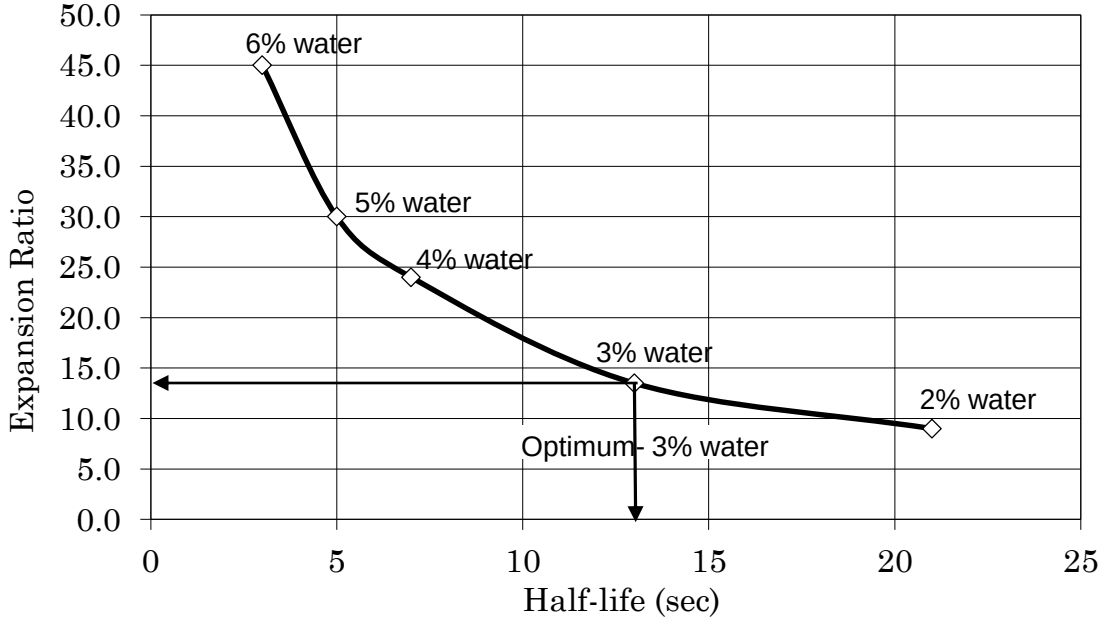

Selected Moisture to be added to PGAC =	3.0	%
Minimum Half Life Requirement =	10.0	sec

Foaming Machine settings:

Water Flow Rate Determination		
PG-AC	58-28	
Tare	2426.2	g
Tare + Binder	3012.0	g
Binder	585.8	g
Timer Setting	5.00	sec
Q_{Binder}	117.2	g/s
Water Content (Foam)	3.0	%
Q_{water}	12.7	L/H

Batch Size	8000	%
Opt. Moisture	7.0	%
Hygros. Moisture	1.44	%
Dry Mass	7886.4	g

	% of Blend	Mass [g]
% Crushed RAP	100	8000
% Gran	0	0
% Other	--	--

$Water_{add}$	300.5	g			
Binder Content [%]	1.2	1.7	2.2	2.7	3.2
WLB10 Timer [sec]	0.81	1.14	1.48	1.82	2.15

A.3: Air Voids

$$\%\text{Air Voids} = \frac{(\text{MRD}-\text{BRD})}{\text{MRD}} \text{ X } 100\%$$

Sample ID	% Air Voids	MRD	BRD
DT-S0	6.30	2.47	2.32
DT-S2	6.85	2.47	2.31
DT-S7	5.93	2.47	2.33
DT-S14	5.77	2.47	2.33
Average =	6.21	2.47	2.32

Sample ID	% Air Voids	MRD	BRD
CIR-S1	6.29	2.47	2.32
CIR-S2	6.63	2.47	2.30
CIR-S3	6.36	2.46	2.30
CIR-S4	6.34	2.46	2.31
CIR-S5	4.81	2.46	2.34
Average =	6.03	2.46	2.31

Sample ID	% Air Voids	MRD	BRD
CIR-S5-F1	5.98	2.46	2.31
CIR-S5-F2	5.13	2.46	2.31
CIR-S5-F3-A	6.15	2.46	2.31
CIR-S5-F3-B	5.95	2.46	2.31
CIR-S5-F4-A	5.99	2.46	2.31
CIR-S5-F4-B	6.97	2.46	2.31
CIR-S5-F5	6.65	2.46	2.31
CIR-S5-F6	6.86	2.46	2.31
CIR-S5-F7	5.27	2.46	2.31
CIR-S5-F8	4.98	2.46	2.31
Average =	5.94	2.46	2.31

Sample ID	% Air Voids	MRD	BRD
CIR-S5-T1	4.51	2.46	2.30

CIR-S5-T2	5.50	2.46	2.30
CIR-S5-T3	6.46	2.46	2.30
CIR-S5-T4	5.59	2.46	2.30
CIR-S5-T5	6.77	2.46	2.30
CIR-S5-T6	8.67	2.46	2.30
Average =	6.87	2.46	2.30

Sample ID	% Air Voids	MRD	BRD
CIREAM-S2	7.50	2.27	2.10
CIREAM-S3	6.84	2.26	2.10
CIREAM-S4	6.28	2.23	2.07
CIREAM-S5	6.96	2.23	2.09
Average =	6.89	2.25	2.09

Sample ID	% Air Voids	MRD	BRD
CIR-N3	6.18	2.53	2.37
CIR-N4	6.69	2.51	2.35
CIR-N5	6.87	2.51	2.34
Average =	6.58	2.52	2.35

Appendix B Dynamic Modulus Results

B.1: Duration Test Results

Equivalent 21°C dynamic modulus values calculated for each sample for the respective temperatures and frequencies:

Temp. (°C)	Freq. (Hz)	Dynamic Modulus |E*| (MPa)			
		DT-S0	DT-S2	DT-S7	DT-S14
-10	1.00E-07	345.42	205.24	185.96	167.38
-10	3.16E-07	404.22	248.32	223.91	206.32
-10	1.00E-06	476.38	303.18	271.27	255.37
-10	3.16E-06	564.98	373.10	330.38	317.06
-10	1.00E-05	673.68	462.15	404.07	394.38
-10	3.16E-05	806.83	575.27	495.73	490.89
4	1.00E-04	969.43	718.35	609.34	610.71
4	3.16E-04	1167.12	898.17	749.46	758.45
4	1.00E-03	1406.12	1122.33	921.24	939.20
4	3.16E-03	1693.05	1398.91	1130.28	1158.40
4	1.00E-02	2034.67	1736.17	1382.49	1421.62
4	3.16E-02	2437.59	2141.92	1683.89	1734.32
21	1.00E-01	2907.80	2622.91	2040.30	2101.63
21	3.16E-01	3450.29	3184.11	2456.97	2527.94
21	1.00E+00	4068.53	3828.12	2938.26	3016.65
21	3.16E+00	4764.10	4554.58	3487.27	3569.88
21	1.00E+01	5536.38	5359.96	4105.48	4188.17
21	3.16E+01	6382.31	6237.51	4792.55	4870.41
37	1.00E+02	7296.44	7177.55	5546.19	5613.72
37	3.16E+02	8271.05	8168.00	6362.12	6413.57
37	1.00E+03	9296.51	9195.06	7234.20	7263.84
37	3.16E+03	10361.66	10244.10	8154.71	8157.16
37	1.00E+04	11454.41	11300.36	9114.62	9085.15
37	3.16E+04	12562.24	12349.78	10104.03	10038.79
54	1.00E+05	13672.80	13379.51	11112.58	11008.76
54	3.16E+05	14774.32	14378.41	12129.87	11985.79
54	1.00E+06	15856.07	15337.26	13145.82	12960.96
54	3.16E+06	16908.58	16248.87	14151.00	13925.95
54	1.00E+07	17923.88	17108.02	15136.92	14873.23
54	3.16E+07	18895.54	17911.36	16096.12	15796.21

Dynamic Modulus values of DT-S samples at a)-10°C b) 4°C and c) 21°C d) 37°C e) 54°C:

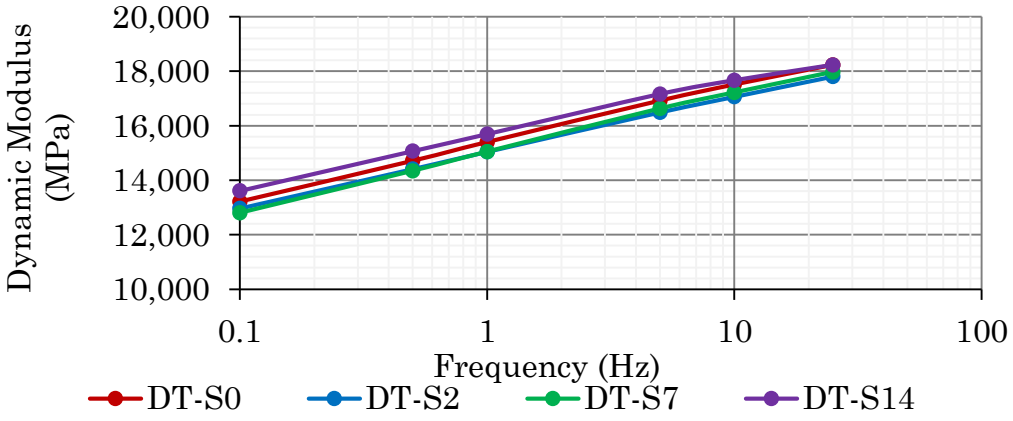

a)

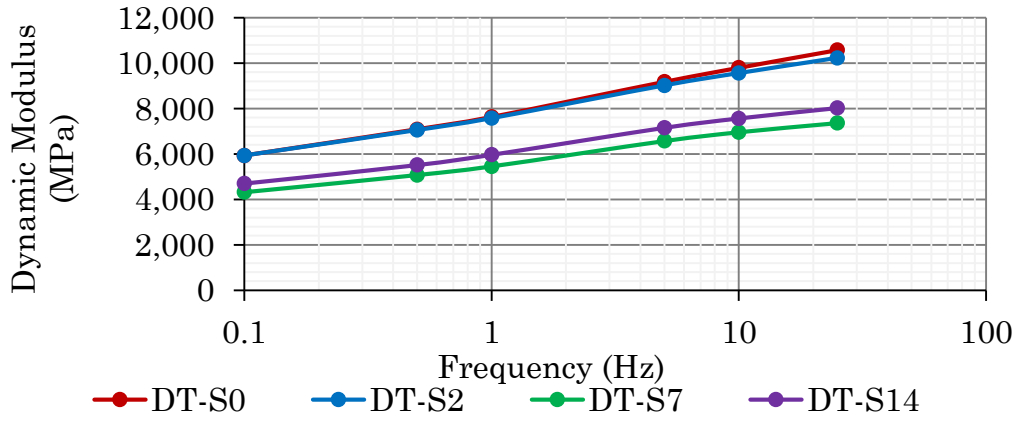

b)

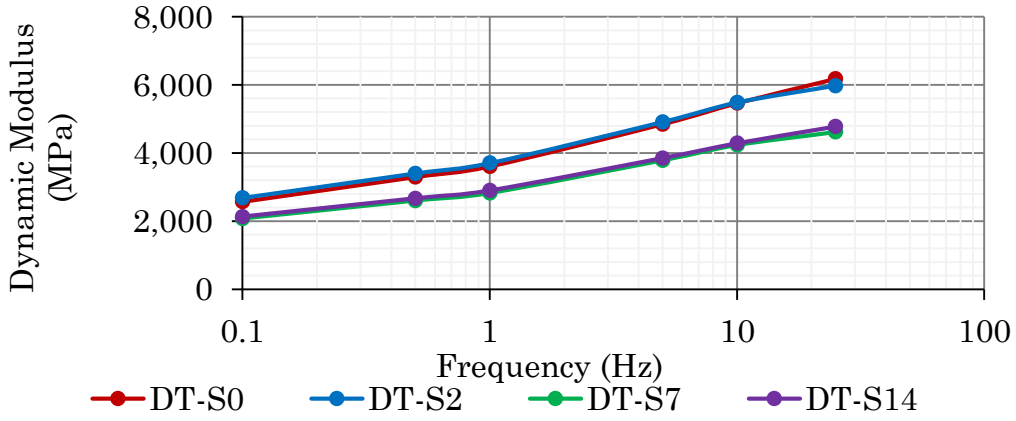

c)

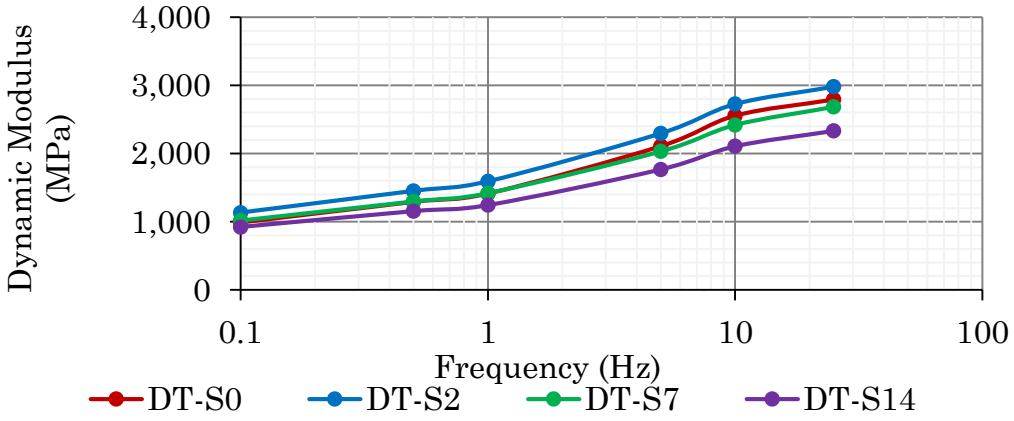
Dynamic Modulus (MPa)
4,000
3,000
2,000
1,000
0
0.1
1
10
100
Frequency (Hz)
DT-S0
DT-S2
DT-S7
DT-S14

d)

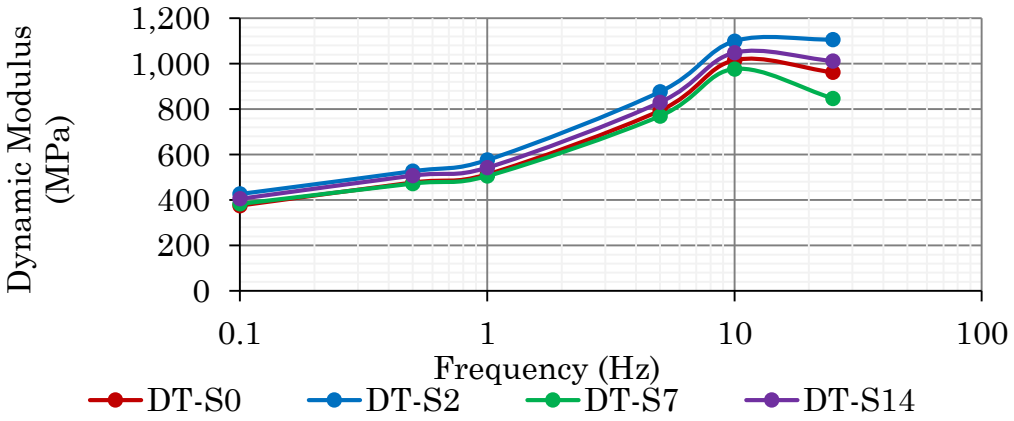
Dynamic Modulus (MPa)
1,200
1,000
800
600
400
200
0
0.1
1
10
100
Frequency (Hz)
DT-S0
DT-S2
DT-S7
DT-S14

e)

B.2: CIR Test Results (Southern RAP)

Equivalent 21°C dynamic modulus values calculated for each sample for the respective temperatures and frequencies:

Temp. (°C)	Freq. (Hz)	Dynamic Modulus |E*| (MPa)				
		CIR-S1	CIR-S2	CIR-S3	CIR-S4	CIR-S5
-10	1.00E-07	136.43	143.82	128.62	341.90	513.30
-10	3.16E-07	161.96	172.42	155.79	367.26	531.86
-10	1.00E-06	193.95	207.62	189.33	398.02	554.10
-10	3.16E-06	234.18	250.97	230.70	435.50	580.83
-10	1.00E-05	284.84	304.33	281.70	481.37	613.04
-10	3.16E-05	348.71	369.92	344.48	537.77	651.99
4	1.00E-04	429.17	450.40	421.57	607.41	699.25
4	3.16E-04	530.38	548.89	515.95	693.73	756.81
4	1.00E-03	657.26	668.98	631.08	801.05	827.16
4	3.16E-03	815.61	814.77	770.92	934.80	913.46
4	1.00E-02	1012.03	990.87	939.94	1101.65	1019.68
4	3.16E-02	1253.83	1202.34	1143.07	1309.72	1150.77
21	1.00E-01	1548.85	1454.60	1385.71	1568.61	1312.88
21	3.16E-01	1905.17	1753.39	1673.63	1889.42	1513.58
21	1.00E+00	2330.67	2104.54	2012.82	2284.45	1761.93
21	3.16E+00	2832.56	2513.81	2409.41	2766.75	2068.67
21	1.00E+01	3416.87	2986.70	2869.46	3349.30	2446.00
21	3.16E+01	4087.86	3528.16	3398.76	4043.94	2907.35
37	1.00E+02	4847.58	4142.37	4002.61	4860.08	3466.67
37	3.16E+02	5695.50	4832.51	4685.62	5803.33	4137.44
37	1.00E+03	6628.34	5600.53	5451.44	6874.31	4931.34
37	3.16E+03	7640.03	6446.97	6302.63	8067.82	5856.70
37	1.00E+04	8721.95	7370.90	7240.45	9372.58	6916.90
37	3.16E+04	9863.27	8369.82	8264.76	10771.63	8109.13
54	1.00E+05	11051.53	9439.69	9373.94	12243.31	9423.65
54	3.16E+05	12273.15	10575.07	10564.91	13762.80	10843.84
54	1.00E+06	13514.12	11769.21	11833.15	15303.85	12347.09
54	3.16E+06	14760.60	13014.31	13172.80	16840.53	13906.40
54	1.00E+07	15999.38	14301.69	14576.86	18348.76	15492.44
54	3.16E+07	17218.38	15622.15	16037.29	19807.53	17075.76

Dynamic Modulus values of CIR-S samples at a)-10°C b) 4°C and c) 21°C d) 37°C e) 54°C:

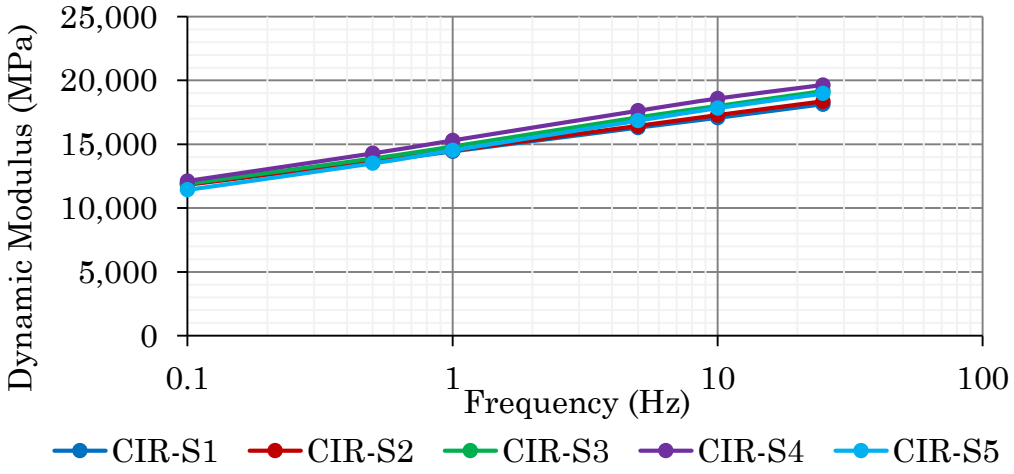

a)

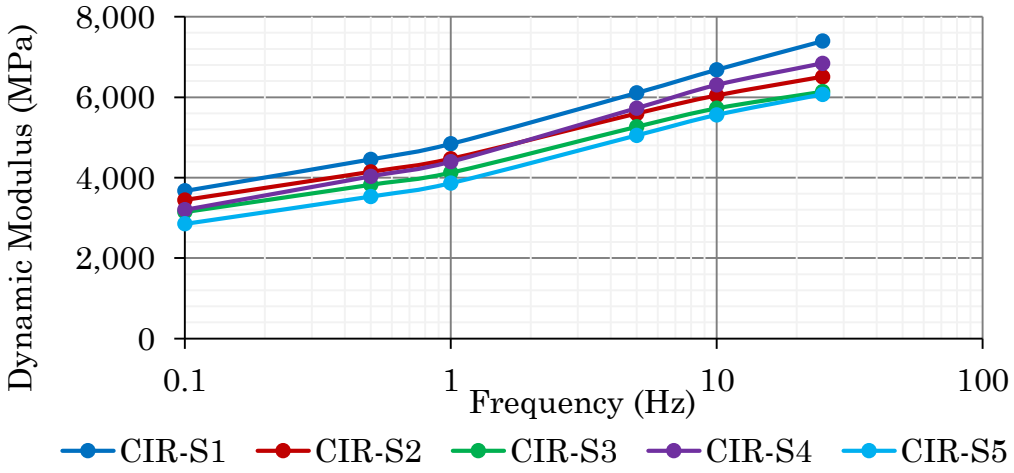

b)

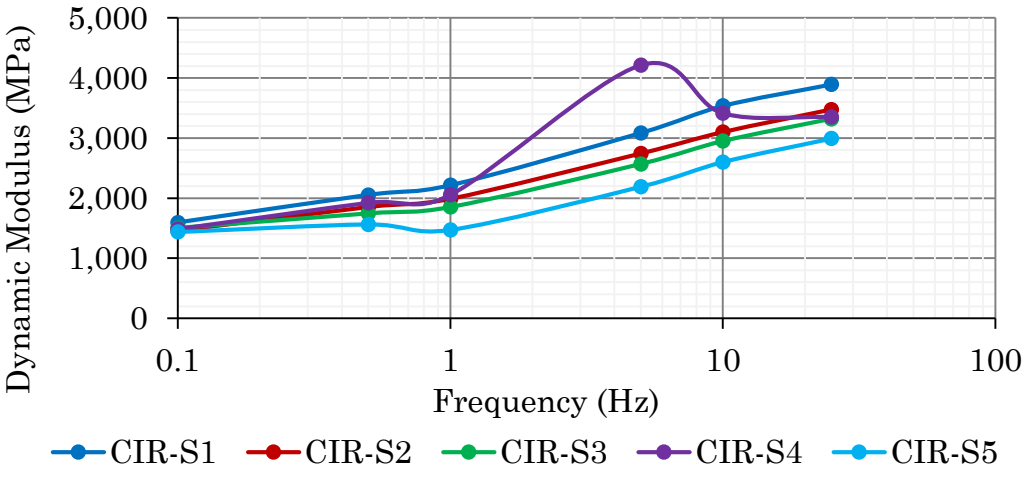

c)

d)

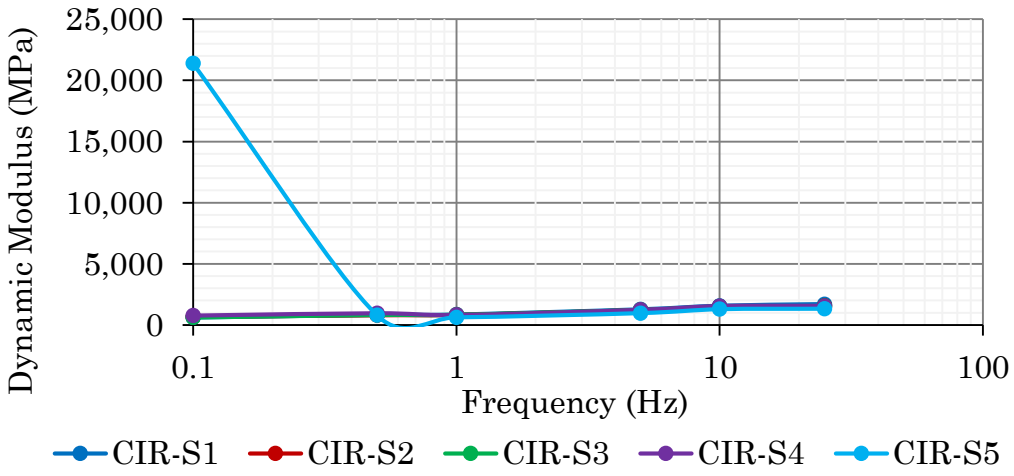
25,000
20,000
15,000
10,000
5,000
0
Dynamic Modulus (MPa)
0.1
1
10
100
Frequency (Hz)
CIR-S1
CIR-S2
CIR-S3
CIR-S4
CIR-S5

e)

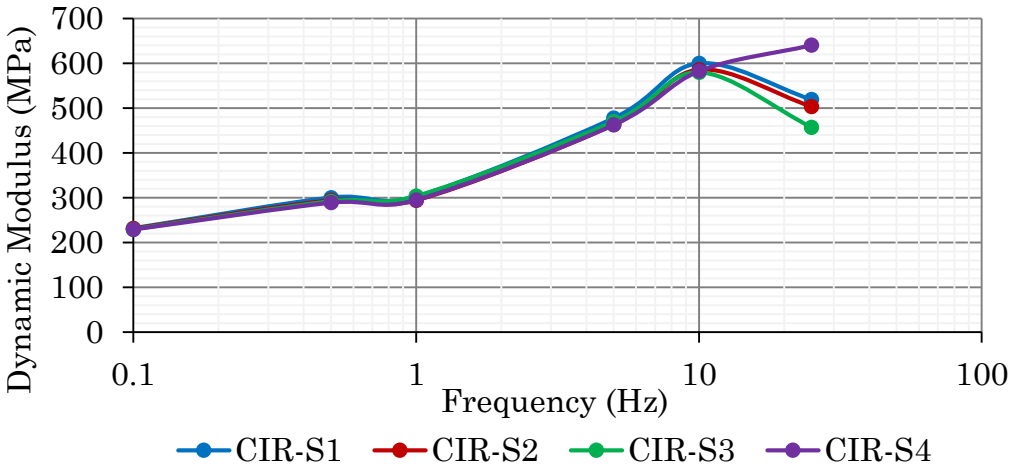
700
600
500
400
300
200
100
0
Dynamic Modulus (MPa)
0.1
1
10
100
Frequency (Hz)
CIR-S1
CIR-S2
CIR-S3
CIR-S4

B.3: CIREAM Test Results (Southern RAP)

Equivalent 21°C dynamic modulus values calculated for each sample for the respective temperatures and frequencies:

Temp. (°C)	Freq. (Hz)	Dynamic Modulus |E*| (MPa)			
		CIREAM-S2	CIREAM-S3	CIREAM-S4	CIREAM-S5
-10	1.00E-07	138.28	235.50	255.16	962.63
-10	3.16E-07	174.74	278.96	304.54	1014.86
-10	1.00E-06	222.24	331.05	364.43	1071.44
-10	3.16E-06	283.82	393.26	436.88	1132.77
-10	1.00E-05	363.12	467.28	524.23	1199.30
-10	3.16E-05	464.26	554.93	629.07	1271.51
4	1.00E-04	591.74	658.14	754.27	1349.92
4	3.16E-04	750.16	778.91	902.86	1435.11
4	1.00E-03	943.88	919.26	1078.02	1527.69
4	3.16E-03	1176.63	1081.12	1282.91	1628.36
4	1.00E-02	1450.98	1266.28	1520.63	1737.85
4	3.16E-02	1768.00	1476.28	1793.99	1856.98
21	1.00E-01	2126.93	1712.32	2105.40	1986.60
21	3.16E-01	2525.08	1975.18	2456.74	2127.69
21	1.00E+00	2957.87	2265.15	2849.17	2281.25
21	3.16E+00	3419.11	2581.96	3283.03	2448.41
21	1.00E+01	3901.43	2924.76	3757.77	2630.34
21	3.16E+01	4396.79	3292.15	4271.90	2828.34
37	1.00E+02	4896.99	3682.15	4823.01	3043.78
37	3.16E+02	5394.18	4092.31	5407.84	3278.12
37	1.00E+03	5881.22	4519.75	6022.32	3532.93
37	3.16E+03	6352.01	4961.28	6661.78	3809.88
37	1.00E+04	6801.59	5413.47	7321.09	4110.70
37	3.16E+04	7226.22	5872.79	7994.81	4437.27
54	1.00E+05	7623.34	6335.71	8677.39	4791.53
54	3.16E+05	7991.45	6798.79	9363.35	5175.50
54	1.00E+06	8329.98	7258.75	10047.39	5591.31
54	3.16E+06	8639.12	7712.57	10724.56	6041.14
54	1.00E+07	8919.67	8157.50	11390.34	6527.25
54	3.16E+07	9172.86	8591.16	12040.72	7051.96

Dynamic Modulus values of CIREAM-S samples at a)-10°C b) 4°C and c) 21°C:

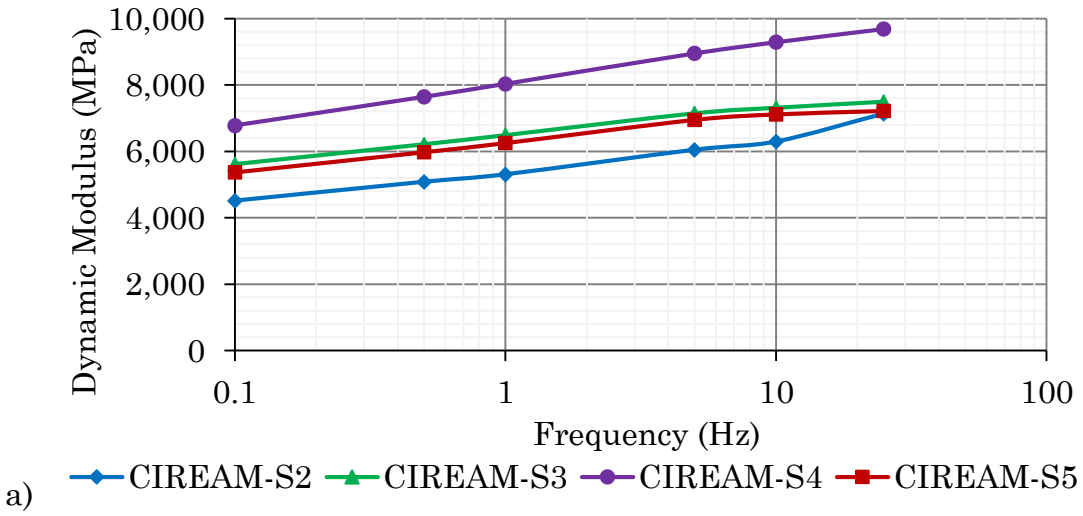

a)

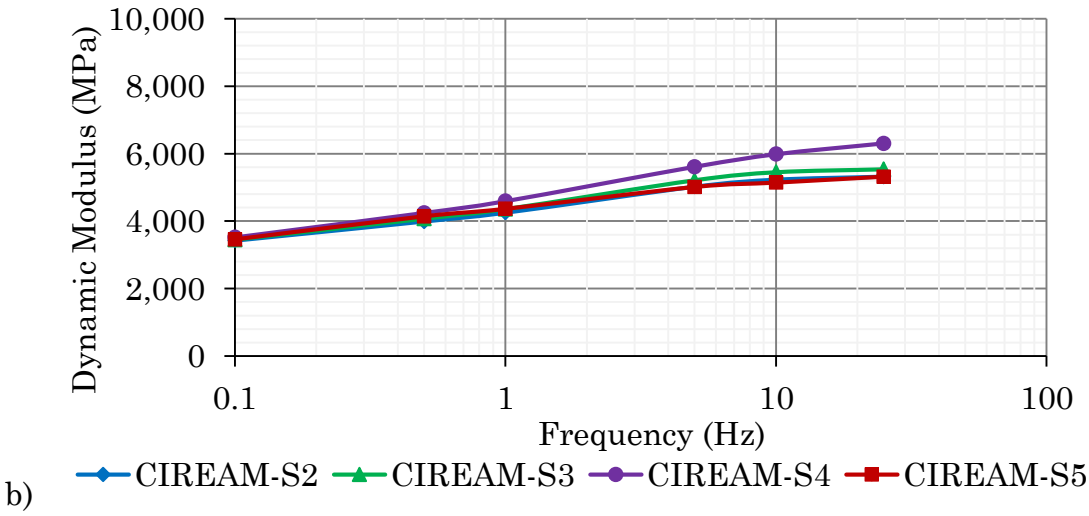

b)

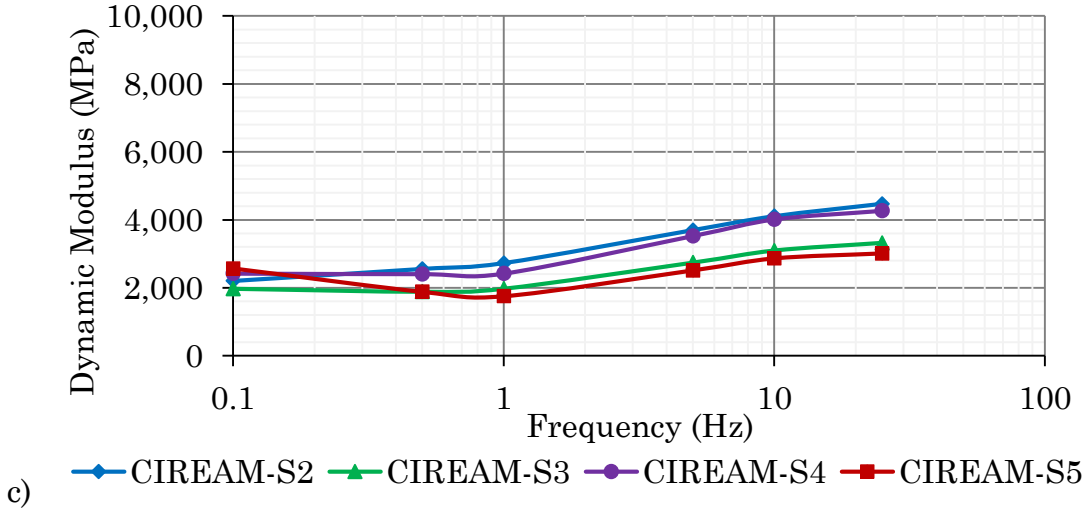

c)

B.4: CIR Test Results (Northern RAP)

Equivalent 21°C dynamic modulus values calculated for each sample for the respective temperatures and frequencies:

Temp. (°C)	Freq. (Hz)	Dynamic Modulus |E*| (MPa)		
		CIR-N3	CIR-N4	CIR-N5
-10	1.00E-07	132.63	130.54	98.26
-10	3.16E-07	152.84	147.51	112.53
-10	1.00E-06	177.64	168.23	130.11
-10	3.16E-06	208.20	193.66	151.90
-10	1.00E-05	245.98	225.03	179.02
-10	3.16E-05	292.82	263.87	212.93
4	1.00E-04	351.00	312.16	255.51
4	3.16E-04	423.36	372.35	309.13
4	1.00E-03	513.36	447.53	376.79
4	3.16E-03	625.20	541.55	462.27
4	1.00E-02	763.87	659.09	570.27
4	3.16E-02	935.24	805.85	706.52
21	1.00E-01	1146.04	988.56	877.94
21	3.16E-01	1403.83	1215.10	1092.72
21	1.00E+00	1716.86	1494.39	1360.33
21	3.16E+00	2093.83	1836.28	1691.42
21	1.00E+01	2543.59	2251.27	2097.64
21	3.16E+01	3074.73	2750.08	2591.24
37	1.00E+02	3695.04	3343.13	3184.56
37	3.16E+02	4410.99	4039.84	3889.36
37	1.00E+03	5227.23	4847.90	4716.07
37	3.16E+03	6146.08	5772.59	5672.92
37	1.00E+04	7167.19	6816.11	6765.23
37	3.16E+04	8287.30	7977.11	7994.73
54	1.00E+05	9500.26	9250.51	9359.12
54	3.16E+05	10797.20	10627.47	10851.88
54	1.00E+06	12166.79	12095.76	12462.45
54	3.16E+06	13595.81	13640.25	14176.53
54	1.00E+07	15069.68	15243.68	15976.82
54	3.16E+07	16573.10	16887.47	17843.75

Dynamic Modulus values of CIR-N samples at a)-10°C b) 4°C and c) 21°C d) 37°C e) 54°C

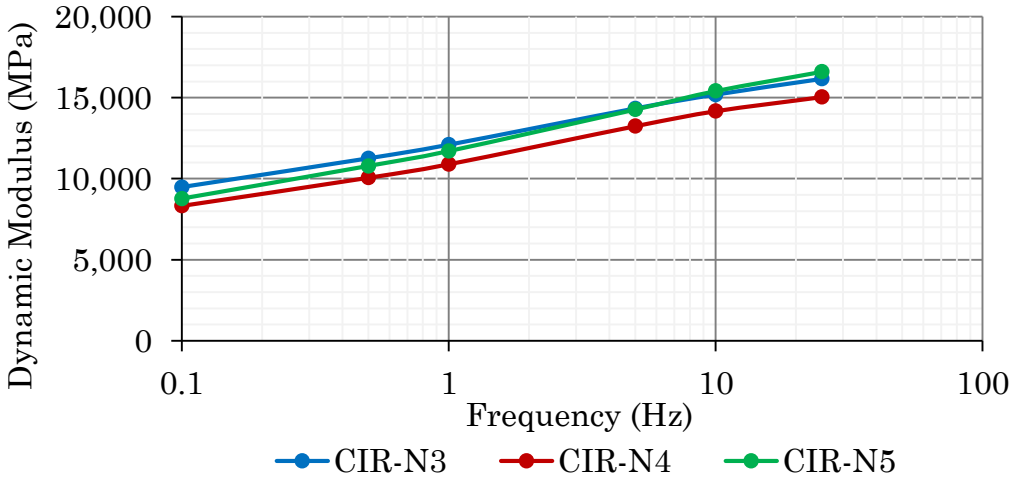

a)

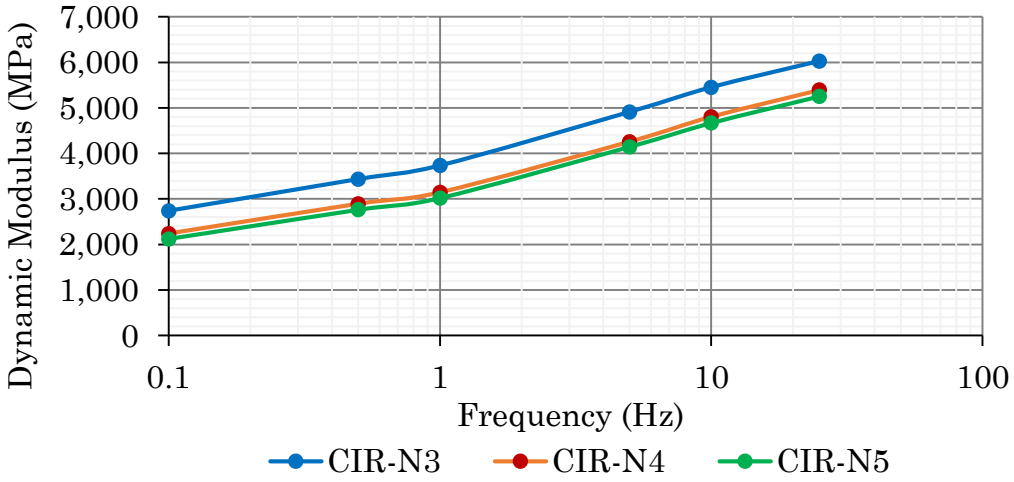

b)

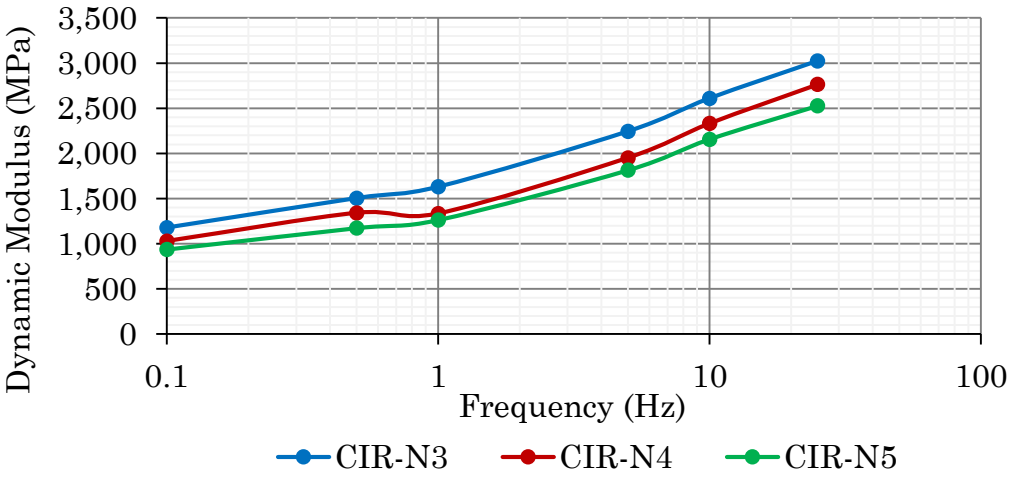

c)

d)

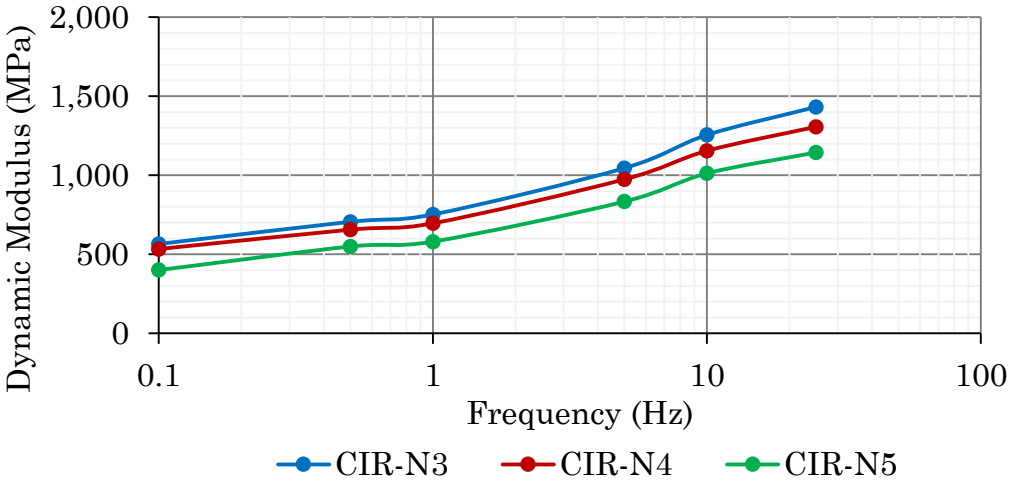
Dynamic Modulus (MPa)
2,000
1,500
1,000
500
0
0.1
1
10
100
Frequency (Hz)
CIR-N3
CIR-N4
CIR-N5

e)

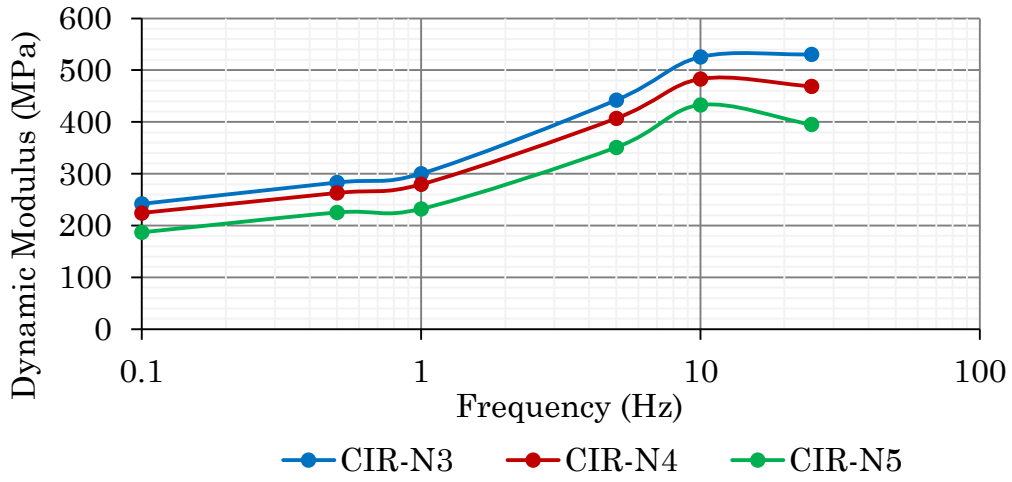
Dynamic Modulus (MPa)
600
500
400
300
200
100
0
0.1
1
10
100
Frequency (Hz)
CIR-N3
CIR-N4
CIR-N5

Appendix C Fatigue Beam Test Results

C.1: CIR Test Results (Southern RAP)

Sample ID	Width (mm)	Height (mm)	Length (cm)
CIR-S5-F8	50.98	63.68	38.10
CIR-S5-F3B	50.10	64.12	38.00
CIR-S5-F9	51.15	65.15	37.70
CIR-S5-F6	51.28	65.28	37.70

Sample ID	Beam LVDT (mm)	Cycles	LOG(cycles)	Variance
CIR-S5-F8	0.25	9800	3.99	-
CIR-S5-F3B	0.25	16500	4.22	0.026
CIR-S5-F9	0.25	25850	4.41	0.019
CIR-S5-F6	0.27	23900	4.38	0.001
	std. dev.=	7344.43	0.19	
	mean =	19012.50		
	cov =	0.39		

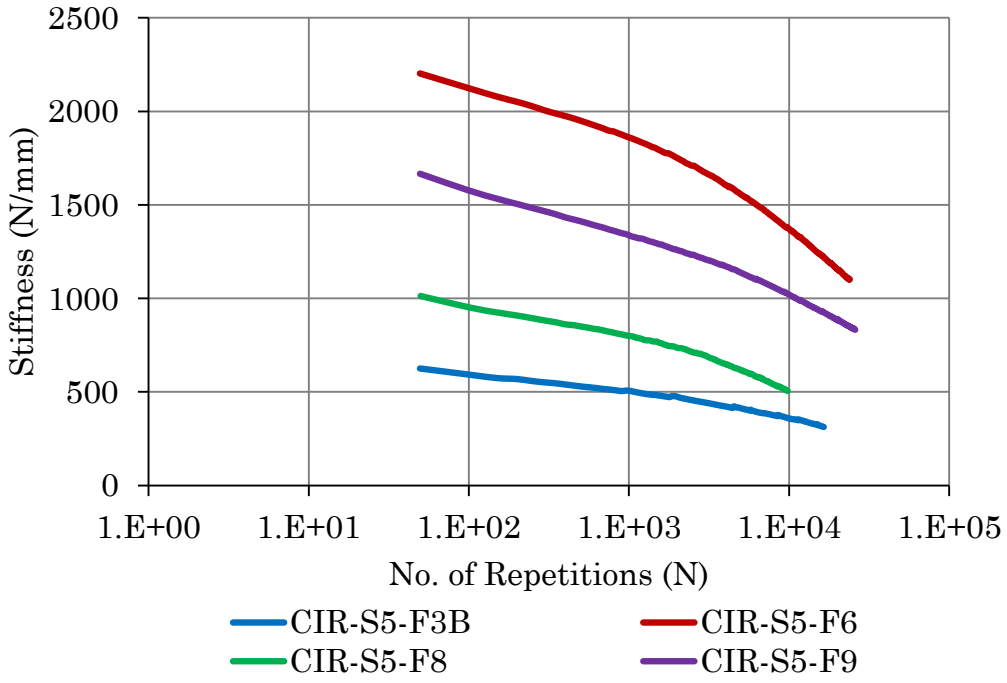

C.2: CIREAM Test Results (Southern RAP)

Sample ID	Width (mm)	Height (mm)	Length (cm)
CIREAM-S5-F1	52.63	63.78	39
CIREAM-S5-F2	49.21	62.6	39
CIREAM-S5-F3	52.46	63.57	39
CIREAM-S5-F4	49.05	64.59	39

Sample ID	Beam LVDT (mm)	Cycles	LOG(cycles)	Variance
CIREAM-S5-F1	0.20	21600	4.33	-
CIREAM-S5-F2	0.20	13950	4.14	0.018
CIREAM-S5-F3	0.20	25950	4.41	0.036
CIREAM-S5-F4	0.20	16550	4.22	0.019
	std. dev.=	5339.07	0.12	
	mean =	19512.50		
	cov =	0.27		

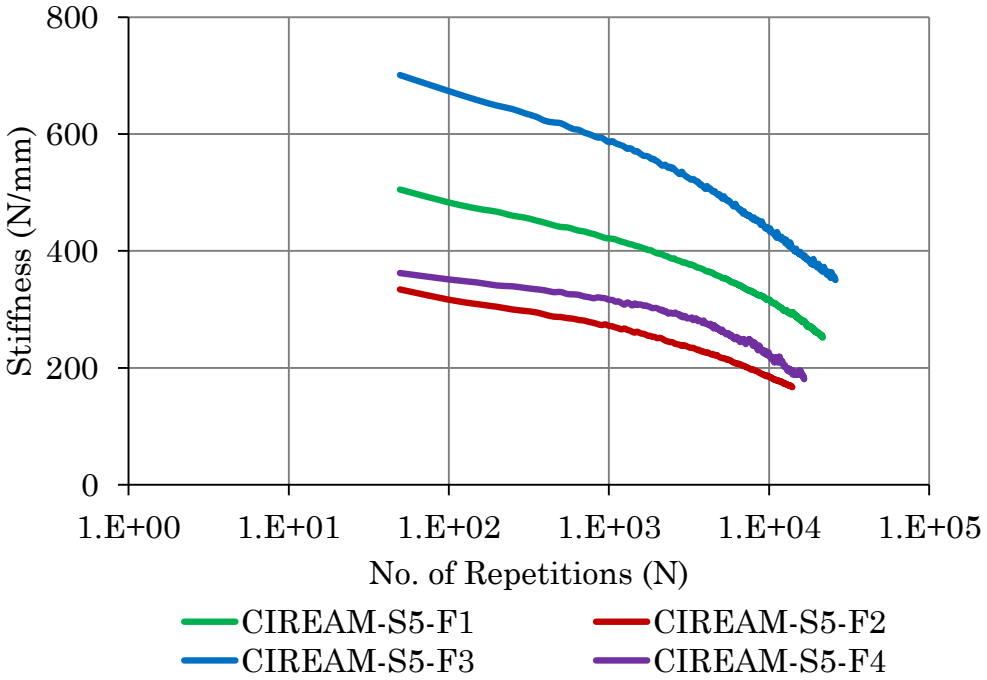

Appendix D TSRST Test Results and Graphs

D.1: CIR Test Results (Southern RAP)

Specimen ID	Length (mm)	Width (mm)	Cross sectional Area (mm^2)
CIR-S5-T1	46.00	51.00	2346
CIR-S5-T2	50.00	50.00	2500
CIR-S5-T3	50.45	45.33	2287
CIR-S5-T6	50.00	51.00	2550
CIR-S5-T7	50.00	51.00	2550

Specimen ID	Temperature (°C)	Max. Load (kN)	Max. Tensile Stress (MPa)
CIR-S5-T1	-29.95	6.41	2.73
CIR-S5-T2	-31.25	6.88	2.75
CIR-S5-T3	-26.13	4.34	1.90
CIR-S5-T6	-26.19	3.98	1.56
Average =	-28.38	5.40	2.24
Std. Dev. =	2.61	1.46	0.60

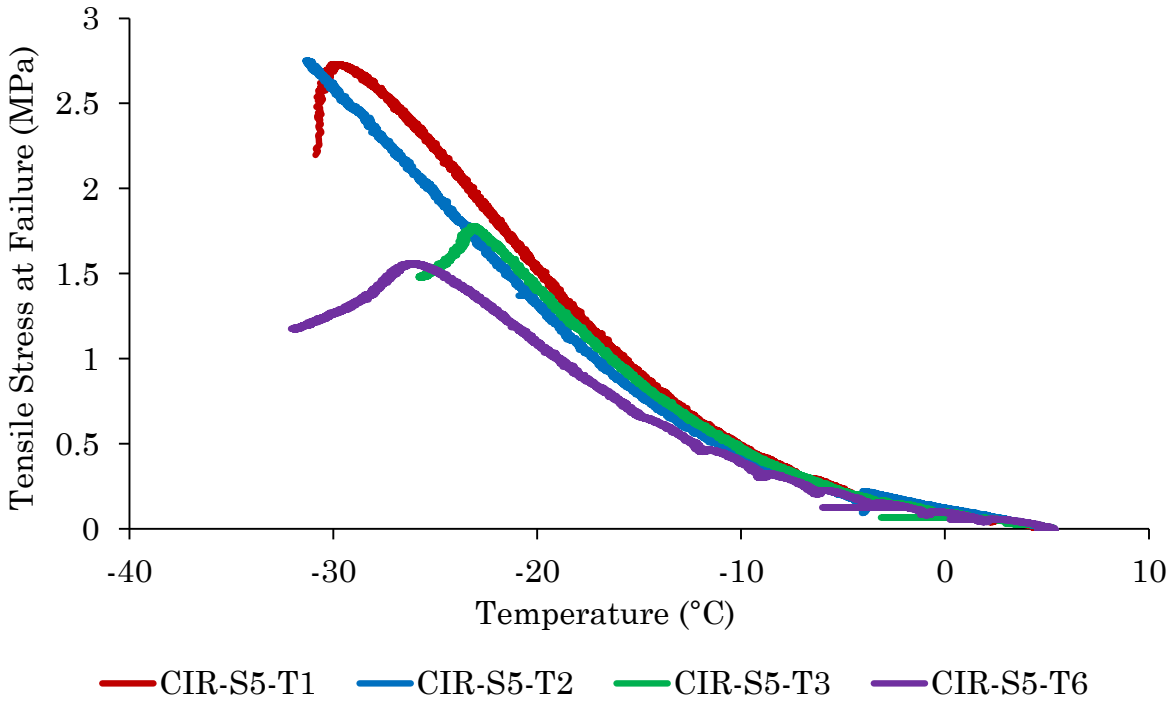

D.2: CIREAM Test Results (Southern RAP)

Specimen ID	Length (mm)	Width (mm)	Cross sectional Area (mm²)
CIREAM-S5-T1	48.00	54.00	2592
CIREAM-S5-T2	49.00	49.00	2401
CIREAM-S5-T3	51.00	49.00	2499
CIREAM-S5-T4	50.00	49.00	2450

Specimen ID	Temperature (°C)	Max. Load (kN)	Max. Tensile Stress (MPa)
CIREAM-S5-T1	-25.70	1.24	0.48
CIREAM-S5-T2	-29.96	1.05	0.44
CIREAM-S5-T3	-25.68	1.48	0.59
CIREAM-S5-T4	-25.93	1.60	0.65
Average =	-26.82	1.34	0.54
Std. Dev. =	2.10	0.24	0.10

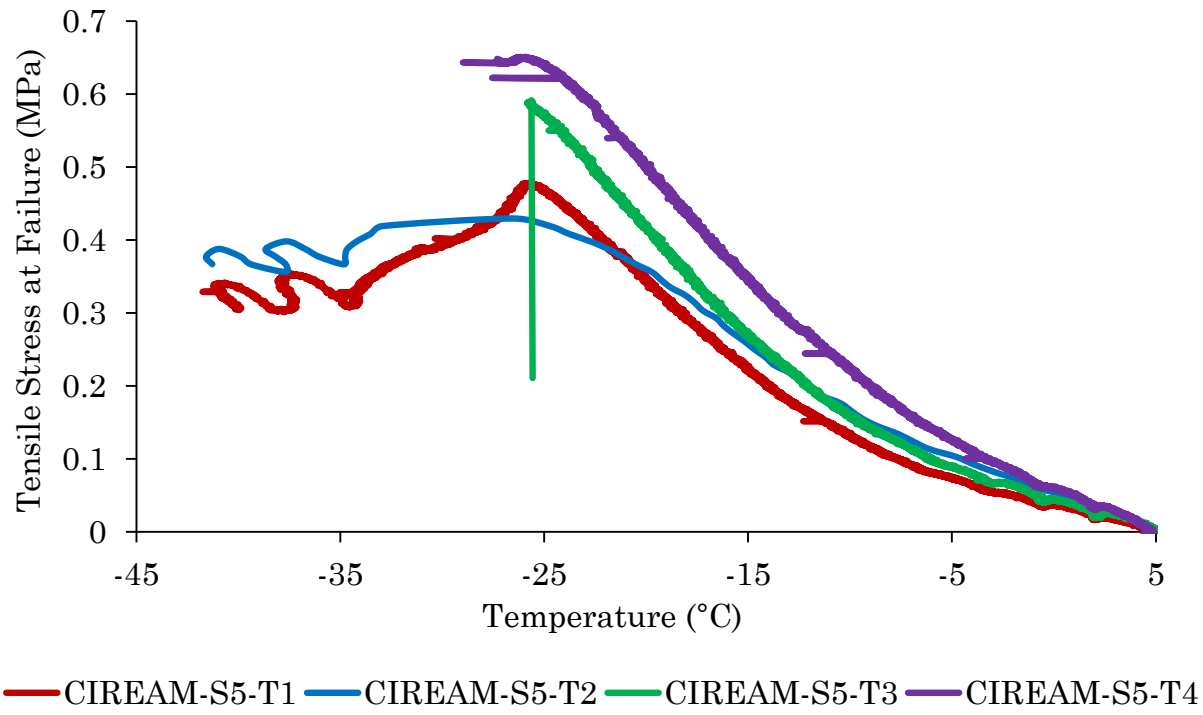

Appendix E Dynamic Modulus Statistical Study

E.1: Duration Test

The Figure below is the same plot that is shown in Figure 4-2:

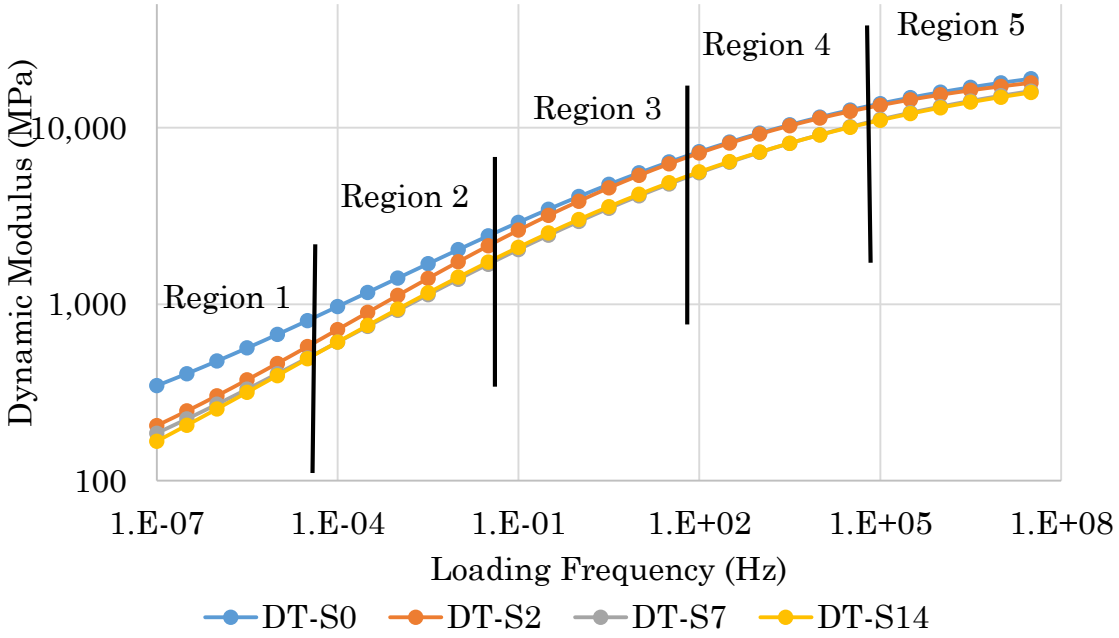

ANOVA summary:

Section ID	F-calc	F-crit	Reject Ho?	P-Value	
Region 1	3.82	3.10	Yes	0.026	--> At least one value is different in this region
Region 2	1.62	3.10	No	0.216	f-calc < f-crit
Region 3	1.64	3.10	No	0.213	f-calc < f-crit
Region 4	2.52	3.10	No	0.087	f-calc < f-crit
Region 5	3.87	3.10	Yes	0.025	--> At least one value is different in this region

t-test (two-tailed) summary:

Section ID	Comparison samples		t - stat	t-crit	Reject H_o?		p-value
Region 1	DT-S0	DT-S2	2.03	2.23	No	|t-stat| < t-crit	0.070

	DT-S0	DT-S7	2.66	2.23	Yes	|t-stat| > t-crit	0.024
	DT-S0	DT-S14	2.78	2.23	Yes	|t-stat| > t-crit	0.019
	DT-S2	DT-S7	0.58	2.23	No	|t-stat| < t-crit	0.576
	DT-S2	DT-S14	0.74	2.23	No	|t-stat| < t-crit	0.475
	DT-S7	DT-S14	0.19	2.23	No	|t-stat| < t-crit	0.850
Region 5	DT-S0	DT-S2	0.58	2.23	No	|t-stat| < t-crit	0.576
	DT-S0	DT-S7	2.45	2.23	Yes	|t-stat| > t-crit	0.034
	DT-S0	DT-S14	2.69	2.23	Yes	|t-stat| > t-crit	0.022
	DT-S2	DT-S7	2.04	2.23	No	|t-stat| < t-crit	0.069
	DT-S2	DT-S14	2.28	2.23	Yes	|t-stat| > t-crit	0.046
	DT-S7	DT-S14	0.19	2.23	No	|t-stat| < t-crit	0.851

From the t-test it can be concluded that samples DT-S7 and DT-S14 are similar to all samples except DT-S0 in both the frequency regions.

E.2: CIR Test (Southern RAP)

The Figure below is the same plot that is shown in Figure 4-3:

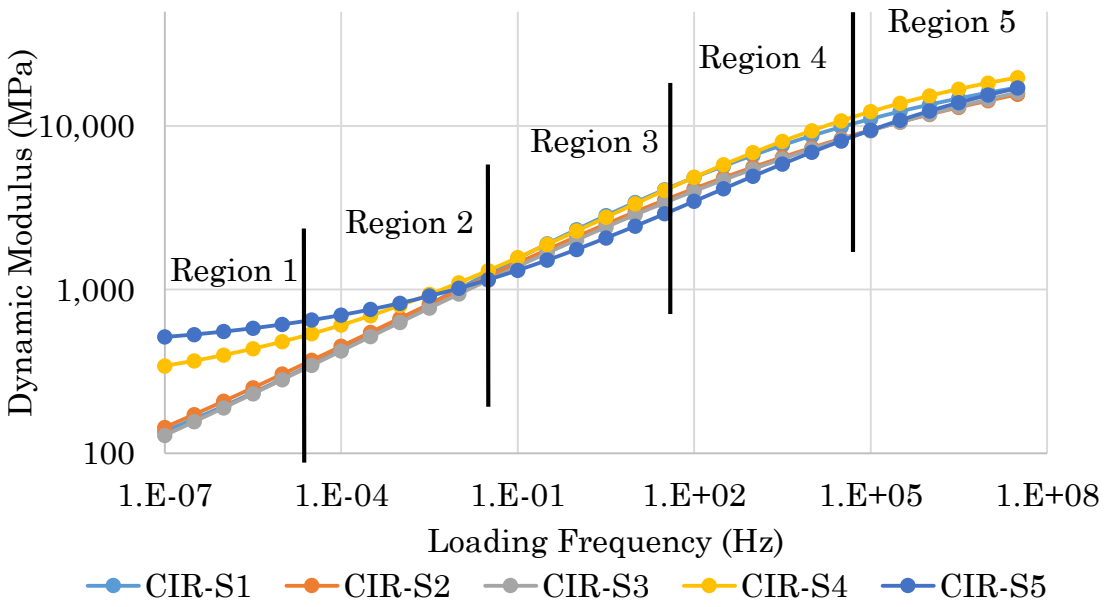

ANOVA summary:

Section ID	F-calc	F-crit	Reject Ho?	P-value	
Region 1	26.31	2.76	Yes	1.22E-08	--> At least one value is different in this region
Region 2	0.50	2.76	No	0.735	f-calc < f-crit
Region 3	0.71	2.76	No	0.590	f-calc < f-crit
Region 4	1.39	2.76	No	0.268	f-calc < f-crit
Region 5	1.98	2.76	No	0.129	f-calc < f-crit

t- test summary:

Section ID	Comparison sam-ples		t - stat	t-crit	Reject Ho?		p- value
Region 1	CIR-S1	CIR-S2	-0.31	2.23	No	|t-stat| < t-crit	0.761
	CIR-S1	CIR-S3	0.11	2.23	No	|t-stat| < t-crit	0.918
	CIR-S1	CIR-S4	-4.53	2.23	Yes	|t-stat| > t-crit	0.001

	CIR-S1	CIR-S5	-8.95	2.23	Yes	|t-stat| > t-crit	0.000
	CIR-S2	CIR-S3	0.41	2.23	No	|t-stat| < t-crit	0.689
	CIR-S2	CIR-S4	-4.05	2.23	Yes	|t-stat| > t-crit	0.002
	CIR-S2	CIR-S5	-8.19	2.23	Yes	|t-stat| > t-crit	0.000
	CIR-S3	CIR-S4	-4.60	2.23	Yes	|t-stat| > t-crit	0.001
	CIR-S3	CIR-S5	-8.97	2.23	Yes	|t-stat| > t-crit	0.000
	CIR-S4	CIR-S5	-4.01	2.23	Yes	|t-stat| > t-crit	0.002

The t-test concludes that samples CIR-S4 and CIR-S5 are statistically different from one another and from the rest of the samples, in Region 1 of the frequencies. Samples CIR-S1. CIR-S2 and CIR-S3 could be considered as statistically similar.

E.3: CIREAM Test (Southern RAP)

The Figure below is the same plot that is shown in Figure 4-4:

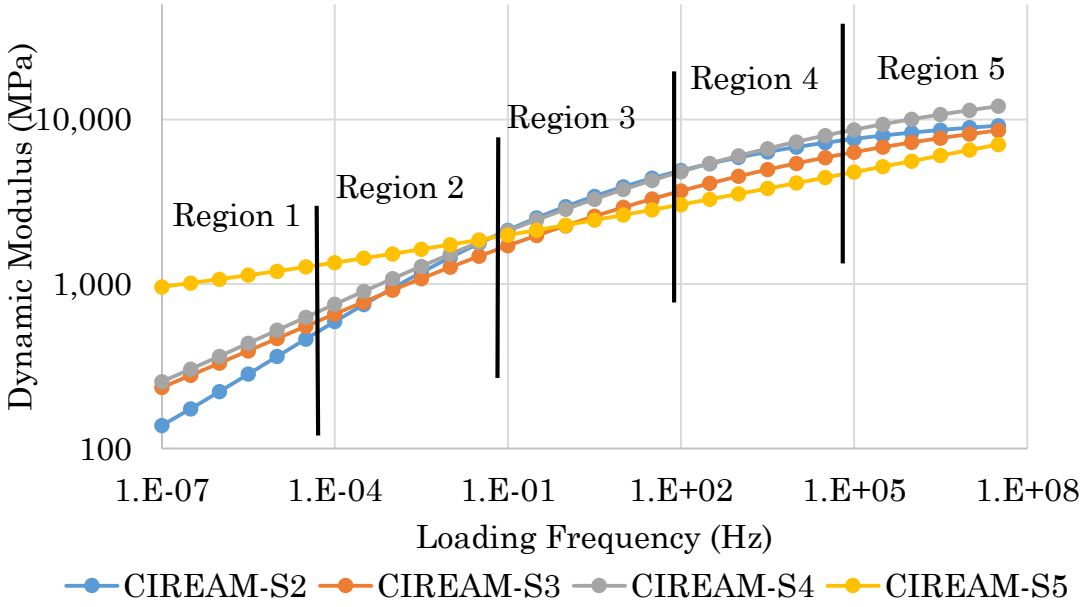

ANOVA Summary:

Section ID	F-calc	F-crit	Reject Ho?	P-value	
Region 1	55.74	3.10	Yes	6.8E-10	--> At least one value is different in this region
Region 2	3.05	3.10	No	0.052	f-calc < f-crit
Region 3	2.48	3.10	No	0.091	f-calc < f-crit
Region 4	11.79	3.10	Yes	0.0001	--> At least one value is different in this region
Region 5	25.44	3.10	Yes	4.97E-07	--> At least one value is different in this region

t-test summary:

Section ID	Comparison samples		t-stat	t-crit	Reject Ho?		p-value
Region 1	CIREAM-S2	CIREAM-S3	-1.46	2.23	No	|t-stat| < t-crit	0.174

	CIREAM-S2	CIREAM-S4	-1.90	2.23	No	|t-stat| < t-crit	0.086
	CIREAM-S2	CIREAM-S5	-12.13	2.23	Yes	|t-stat| > t-crit	0.000
	CIREAM-S3	CIREAM-S4	-0.56	2.23	No	|t-stat| < t-crit	0.588
	CIREAM-S3	CIREAM-S5	-10.77	2.23	Yes	|t-stat| > t-crit	0.000
	CIREAM-S4	CIREAM-S5	-9.29	2.23	Yes	|t-stat| > t-crit	0.000
Region 4	CIREAM-S2	CIREAM-S3	2.73	2.23	Yes	|t-stat| > t-crit	0.021
	CIREAM-S2	CIREAM-S4	-0.46	2.23	No	|t-stat| < t-crit	0.652
	CIREAM-S2	CIREAM-S5	5.75	2.23	Yes	|t-stat| > t-crit	0.000
	CIREAM-S3	CIREAM-S4	-2.74	2.23	Yes	|t-stat| > t-crit	0.021
	CIREAM-S3	CIREAM-S5	2.66	2.23	Yes	|t-stat| > t-crit	0.024
	CIREAM-S4	CIREAM-S5	5.04	2.23	Yes	|t-stat| > t-crit	0.001
Region 5	CIREAM-S2	CIREAM-S3	2.32	2.23	Yes	|t-stat| > t-crit	0.043
	CIREAM-S2	CIREAM-S4	-3.40	2.23	Yes	|t-stat| > t-crit	0.007
	CIREAM-S2	CIREAM-S5	6.16	2.23	Yes	|t-stat| > t-crit	0.000
	CIREAM-S3	CIREAM-S4	-4.68	2.23	Yes	|t-stat| > t-crit	0.001
	CIREAM-S3	CIREAM-S5	3.30	2.23	Yes	|t-stat| > t-crit	0.008
	CIREAM-S4	CIREAM-S5	7.28	2.23	Yes	|t-stat| > t-crit	0.000

The t-test concludes that in Region 1, CIREAM-S5 has significant difference in comparison to all other mixes; in Region 4, all mixes are significantly different from each other with the exception of no significant difference between CIREAM-S2 and CIREAM-S4; in Region 5, all mixes are significantly different from one another.

E.4: CIR Test (Northern RAP)

The Figure below is the same plot that is shown in Figure 4-5:

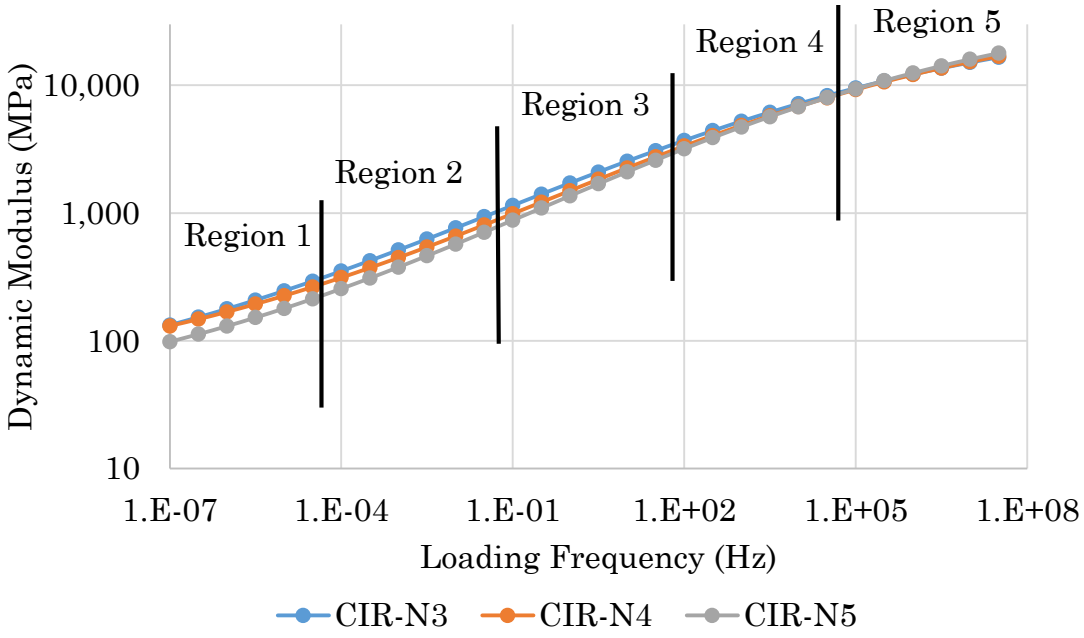

ANOVA Summary:

Section ID	F-calc	F-crit	Reject Ho?	P-value	
Region 1	1.80	3.68	No	0.199	f-calc < f-crit
Region 2	0.98	3.68	No	0.3997	f-calc < f-crit
Region 3	0.48	3.68	No	0.629	f-calc < f-crit
Region 4	0.11	3.68	No	0.896	f-calc < f-crit
Region 5	0.06	3.68	No	0.945	f-calc < f-crit

The ANOVA summary shows that no t-test was required. None of the mixes have any significant difference from one another in any of the regions.

Appendix F Field Performance Data

F.1: United Counties of Stormont, Dundas and Glengarry:

Section ID	Treatment	AADT	Year Com-pleted	Age	Physical Condition	Drainage Rating
02-060	CIR	3862	2008	7	85	15
02-081	CIR	2540	2008	7	65	15
02-104	CIR	2540	2008	7	80	15
02-159	CIR	2540	2008	7	80	15
02-175	CIR	2540	2008	7	80	15
02-841	CIR	1196	2008	7	55	12
02-841	CIR	1196	2008	7	55	12
03-080	CIR	969	2011	4	30	15
09-000	CIR	484	2005	10	55	15
09-977	CIR	356	2005	10	60	15
13-000	CIR	974	2011	4	35	15
34-347	CIR	3656	2010	5	85	15
34-369	CIR	2246	2010	5	85	15
35-000	CIR	1902	2008	7	80	15
35-012	CIR	1902	2008	7	85	15
43-042	CIR	4536	2010	5	55	15
43-042	CIR	4536	2010	5	55	15
43-135	CIR	3618	2008	7	90	15
07-213	CIR	1900	2012	3	25	15
14-019	CIR	1627	2012	3	35	15
18-348	CIR	399	2003	12	35	15
14-047	CIREAM	897	2014	1	85	15
31-265	CIREAM	5674	2014	1	30	15
08-078	CIREAM	776	2004	11	45	15
12-226	CIREAM	1993	2008	7	85	15
12-228	CIREAM	1993	2008	7	70	15
12-236	CIREAM	1993	2008	7	95	15
13-045	CIREAM	931	2007	8	70	15
14-044	CIREAM	1123	1999	16	100	15
14-047	CIREAM	1123	1999	16	85	15
24-160	CIREAM	526	2005	10	55	13
24-160	CIREAM	526	2005	10	55	13
01-305	CIREAM /FDR	1510	2007	8	80	15

F.2: Region of Waterloo:

Section ID	Treatment	%Truck	AADT	Physical Condition	Speed Limit	Drainage Rating
W1	CIR	1.72	12,445	80	60	15
W10	CIR		1,312	55	50	13
W11	CIR	8.72	2,111	90	80	15
W12	CIR	6.79	3,669	55	80	13
W13	CIR		1,500	85	80	14
W14	CIR	20.02	6,081	55	80	15
W15	CIR	4.16	9,670	85	80	13
W16	CIR	6.72	7,248	30	80	14
W17	CIR	2.57	6,506	90	80	14
W18	CIR		5,000	60	80	13
W19	CIR	4.87	2,648	55	80	15
W2	CIR	2.66	6,016	95	80	14
W20	CIR	7.67	7,652	30	80	12
W21	CIR	5.97	3,282	85	80	14
W22	CIR	3.06	4,178	50	80	14
W3	CIR	11.29	23,317	80	80	15
W4	CIR		7,500	30	80	13
W5	CIR		7,500	70	80	14
W6	CIR	6.05	4,824	70	80	13
W7	CIR		8,000	55	80	15
W8	CIR	10.49	7,465	100	80	15
W9	CIR		1,500	85	60	14
W23	CIR,CIREAM		500	80	80	15
W24	CIR,CIREAM	8.68	8,224	95	50	15
W25	CIR,CIREAM	11.68	3,466	20	80	15
W26	CIR,CIREAM	5.95	1,919	70	80	15
W27	CIREAM		10,000	80	80	15
W29	CIREAM	3.24	3,833	25	80	13
W32	CIREAM	5.97	3,283	85	60	14
W33	CIREAM		8,000	70	80	14

F.3: County of Perth:

Section ID	Treatment	AADT	Most Recent Activity Year	Age	Physical Condition	Drainage Rating
020022	CIR, 2" HL4	2575	1997	18	100	15
020040	CIR, 2" HL4	2575	1997	18	100	15
020060	CIR, 50mm HL3 Shingle Mix, Modified Slurry 2007	2420	2000	15	100	15
020080	CIR, 50mm HL3 Shingle Mix, Modified Slurry 2007	2685	2000	15	100	15
020100	CIR, 50mm HL3 Shingle Mix, Modified Slurry 2007	2685	2000	15	95	15
020120	CIR, 50mm HL3 Shingle Mix, Modified Slurry 2007	2685	2000	15	95	15
020140	CIR, 50mm HL3 Shingle Mix, Modified Slurry 2007	2685	2000	15	100	15
020160	CIR, 50mm HL3 Shingle Mix, Modified Slurry 2007	2685	2000	15	100	15
020172	CIR, 50mm HL3 Shingle Mix, Modified Slurry 2007	2685	2000	15	85	15
026053	CIR, R1	4160	2002	13	30	14
026085	CIR, R1	2705	2002	13	20	14
026111	CIR, R1	2705	2002	13	20	14
044138	CIR, R1	1076	1999	16	75	15
044158	CIR, R1	1076	1999	16	75	15
044178	CIR, R1	1076	1999	16	75	15
044198	CIR, R1	1240	1999	16	85	15
044218	CIR, R1	1240	1999	16	85	15

055000	CIR, R1	1965	2005	10	80	15
055019	CIR, R1	1735	2005	10	85	15
055039	CIR, R1	1735	2005	10	85	15
055129	CIR, R1	1125	2002	13	75	15
055152	CIR, R1	1125	2002	13	75	15
055172	CIR, R1	1125	2008	7	85	15
055193	CIR, R1	1125	2008	7	100	15
056000	CIR, R1	2655	2001	14	60	15
056040	CIR, R1	2600	2001	14	40	15
056063	CIR, R1	2600	2001	14	55	15
072000	CIR, R1	2730	1998	17	70	15
072017	CIR, R1	2570	2007	8	80	15
072036	CIR, R1	2570	2007	8	85	15
072054	CIR, R1	2570	2007	8	85	15
072072	CIR, R1	2310	2006	9	95	15
072090	CIR, R1	2310	2006	9	95	15
072108	CIR, R1	2310	1998	17	55	15
072135	CIR, R1	1870	1998	17	55	15
072156	CIR, R1	1870	1998	17	55	15
072176	CIR, R1	1870	1998	17	55	15
086000	CIR, R1	7755	1998	17	65	15
086018	CIR, R1	7170	1998	17	85	15
086036	CIR, R1	7170	1998	17	60	15
086054	CIR, R1	7170	2008	7	60	15
086072	CIR, R1	7120	2008	7	95	15
086090	CIR, R1	7120	2008	7	95	15
086108	CIR, R1	7120	2008	7	95	15
086131	CIR, R1	7250	2008	7	100	15
086223	CIR, R1	4605	1999	16	85	15
086241	CIR, R1	4605	1999	16	85	15
086259	CIR, R1	4605	1999	16	85	15
091000	CIR, R1	1970	1995	20	100	15
091018	CIR, R1	1970	1995	20	100	15
093000	CIR, R1	2680	1998	17	40	15
093022	CIR, R1	2680	1998	17	55	15
093057	CIR, R1	2680	1995	20	85	15
107004	CIR, R1	4400	2008	7	100	10
107024	CIR, R1	5670	2008	7	100	10
107046	CIR, R1	3385	1992	23	65	10
107064	CIR, R1	3385	1992	23	75	10

107084	CIR, R1	3385	1992	23	30	10
107102	CIR, R1	3410	1992	23	35	10
112000	CIR, R1	2490	1994	21	60	15
112023	CIR, R1	2490	1994	21	70	15
112035	CIR, R1	2490	1994	21	70	15
113019	CIR, R1, 1995 40mm HL4	3975	1994	21	60	15
113041	CIR, R1	3655	1995	20	25	15
118000	CIR, R1	3755	1997	18	100	15
118001	CIR, R1	1010	1997	18	30	15
121000	CIR, R1	2080	2003	12	80	15
121030	CIR, R1	2080	2003	12	85	15
121057	CIR, R1	2080	2003	12	85	15
121094	CIR, R1	1880	2004	11	40	15
121109	CIR, R1	1880	2004	11	60	15
121134	CIR, R1	1880	2004	11	75	15
121158	CIR, R1	1880	2004	11	75	15
121167	CIR, R1	1880	2004	11	75	15
123000	CIR, R1	2125	2001	14	95	14
130000	CIR, R1	2415	1997	18	100	15
130083	CIR, R1	3095	1997	18	65	15
130125	CIR, R1	3095	2001	14	80	15
130145	CIR, R1	3460	2001	14	85	15
131050	CIR, R1	2830	2003	12	70	15
131084	CIR, R1	1775	2003	12	80	15
131110	CIR, R1	1775	2003	12	65	15
131136	CIR, R1	1775	2003	12	55	15
131162	CIR, R1	1775	2003	12	50	15
135000	CIR, R1	1685	1992	23	75	15
135020	CIR, R1	1685	1992	23	75	15
135030	CIR, Rap, R1	2145	2009	6	75	15
135061	CIR, Rap, R1	2145	2009	6	85	15
135081	CIR, Rap, R1	2145	2009	6	85	15
135104	CIR, R1	1535	2009	6	85	15
135122	CIR, R1	1535	2009	6	85	15
135142	CIR, R1	1535	2009	6	85	15
139000	CIR, R1	1958	2009	6	85	15
139015	CIR, R1	1958	2009	6	95	15
139035	CIR, R1	1958	2009	6	95	15
139056	CIR, R1	1958	2009	6	85	15

139071	CIR, R1	4835	2009	6	85	15
140000	CIR, 65mm HL	1790	1990	25	100	15
140027	CIR, 65mm HL	1790	1990	25	85	15
140135	CIR, R1	1780	2009	6	80	15
140162	CIR, R1	1780	2009	6	80	15
163000	CIR, R1	2365	2007	8	95	15
163019	CIR, R1	1340	2007	8	85	15
163047	CIR, R1	1340	2007	8	85	15
163071	CIR, R1	1340	2007	8	95	15
163072	CIR, R1	1340	2007	8	85	15
180062	CIR, R1	1660	1993	22	35	15
180082	CIR, R1	1660	1993	22	30	15
180102	CIR, R1	1660	1993	22	50	15
180206	CIR 100mm, HL4 50mm	1450	2009	6	100	15
180227	CIR 100mm, HL4 50mm	1115	2009	6	95	15
180247	CIR 100mm, HL4 50mm	1115	2009	6	100	15
180267	CIR 100mm, HL4 50mm	1115	2009	6	100	15
180287	CIR 100mm, HL4 50mm	1115	2009	6	100	15
072007	CIR, R1	2730	1998	17	70	15
072050	CIR, R1	2570	2007	8	100	15
107000	CIR, R1	4400	2008	7	95	10
121074	CIR, R1	2070	2003	12	85	15
121082	CIR, R1	1880	2004	11	50	15
091044	CIR, R1	1970	1998	17	95	15
135096	CIR, R1	1535	2009	6	85	15
024000	CIR, R1	515	2004	11	90	15
024020	CIR, R1	515	2004	11	70	15
024040	CIR, R1	515	2004	11	85	15
024060	CIR, R1	515	2004	11	85	15
147000	CIR, R1	680	2001	14	80	13
147020	CIR, R1	680	2001	14	85	13
147040	CIR, R1	680	2001	14	75	13
178077	CIR, R1	520	1998	17	50	15
178126	CIR, R1	700	2004	11	80	15

178161	CIR, R1	700	2004	11	85	15
101000	CIREAM, 37mm HL3/4	6710	2005	10	75	15
101011	CIREAM, 37mm HL3/4	6710	2005	10	70	15
101033	CIREAM, 37mm HL3/4	6710	2005	10	55	15
101055	CIREAM, 37mm HL3/4	6710	2005	10	60	15
101075	CIREAM, 37mm HL3/4	6710	2005	10	30	15

F.4: MTO Sections:

MTO Sections: Contract ID	Treatment	Const. Year	Age	AADT	Truck %	IRI 2013	PCI 2013	Rut Values 2013
2008-3020	CIR	2009	6	7050	10.6	1.33	82.62	3.95
2008-3024	CIR	2009	6	3800	17.3	0.89	83.03	2.52
2008-3024	CIR	2010	5	3100	16.8	0.93	83.5	3.35
2008-3024	CIR	2010	5	3100	20.7	0.78	86.56	4.68
2008-4014	CIR	2011	4	8600	14.1	0.86	93.89	1.78
2009-3006	CIR	2009	6	5000	10.8	0.97	92.02	2.86
2009-3023	CIR	2011	4	3200	9.4	0.81	93.85	3.29
2009-4017	CIR	2010	5	4150	11.7	3.52	74.74	5.37
2010-3001	CIR	2010	5	6000	7.7	1.26	83.04	1.47
2010-3005	CIR	2010	5	2900	9.8	0.63	93.81	1.39
2010-3005	CIR	2010	5	2500	11.8	1.07	86.02	1.94
2010-3005	CIR	2010	5	1950	3.1	0.95	90.76	2.06
2010-3007	CIR	2010	5	8550	9.4	0.86	89.48	4.2
2010-4001	CIR	2011	4	8300	14.1	0.86	93.89	1.78
2011-3005	CIR	2011	4	3750	11.1	0.77	96	4.38
2011-3006	CIR	2011	4	7900	11	0.88	92.86	2.57
2011-3006	CIR	2011	4	3400	15.8	1.14	92.18	3.6
2011-4048	CIR	2011	4	8300	14.1	0.86	93.89	1.78
2002-4040	CIREAM	2003	12	12700	8	3.73	69.34	69.34
2005-5140	CIREAM	2005	10	1100	51.5	1.40	81.45	81.45
2006-2015	CIREAM	2007	8	16000	3.2	1.50	79.23	79.23
2007-2263	CIREAM	2007	8	12800	7.2	1.27	84.81	84.81
2007-5192	CIREAM	2008	7	5150	15.4	1.10	84.93	84.93
2008-4008	CIREAM	2008	7	6200	12.2	1.38	87.5	87.5

2008-4015	CIREAM	2009	6	8200	6.9	3.19	73.82	73.82
2008-4016	CIREAM	2009	6	7983	11.7	1.18	86.17	86.17
2008-4030	CIREAM	2010	5	4850	13	3.79	75.18	75.18
2008-5108	CIREAM	2009	6	1867	36.3	0.89	92.75	92.75
2008-5132	CIREAM	2009	6	4217	26.3	1.24	91.39	91.39
2008-5133	CIREAM	2009	6	4583	8.4	1.31	79.85	79.85
2009-3011	CIREAM	2009	6	5650	12.3	1.25	88.09	88.09
2009-3020	CIREAM	2010	5	2106	8	1.24	85.48	85.48
2009-3024	CIREAM	2010	5	5094	11.7	0.86	95.17	95.17
2009-4014	CIREAM	2009	6	1583	17.8	1.22	86.59	86.59
2009-4729	CIREAM	2010	5	3300	12.4	1.18	94.9	94.9
2009-5002	CIREAM	2009	6	4000	11.8	0.88	94.39	94.39
2009-5126	CIREAM	2009	6	9050	14.5	1.11	87.37	87.37
2009-6007	CIREAM	2009	6	16533	8.7	1.27	92.25	92.25
2009-6007	CIREAM	2009	6	18533	6.2	1.30	91.76	91.76
2010-2002	CIREAM	2010	5	9606	14.5	1.75	82.21	82.21
2010-2002	CIREAM	2010	5	7961	7.6	1.60	89.77	89.77
2010-2009	CIREAM	2010	5	9311	10.4	1.21	94.36	94.36
2010-3011	CIREAM	2010	5	2056	13	0.90	92.55	92.55
2010-4000	CIREAM	2010	5	35800	15.2	1.03	93.46	93.46
2010-4014	CIREAM	2010	5	6517	9.3	1.13	93.32	93.32
2010-4016	CIREAM	2010	5	6650	2.8	1.29	88.79	88.79
2010-4021	CIREAM	2010	5	25700	8.6	1.18	90.76	90.76
2010-5109	CIREAM	2010	5	2700	18.1	1.04	86.86	86.86
2010-5133	CIREAM	2011	4	5551	17.3	0.88	93.31	93.31
2010-5142	CIREAM	2011	4	3050	27.3	0.80	97.6	97.6
2010-5142	CIREAM	2011	4	3050	27.3	0.85	97.24	97.24
2011-3004	CIREAM	2011	4	3361	10.6	0.99	93.08	93.08

2011-3013	CIREAM	2011	4	6411	10.1	0.99	92.45	92.45
2011-3014	CIREAM	2011	4	4441	10.7	0.96	92.09	92.09
2011-3020	CIREAM	2011	4	11400	18.2	0.78	94.7	94.7
2011-4033	CIREAM	2011	4	8000	13.9	1.73	81.21	81.21

Appendix G Field Performance Pictures

G.1: City of Waterloo

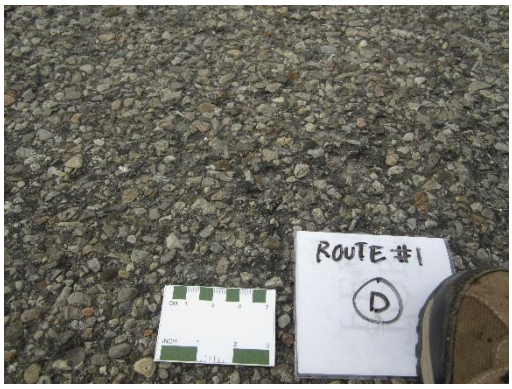

Ravelling/ Aggregate Loss

Severe Thermal transverse cracking

Alligator cracking

Structural damage due to poor drainage

Some Thermal cracking

Wheel path cracking

Cracking near the shoulders (poor drainage)

Combination of transverse and wheel path cracking

Wheel path cracking on just one side(poor to no drainage)

Severe damage repairs (possible potholes)

Micro cracking on wheel path

Centreline cracking

Minor to no thermal cracking

Some Aggregate loss

Crack at construction joints

Some wheel path rutting

Micro cracking

Asphalt Flushing

Severe cracking and possible structural damage (poor drainage)

Severe wheel path damage (near an entrance; thus, slow moving traffic)

Heavy truck traffic on roadways

Road in good condition

Combination of thermal and wheel path micro cracking

Micro cracking

Thermal cracking in the middle of the road

Large severe pothole and aggregate loss

Large severe pothole and aggregate loss

Construction joint cracking

Severe alligator cracking near the centreline

Thermal transverse cracking

G.2: Haldimand County

Centreline cracking (RR 3, Haldimand County)

Ravelling and aggregate loss (RR 3, Haldimand County)

Severe wheel path cracking (RR 3, Haldimand County)

Severe alligator cracking (RR 3, Haldimand County)

Severe wheel path rutting and cracking (RR 3, Haldimand County)

Severe cracking near railway tracks (RR 3, Haldimand County)

Appendix H Field Data Analysis

H.1: Physical Condition Values vs. Age for CIR Sections

Regression Statistics	
Multiple R	0.711
R Square	0.505
Adjusted R Square	0.500
Standard Error	15.477
Observations	95.000

	Coeffi-cients	Standard Error	t Stat	P-value	Lower 95%	Upper 95%
Intercept	103.10	3.61	28.54	0.00	95.93	110.27
Age	-2.93	0.30	-9.75	0.00	-3.53	-2.34

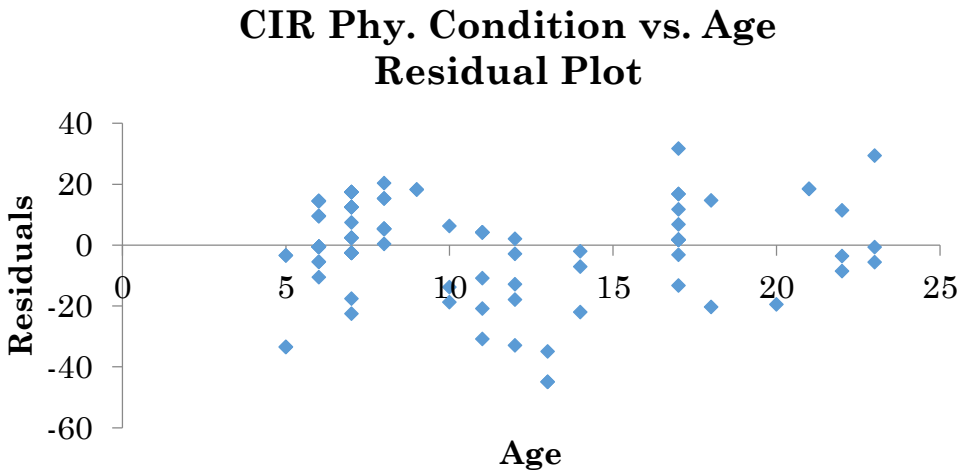

The regression analysis shows a 95% prediction interval of (95.93, 110.27). The residual plot shows no trend, thus the regression is significant. The p-value for age is 0.00 and thus, age showed a significant effect on physical condition.

H.2: Physical Condition Values vs. Age for CIREAM Sections

Regression Statistics	
Multiple R	0.216
R Square	0.047
Adjusted R Square	-0.017
Standard Error	20.798
Observations	17.000

	Coeffi-cients	Standard Error	t Stat	P-value	Lower 95%	Upper 95%
Intercept	57.29	12.78	4.48	0.00	30.06	84.53
Age	1.13	1.31	0.86	0.40	-1.67	3.92

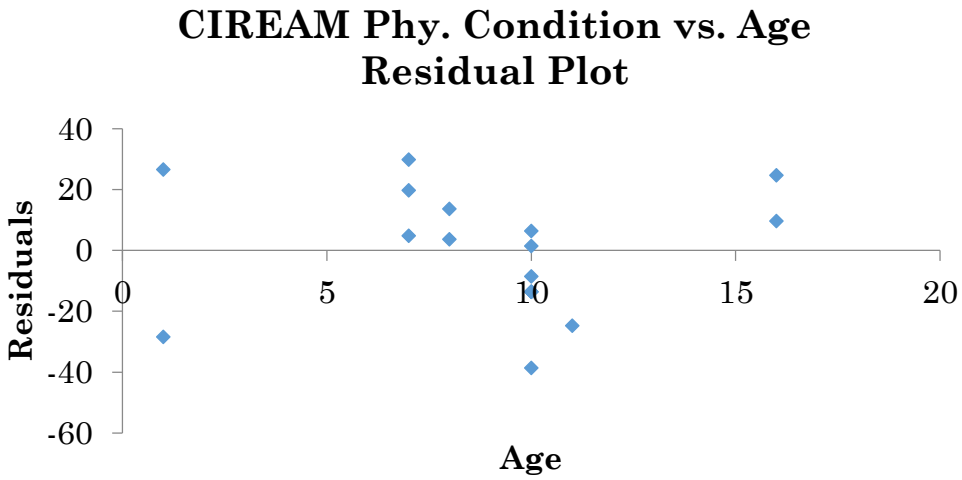

The regression analysis shows a 95% prediction interval of (30.06, 84.53). The residual plot shows no trend, thus the regression is significant. The p-value for age is 0.40 and thus, age showed an insignificant effect on physical condition.

H.3: Physical Condition Values vs. Truck Traffic for CIR Sections

Regression Statistics	
Multiple R	0.012
R Square	0.0001
Adjusted R Square	-0.077
Standard Error	23.614
Observations	15.000

	Coeffi-cients	Standard Error	t Stat	P-value	Lower 95%	Upper 95%
Intercept	69.79	7.90	8.84	0.00	52.73	86.84
AADTT	0.00	0.01	0.04	0.97	-0.02	0.02

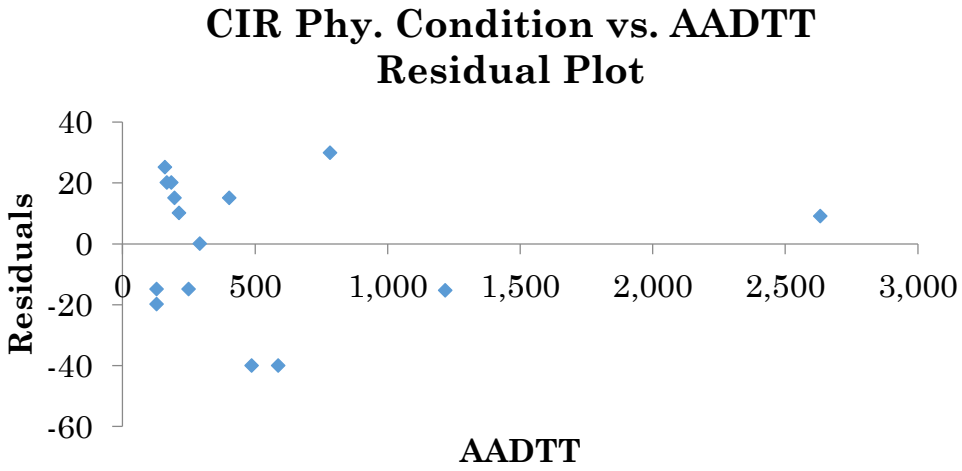

The regression analysis shows a 95% prediction interval of (52.73, 86.84). The residual plot shows no trend, thus the regression is significant. The p-value for AADTT is 0.97 and thus, AADTT showed an insignificant effect on physical condition.

H.4: Physical Condition Values vs. Truck Traffic for CIREAM Sections

Regression Statistics	
Multiple R	0.465
R Square	0.216
Adjusted R Square	-0.176
Standard Error	35.143
Observations	4.000

	Coeffi-cients	Standard Error	t Stat	P-value	Lower 95%	Upper 95%
Intercept	73.37	36.07	2.03	0.18	-81.82	228.56
AADTT	-0.11	0.15	-0.74	0.54	-0.76	0.53

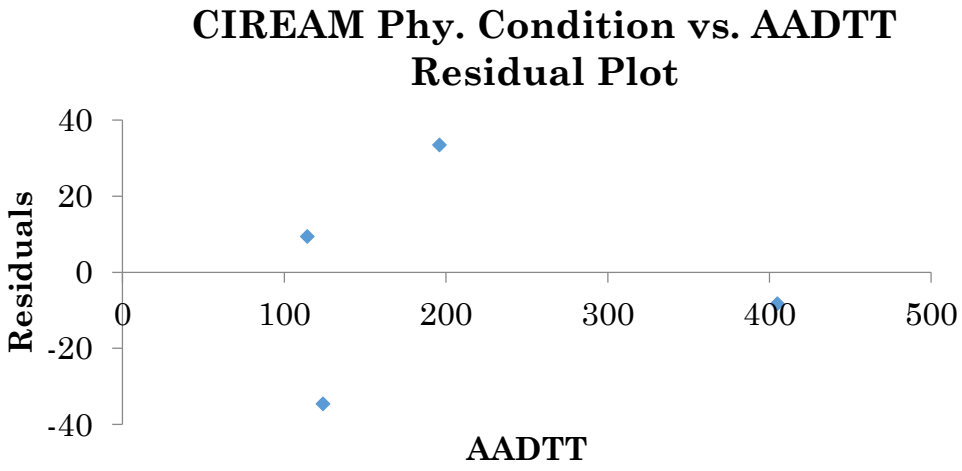

The regression analysis shows a 95% prediction interval of (-81.82, 228.56). The residual plot shows no trend, thus the regression is significant. The p-value for AADTT is 0.54 and thus, AADTT showed an insignificant effect on physical condition.

H.5: MTO PCI Values vs. AADT for CIR Sections

Regression Statistics	
Multiple R	0.202
R Square	0.041
Adjusted R Square	-0.019
Standard Error	5.820
Observations	18.000

	Coeffi-cients	Standard Error	t Stat	P-value	Lower 95%	Upper 95%
Intercept	86.53	3.30	26.25	0.00	79.54	93.52
AADT	0.00	0.00	0.83	0.42	0.00	0.00

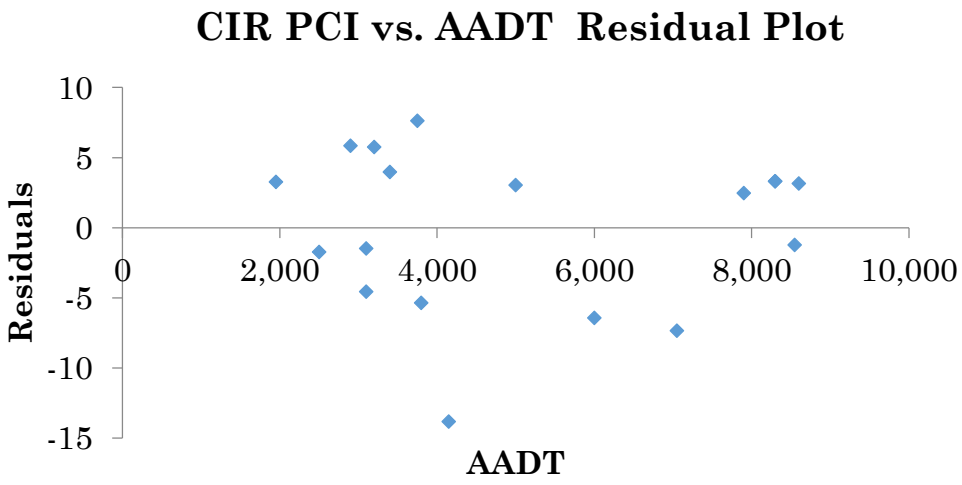

The regression analysis shows a 95% prediction interval of (79.54, 93.52). The residual plot shows no trend, thus the regression is significant. The p-value for AADT is 0.42 and thus, AADT showed an insignificant effect on PCI.

H.6: MTO PCI Values vs. AADT for CIREAM Sections

Regression Statistics	
Multiple R	0.019
R Square	0.0001
Adjusted R Square	-0.027
Standard Error	6.786
Observations	38.000

	Coeffi-cients	Standard Error	t Stat	P-value	Lower 95%	Upper 95%
Intercept	88.47	1.68	52.63	0.00	85.06	91.88
AADT	0.00	0.00	-0.12	0.91	0.00	0.00

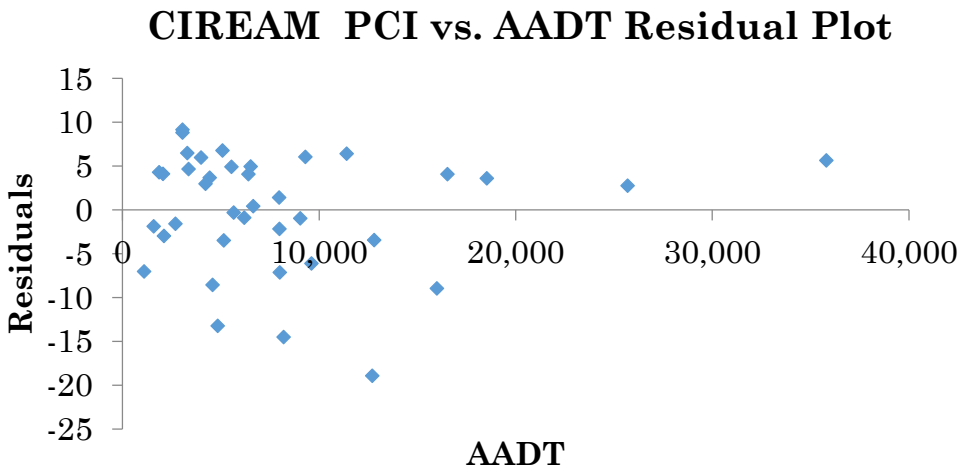

The regression analysis shows a 95% prediction interval of (85.06, 91.88). The residual plot shows no apparent trend, thus the regression is significant. The p-value for AADT is 0.91 and thus, AADT showed an insignificant effect on PCI.

H.7: MTO Rut Values vs. AADT for CIR Sections

Regression Statistics	
Multiple R	0.173
R Square	0.030
Adjusted R Square	-0.031
Standard Error	1.232
Observations	18.000

	Coeffi-cients	Standard Error	t Stat	P-value	Lower 95%	Upper 95%
Intercept	3.39	0.70	4.85	0.00	1.91	4.87
AADTT	0.00	0.00	-0.70	0.49	0.00	0.00

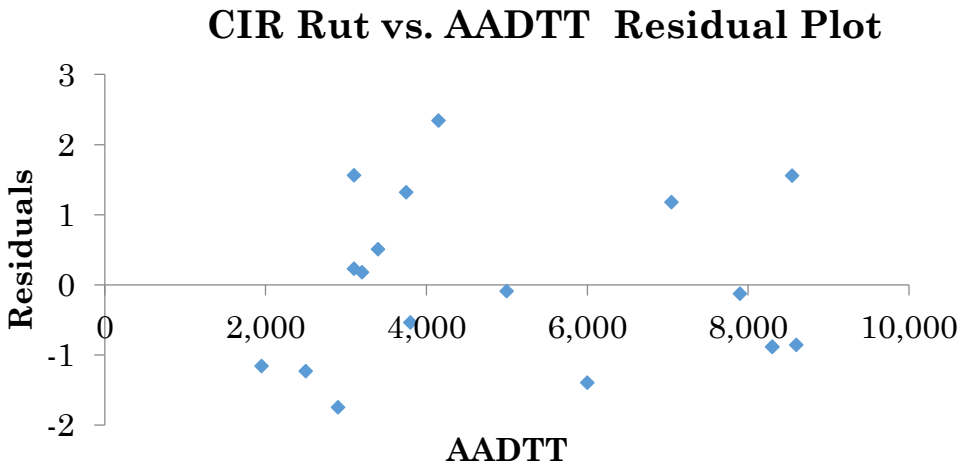

The regression analysis shows a 95% prediction interval of (1.91, 4.87). The residual plot shows no apparent trend, thus the regression is significant. The p-value for AADTT is 0.49 and thus, AADTT showed an insignificant effect on rutting.

H.8: MTO Rut Values vs. AADT for CIREAM Sections

Regression Statistics	
Multiple R	0.244
R Square	0.060
Adjusted R Square	0.033
Standard Error	1.591
Observations	38.000

	Coeffi-cients	Standard Error	t Stat	P-value	Lower 95%	Upper 95%
Intercept	2.27	0.39	5.76	0.00	1.47	3.07
AADTT	0.00	0.00	1.51	0.14	0.00	0.00

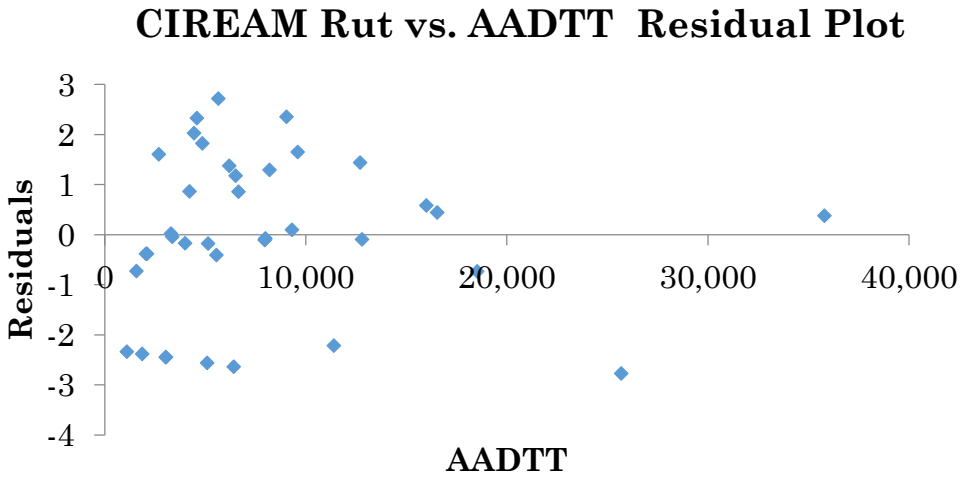

The regression analysis shows a 95% prediction interval of (1.47, 3.07). The residual plot shows no apparent trend, thus the regression is significant. The p-value for AADTT is 0.14 and thus, AADTT showed an insignificant effect on rutting.